ARCHIVES OF ACOUSTICS
22, 4, (1997)

Professor Roman Wyrzykowski

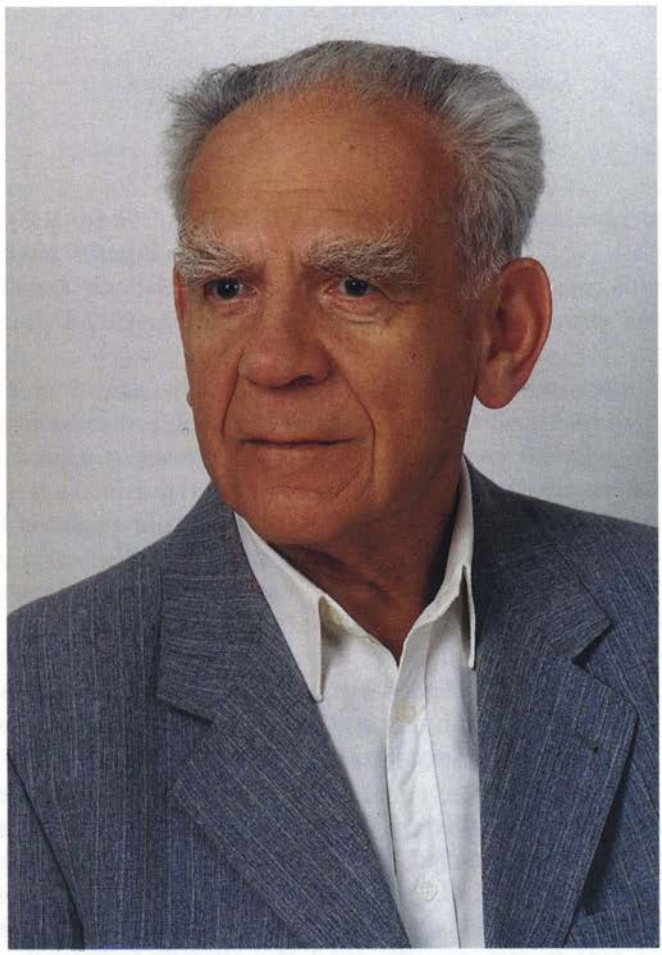

Phot.: Zakład Fotograficzny Franciszek Kasowski

ARCHIVES OF ACOUSTICS
22, 4, 375–382 (1997)

PROFESSOR ROMAN WYRZYKOWSKI

ON THE OCCASION OF THE 75TH BIRTHDAY AND THE 50TH ANNIVERSARY OF SCIENTIFIC ACTIVITY

H. CZYŻ, A. SNAKOWSKA

Institute of Physics, Pedagogical University
(35–311 Rzeszów, Rejtana 16a, Poland)

The year 1997 is the 50th year of Professor's Roman Wyrzykowski, one of the leading Polish acousticians, scientific activity.

Professor Roman Wyrzykowski is an outstanding personage; his knowledge, that surpasses significantly his scientific speciality, makes him an authority both as acoustician and a human.

He was born on the 5th of September 1922 in Grodzisk Mazowiecki in an intellectual family. His grandfather was doctor of medicine and his father a violin player (he even took his degree from an academy of music) and a lawyer, so, when he was employed in the Bank of Poland, the family moved to Warsaw. His mother graduated from a Pedagogical University and became a physicist.

The affiliation to the intelligentsia meant that the parents of Professor Wyrzykowski paid special attention to his education and his good knowledge of languages. Roman Wyrzykowski himself graduated from the Zamoyski Gymnasium in Warsaw which at that time, as well as today, was recognised as one of the leading schools in the city. He took his secondary-school certificate after completing on the study in clandestine classes. Before the Second World War had begun, a decision, which reflected his parents expectations, was made to base young Roman's career on versatile studies combinning physics and technical knowledge.

The events of the Second World War had a great influence on his life. He fought in the conspiracy, took part in the Warsaw Uprising as soldier of the Home Army, was seriously injured and, in consequence, lost his leg. In 1947, under supervision of prof. Sołtan, Professor Wyrzykowski took his first science degree at the Warsaw Institute of Technology situated at that time in Łódź (Warsaw was at that time a completely destroyed city); this degree is an equivalent to the nowadays' Master of Engineering degree. He started working at the Warsaw University together with his colleagues, at that time engineers, Marian Danysz, Zbigniew Wilhelmi and Olgierd Wołczek, a team of scientists interested in physics and completed by prof. Sołtan for starting research on

nuclear physics. It is worthy of mentioning here that during the first hydrogen bomb test on the Bikini Atoll (on the Pacific Ocean) a group of outstanding physicists, including professors Pieńkowski and Sołtan, was present there watching the test from a ship 16 miles away from the island and being protected only by dark glasses. None of them lived after that longer than few years.

Roman Wyrzykowski, after he had won the contest for a researcher post at the Industrial Chemistry Institute in Poznań, became head of the ultrasound laboratory in which the production of sirens and strong acoustical field generators has been set up. This way he became interested in acoustics. In 1951 he was dismissed from his work and accused, on the grounds of the infamous clause 49, of concealing in his CV the affiliation to the military college of the Home Army.

Between 1952 and 1956 he was lecturer at the Department of Theoretical Physics at the Adam Mickiewicz University in Poznań, working first with prof. Szczeniowski, later with prof. Kwiek. In the years 1956–61 he was assistant professor at the Physics Department of the Institute of Technology in Łódź.

For the first time he presented his thesis for the candidate of science degree (now the PhD degree) in 1957. His referees had to fight a real "battle" in the Central Qualifying Commission for the acceptance of his thesis, however the opinion of the Commission was negative. At the same time, a paper presenting a solution to the problem that was subject of Professor Wyrzykowski's thesis was published in one of the American journals; this fact could not have been known to Professor Wyrzykowski at that time. In 1960, the title of Doctor of Technics was conferred on Roman Wyrzykowski by the Board of the Communication Department of the Warsaw Institute of Technology basing on the thesis "The near field of a rectangle". The degree of assistant-professor was given to him already in 1963 by the Board of the Division of Communications of the Technical University of Wrocław, in virtue of the dissertation "The influence of the shape of the acoustic pulse on the shape of a wave generated by an acoustic siren". In the years 1961–1966, he was employed at the Institute of Physics of the Technical University in Wrocław and since 1966 he has worked at the Pedagogical University of Rzeszów being elected there head of the Physics Department, later he became head of the Acoustics Department and finally Director of the Institute of Physics. After the martial law was declared in 1981, he was relieved from his post of Director of the Institute of Physics and sent to an internment camp. This post was given back to him in consequence of the investigations of the Senate Commission for martial low victim affairs and was on duty again in the years 1990–1992. In 1973 he received the title of associate professor, however, he has not received the title of full professor until 1991 because of political reasons. In 1992 he retired, but even today he is still active in scientific work publishing papers with his younger colleagues, often the previous students or promoted doctors. He still gives lectures and carries on seminars for students preparing their thesis for the Master of Science degree.

His interests concerned mainly theoretical acoustics, especially the theory of diffraction and its application to the generation of strong acoustic fields and noise control.

Professor Wyrzykowski created his own school of theoretical acoustics inventing a new mathematical approach applying the methods of statistical physics. He is the author of

about fifty scientific papers that are well known both in Poland and abroad. Due to his scientific activity, many new developments, designed to reduce noise in workshops and factories, have been created and installed.

Professor Wyrzykowski was many times representative of polish science at acoustical congresses abroad, for example at the biggest one – the International Congresses on Acoustics in London in 1974 and in Madrid in 1977, a couple of times he participated in conferences in Germany, Hungary, France and Switzerland. During his professional career he has been a member of the French Acoustical Society, the Polish Acoustical Society, the Polish Physical Society and also of the Committee of Acoustics of the Polish Academy of Sciences. In 1973, thanks to his efforts, the division of the Polish Acoustical Society was established in Rzeszów and Prof. Wyrzykowski was elected its chairman for many succeeding terms of office; he was also active in the Ecology Club in Rzeszów. His younger friends have always felt to be supported by him, by his knowledge and experience. He has given lectures on many fields of theoretical physics and advanced mathematical methods for physicists. The wide range of his didactic activities led to the preparation and issue of many monographic books and textbooks. A striking feature of his books and publications is the intelligible manner of presentation of even the most difficult problems.

Under his supervision some hundreds of students received their Master of Science degree. He promoted twelve Philosophy Doctors (PhD); three others, because of some formal reasons, were confided to someone else's supervision. He was a reviewer of about 40 thesis for the PhD degree and of two thesis for assistant-professorship and wrote one review in the procedure of conferring the title of full professor to one of his former students.

The papers and researches made by him or inspired by him deal with the theory of diffraction, acoustical coagulation and high efficiency sirens.

On the occasion of his 50 scientific activity jubilee, a circle of his colleagues would like to express their admiration. We share a very common opinion – he is an outstanding acoustician. For many years we have had the opportunity to admire his accomplishments. This is why we feel obliged to tell a few words about his personality which had such a great influence on the interests of many young acousticians and filled them with enthusiasm for scientific research. He never gave up watching carefully the careers of his students, taking interest in their achievements, encouraging, making suggestions and raising spirits. He has been always happy about his pupils' successes, the "acoustical children and grandchildren" as he usually calls them.

Professor Wyrzykowski has always taught us a beautiful style of giving lectures, introduced us into his own researches and encouraged to new projects carried out under his mastery supervision.

The scientific and didactic activities are not the only passions of Professor Wyrzykowski, he is interested in literature, music, history and speaks several languages fluently. Travelling, connected with his professional activities, is also a great passion of his life giving him opportunity to meet interesting people and other scientists. Intelligence, good manners and diligence are the features he considers to be the most valuable and virtue.

Professor Wyrzykowski is always hopeful, very elegant, natural and stylish in his manners. We would like to express our congratulations and wish the continuation of scientific work to be always a source of happiness and satisfaction to Professor Wyrzykowski.

References

1. R. WYRZYKOWSKI, *Ochronniki akustyczne*, Biuletyn CIOP, Warszawa (1951).
2. R. WYRZYKOWSKI, *Zagadnienia naukowe w budowie syren ultradźwiękowych*, Biuletyn CIOP, Warszawa (1952).
3. R. WYRZYKOWSKI, *Akustyczne obliczenie syren*, Materiały I Konf. Techniki Ultradźwiękowej PAN 1953, Warszawa PWN (1956).
4. R. WYRZYKOWSKI, *Opór pobocznicy walca o skończonej długości*, Postępy Akustyki, Poznań (1956).
5. R. WYRZYKOWSKI, *Metody oczyszczania gazów przemysłowych*, Biuletyn KCMP Politechniki Łódzkiej, Łódź (1957).
6. R. WYRZYKOWSKI, *Teoria koagulacji dźwiękowej*, Zeszyty Naukowe Politechniki Łódzkiej, Fizyka Nr 20, Łódź (1958).
7. R. WYRZYKOWSKI, *Dźwiękowa koagulacja aerosoli*, Materiały II Konf. Techniki Ultradźwiękowej PAN 1956, Warszawa PWN (1958).
8. R. WYRZYKOWSKI, *Akustyczne pole bliskie prostokąta*, Zeszyty Naukowe Politechniki Łódzkiej, Fizyka, Nr 25, Łódź (1959).
9. R. WYRZYKOWSKI, *Dźwiękowa aglomeracja*, Zeszyty Naukowe Politechniki Łódzkiej Nr 20, Elektr., 2, 3 (1960).
10. R. WYRZYKOWSKI, *Kryteria porównawcze i podstawy obliczania urządzeń odpylających*, Zeszyty Naukowe Politechniki Wrocławskiej, Fizyka III Nr 46, Wrocław (1961).
11. R. WYRZYKOWSKI, *Analiza możliwości podniesienia sprawności pracy syren*, cz. I, Zeszyty Naukowe Politechniki Wrocławskiej, Fizyka III, Nr 48, Wrocław (1961).
12. R. WYRZYKOWSKI, *Analiza możliwości podniesienia sprawności pracy syren*, cz. II, Zeszyty Naukowe Politechniki Wrocławskiej, Fizyka III, Nr 48, Wrocław (1963).
13. R. WYRZYKOWSKI, *Wpływ kształtu impulsu na kształt fali i warunki pracy syreny*, Zeszyty Naukowe Poltechniki Wrocławskiej, Fizyka V Nr 75, Wrocław (1963).
14. R. WYRZYKOWSKI, *Fizyka dla Wydziału Inżynierii Sanitarnej*, Tom I. Termodynamika i akustyka, str. 168, Tom II. Elektryczność i magnetyzm, str. 195, Wydawnictwo Politechniki Wrocławskiej, Wrocław (1965).
15. R. WYRZYKOWSKI, *Obniżenie kosztów eksploatacji urządzenia odpylającego przy pomocy regeneracji ciepła*, Zeszyty Naukowe Politechniki Wrocławskiej, Fizyka XII, Nr 108, Wrocław (1966).
16. R. WYRZYKOWSKI, *Analogie elektromagnetyczne*, Zeszyty Naukowe Politechniki Wrocławskiej, Fizyka X, Wrocław (1966).

17. R. WYRZYKOWSKI, *Fizyka współczesna*, str. 140, Wydawnictwo Politechniki Wrocławskiej, Wrocław (1967).

18. R. WYRZYKOWSKI, *Teorie koagulacji akustycznej*, Zeszyty Naukowe WSP Rzeszów, Prace Mat.-Przyr. RTPN, 1, 125–135 (1969).

19. R. WYRZYKOWSKI, *Dydaktyczne ujęcie równania Schrödingera*, Rocz. Nauk.-Dydakt. WSP Rzeszów, z. 7, Nauki Mat.-Przyr. z. 2 (1970).

20. R. WYRZYKOWSKI, *Możliwości obliczenia częstości optymalnej przy akustycznej koagulacji aerozoli*, Zeszyty Naukowe WSP Rzeszów, Prace Mat.-Przyr. RTPN, 2, 173–181 (1970).

21. J. MORAWIEC, J. OLSZOWY, B. WYRZYKOWSKA, R. WYRZYKOWSKI, *Wybrane metody analizy hałasów niestacjonarnych*, Medycyna Pracy, 22, 527–537 (1971).

22. W. RDZANEK, B. WYRZYKOWSKA, R. WYRZYKOWSKI, *Elektrodynamika teoretyczna*, Wyd. WSP w Rzeszowie, str. 286 (1971).

23. Cz. SOŁTYS, R. WYRZYKOWSKI, *Obliczanie impedancji akustycznej źródeł dźwięku o znanej kierunkowości*, Archiwum Akustyki, **7**, 3/4, 327–335 (1972).

24. R. WYRZYKOWSKI, *Podstawy teorii mechaniki ośrodków ciągłych*, Wyd. WSP w Rzeszowie, str. 153 (1972).

25. R. WYRZYKOWSKI, *Liniowa teoria pola akustycznego ośrodków gazowych*, Rzeszów, RTPN – WSP, 437 s. (1972).

26. R. WYRZYKOWSKI, T. NIEDZIELSKI, *Nowe rozwiązania filtrów akustycznych do tłumienia hałasów wytworzonych przez sprężone gazy*, Ochrona Pracy, 5, 15–17 (1972).

27. W. RDZANEK, R. WYRZYKOWSKI, *Zastosowanie funkcji Greena w układzie współrzędnych cylindrycznych do obliczenia akustycznej impedancji dla układu szczelin w pobocznicy walca kołowego*, Archiwum Akustyki, **7**, 2, 183–193 (1972).

28. Cz. SOŁTYS, R. WYRZYKOWSKI, *Własności źródła o gaussowskim rozkładzie amplitudy prędkości drgań*, Archiwum Akustyki, **8**, 1, 81–89 (1973).

29. H. CZYŻ, R. WYRZYKOWSKI, *Obliczanie współczynnika odbicia płaskiej fali sinusoidalnej w ośrodkach niejednorodnych*, Mat. XX OSA'73, UAM, Poznań, 153–157 (1973).

30. R. WYRZYKOWSKI, *Podstawy mechaniki kwantowej*, Wydawnictwo WSP Rzeszów, str. 219 (1973).

31. R. WYRZYKOWSKI, J. SMELA, *Statystyczna metoda obliczania prędkości dźwięku w dwuatomowych gazach doskonałych*, Archiwum Akustyki, **8**, 3, 299–309 (1973).

32. R. WYRZYKOWSKI, *Nowe rozwiązanie filtrów akustycznych*, Bezpieczeństwo Pracy, Nr 1, 20 (1973).

33. A. SNAKOWSKA, R. WYRZYKOWSKI, K. ZIMA, *Pole bliskie na osi głównej źródła o gaussowskim rozkładzie amplitudy prędkości drgań*, Mat. XXI OSA'74, Rzeszów, 121–124 (1974).

34. R. WYRZYKOWSKI, M. ZWIERNIK, *Równania adiabat gazu idealnego składającego się z cząsteczek wieloatomowych w wysokich temperaturach uwzględniające zależność*

ciepła właściwego od temperatury, Rocznik Nauk.-Dydakt. WSP w Rzeszowie, 2, 79–94 (1974).

35. R. WYRZYKOWSKI, M. ZWIERNIK, *Prędkość fali akustycznej w gazach wieloatomowych w wysokich temperaturach*, Archiwum Akustyki, **9**, 4, 437–443 (1974).
36. W. RDZANEK, R. WYRZYKOWSKI, T. ZAMORSKI, *Obliczenie syreny akustycznej z uwzględnieniem wzajemnych oddziaływań otworów statora*, Archiwum Akustyki, **9**, 4, 413–423 (1974).
37. R. WYRZYKOWSKI, *XXI Seminarium z Akustyki. Rzeszów, 9-14.IX.1974r.*, Archiwum Akustyki, **10**, 2, 191–197 (1975).
38. A. SNAKOWSKA, R. WYRZYKOWSKI, K. ZIMA, *Pole bliskie na osi głównej membrany o gaussowskim rozkładzie amplitudy prędkości drgań*, Archiwum Akustyki, **10**, 3, 285–295 (1975).
39. H. CZYŻ, R. WYRZYKOWSKI, *Aproksymacja przebiegów temperaturowych w akustycznej wieży koagulacyjnej za pomocą funkcji Mathieu*, Archiwum Akustyki, **10**, 4, 425–432 (1975).
40. R. WYRZYKOWSKI, *Metody matematyczne w akustyce teoretycznej*, Wydawnictwo WSP Rzeszów, str. 223 (1975).
41. R. WYRZYKOWSKI, *Kryteria techniczno-ekonomiczne akustycznej koagulacji aerozoli*, Ochrona Pracy, 10, 20–21 (1975).
42. W. RDZANEK, R. WYRZYKOWSKI, *Pole akustyczne walca*, Wyd. WSP, Rzeszów, str. 161 (1975).
43. A. SNAKOWSKA, R. WYRZYKOWSKI, *Impedancja wylotu półnieskończonej rury o przekroju kołowym*, Mat. XXIII OSA'76, Wisła, 156–157 (1976).
44. A. PUCH, J. K. SNAKOWSKI, R. WYRZYKOWSKI, *Filtry akustyczne*, Wydawnictwo Uczelniane WSP Rzeszów (1977).
45. R. WYRZYKOWSKI, A. PUCH, J. TRZEŚNIOWSKI, T. ZAMORSKI, *High-efficiency acoustical siren*, Proceedings ICA'97, Madrid (1977).
46. T. ZAMORSKI, R. WYRZYKOWSKI, *Promieniowanie tuby akustycznej poniżej częstości granicznej*, Mat. XXIV OSA'77, Gdańsk-Władysławowo, 295–298 (1977).
47. T. ZAMORSKI, R. WYRZYKOWSKI, *Tuby hiperboliczne o pierścieniowym przekroju poprzecznym*, Mat. XXV OSA'78, Poznań-Błażejewko (1978).
48. H. CZYŻ, R. WYRZYKOWSKI, *Dryf cząstek aerosolu w polu fali stojącej*, Mat. XXVI OSA'79, Wrocław, 377–378 (1979).
49. T. ZAMORSKI, R. WYRZYKOWSKI, *Wpływ własności tuby katenoidalnej o pierścieniowym przekroju poprzecznym na emisję mocy akustycznej osiowego generatora dynamicznego*, Mat. XXVI OSA'79, Oleśnica (1979).
50. R. WYRZYKOWSKI, J. SMELA, *Analiza temperaturowej zależności stałych sprężystości w szerokim zakresie temperaturowym dla izotropowych ciał stałych*, Rocznik Nauk.-Dydakt. WSP Rzeszów, 6 (1980).

51. T. ZAMORSKI, R. WYRZYKOWSKI, *Rozszerzenie zakresu stosowalności modelu teoretycznego dynamicznych generatorów przepływowych do wyższych ciśnień zasilania*, Mat. XXVII OSA'80, Puławy (1980).

52. T. ZAMORSKI, R. WYRZYKOWSKI, *Approximate methods for the solution of the equation of acoustic wave propagation in horn*, Archives of Acoustics, **6**, 237–285 (1981).

53. J.K. SNAKOWSKI, R. WYRZYKOWSKI, *Diffraction of a sonic wave by the edge*, Archives of Acoustics, **7**, 2, 143–154 (1982).

54. R. WYRZYKOWSKI, *Zastosowanie transformacji całkowej Fouriera w ogólnej teorii dyfrakcji*, Archiwum Akustyki, **4**, 417–429 (1983) oraz w j. ang. Archives of Acoustics (1983).

55. A. SNAKOWSKA, R. WYRZYKOWSKI, *Wybrane zagadnienia z teorii dyfrakcji*, Wyd. WSP Rzeszów, 298 str. (1984).

56. M. LEŚNIAK, A. DRZYMAŁA, S. KLIMCZYK, R. WYRZYKOWSKI, *Obliczanie materiałów dźwiękochłonnych na zasadzie analogii elektroakustycznych przy uwzględnieniu impedancji Rayleigha*, Archiwum Akustyki, **20**, 3–4, 183–192 (1985) oraz w j. ang. Archives of Acoustics (1985).

57. A. SNAKOWSKA, R. WYRZYKOWSKI, *Calculation of the acoustical field of a semi-infinite cylindrical wave-guide by means of the Green function expressed in cylindrical coordinates*, Archives of Acoustics, **11**, 261–285 (1986).

58. R. WYRZYKOWSKI, *The velocity of sound on the axis of a circular ring*, Archives of Acoustics, **11**, 4 (1986).

59. R. WYRZYKOWSKI, *Phase velocity of a pressure wave on the axis of an acoustic field of a circular ring in an acoustic baffle*, Archives of Acoustics, **11**, 4, 331–337 (1986).

60. R. WYRZYKOWSKI, R. HNATKÓW, *Sirene mit hoher akustischer Leistung*, Acustica (Stuttgart), 59, 225–229 (1986).

61. R. WYRZYKOWSKI, *Propagation velocity of a vibration velocity wave, i.e. acoustic velocity wave*, Archives of Acoustics, **12**, 1, 17–31 (1987).

62. A. SNAKOWSKA, R. WYRZYKOWSKI, *Impedance of the semi-infinite unbaffled cylindrical wave-guide outlet*, Archives of Acoustics, **13**, 137–145 (1988).

63. A. SNAKOWSKA, R. WYRZYKOWSKI, *Powstawanie fali bocznej przy odbiciu fali kulistej od płaskiej granicy dwóch ośrodków*, Mat. XXXVI OSA'89, Szczyrk-Biła, 387–393 (1989).

64. R. WYRZYKOWSKI, *Metody matematyczne fizyki*, FOSZE, Rzeszów (1992).

65. R. WYRZYKOWSKI, *Sound sources of high directivity*, Archives of Acoustics, **17**, 307–320 (1992).

66. R. WYRZYKOWSKI, A. CZYRKA, *Properties of sound source with Gauss's velocity distribution*, Archives of Acoustics, **17**, 543–553 (1992).

67. A. CZYRKA, R. WYRZYKOWSKI, *Źródła dźwięku o absolutnej kierunkowości*, Archives of Acoustics, **18**, 3 (1993).

68. R. WYRZYKOWSKI, *Kierunkowość płaskich harmonicznych źródeł fal akustycznych w odgrodzie i zagadnienia z tym związane*, FOSZE, Rzeszów, ss. 79 (1993).
69. R. WYRZYKOWSKI, *The Dependence of the Speed of Sound on Space Coordinates*, Acustica, 79, 2, 128–134 (1993).
70. R. WYRZYKOWSKI, A. CZYRKA, *The applications of Hankel transform to the computation of nearfields of circular baffled sources*, Archives of Acoustics, **18**, 457–469 (1993).
71. R. WYRZYKOWSKI, H. CZYŻ, L. LENIOWSKA, W. RDZANEK, A. SNAKOWSKA, P. WITKOWSKI, B. WYRZYKOWSKA, T. ZAMORSKI, *Wybrane zagadnienia z teorii pola akustycznego*, FOSZE, Rzeszów, str. 515 (1994).
72. L. LENIOWSKA, R. WYRZYKOWSKI, *Wpływ korekty fazy na kierunkowość źródła fali*, XLIII Otwarte Seminarium z Akustyki, Gliwice-Ustroń, 425–430 (1996).

Doctors promoted by professor R. Wyrzykowski

1. IRENEUSZ WILK, *Rozwiązanie zagadnienia rozchodzenia się fali akustycznej w słupie powietrza z niezerowym gradientem temperatury* (1968).
2. WITOLD RDZANEK, *Zastosowanie funkcji Greena w układzie współrzędnych cylindrycznych do obliczania akustycznej impedancji dla układu szczelin na pobocznicy walca* (1970).
3. LUDMIŁA BIGDA, *Wpływ stanu naelektryzowania cząstek aerozolu na proces koagulacji akustycznej* (1973).
4. WIESŁAW KASPRZYK, *Teoria zjawisk hydrodynamicznych wynikająca z rozwiązania równania Naviera–Stokesa dotycząca opływu cząsteczki kulistej ruchem drgającym i uwzględniająca asymetrię pola opływu* (1976).
5. BOGDAN MĄCZEWSKI–ROWIŃSKI, *Nowe metody akustycznej koagulacji aerozolu* (1976).
6. JERZY SMELA, *Zależność prędkości dźwięku od temperatury w prętach i izotropowych ciałach stałych obliczona metodami statystycznymi* (1978).
7. ANDRZEJ PUCH, *Wpływ warunków pracy osiowego generatora dynamicznego o wspólnej dla kanałów statora tubie i komorze ciśnieniowej na jego parametry akustyczne* (1978).
8. MIECZYSŁAW ROCZNIAK, *Wpływ zmian stężenia wybranego aerozolu na natężenie fali akustycznej wymagane do osiągnięcia stałych efektów koagulacji* (1979).
9. RYSZARD HNATKÓW, *Zależność współczynników absorpcji fali akustycznej od parametrów wybranego aerozolu i pola akustycznego w procesie koagulacji akustycznej* (1979).
10. TOMASZ ZAMORSKI, *Wpływ zjawisk tuby o skończonej długości na warunki pracy syreny akustycznej* (1980).
11. ANNA SNAKOWSKA, *Impedancja akustyczna wylotu falowodu cylindrycznego bez odgrody* (1980).
12. HENRYKA CZYŻ, *Dryf cząstek aerozolu w polu fali stojącej* (1982).

ARCHIVES OF ACOUSTICS
22, 4, 383–395 (1997)

MODEL OF AN ACOUSTIC SOURCE WITH DISCONTINUOUS OPTIMAL ELEMENTS

A. BRAŃSKI

Institute of Technics, Pedagogical University
(35-310 Rzeszów, Reytana 16a, Poland)

A new multi-elements model is considered. This model is composed of a sequence of discontinuous elements. They are constructed basing on the zeros of the Tchebycheff's polynomial. In this case, the discontinuous elements, and consequently the discontinuous model, are obtained. Such a model is particularly useful for modelling a source with corners and arbitrary boundary conditions.

It has been proved that the new model is of better quality than other ones applied in the BEM up to now. To confirm this conclusion, the error of the new model and their acoustic fields have been compared with those of different other models.

In order to clearly demonstrate the advantages of the new model, a plane and fully axisymmetric source has been taken into account, however the idea of the model with discontinuous elements can be applied to more practical problems.

Notations

x_i	nodes, to model $M_{\mathcal{W};n+1}$; $i = 0, 1, ..., n$,
$\mathcal{W}_q(x)$	polynomial of degree q,
$M_{\mathcal{W};n+1}$	one-element model of degree q with $n+1$ nodes; $q = n$,
μ_j	break points, j-subinterval (j-element) $\in [\mu_{j-1}, \mu_j)$, to $M_{\mathcal{P};n_j,n_{ij}+1}$; $j = 1, 2, ...n_j$,
ν_i	nodes separately numbered on each element, to model $M_{\mathcal{P};n_j,n_{ij}+1}$; $i = 1, 2, ...n_{ij}$,
$\mathcal{P}_q(x)$	piecewise polynomial of degree q,
$M_{\mathcal{P};n_j,n_{ij}+1}$	n_j-elements model of degree q with $n_{ij}+1$ nodes on each element; $q = \max_j n_{ij}$,
$f(x), \widetilde{f}(x)$	given any function, interpolating function,
k	wave number,
$J_0(\ldots)$	Bessel function of zero order,
$G(r)$	infinite space solution of the Helmholtz equation for the point source [16] p. 641,
$f_{i..n}$	n-th divided difference of the function $f(x)$ at the nodes x_i, [3], [8] p. 193,
$P_i(x)$	finite product, [3], [8] p. 193,
x_b	radius of the membrane,
$[a, b] \equiv [0, x_P]$	from mathematical point of view.

1. Introduction

The first step of BEM is the discretization of the source boundary into elements [14] (boundary ≡ geometry and acoustic variables defined on the geometry). Next, applying

the interpolation theory, the model of each element source is built. From the mathematical point of view, the model of the source constitutes the piecewise polynomials [11, 12]. Hereafter, for simplicity: model of the element $\equiv$ element, model of the source $\equiv$ model.

Because the elements may be connected in an arbitrary manner, the model, in general, is a discontinuous function at singular points, i.e. at the points of discontinuity of the physical variables and/or those of discontinuity of the geometry (corners). However, the BEM requires, at these points, the existence of derivatives of the boundary [7, 17]. Under these circumstances the derivatives may not be determined and they require special attention.

Two main techniques to circumvent to the singular points are proposed:

- by duplicating the singular point with a small gap between [15, 17]. However, the problem arises how large the gap should be to ensure a good quality of the model,
- by using discontinuous (nonconforming) elements in which the nodes are shifted inside the elements; in order words, the extreme nodes are not placed at the borders of element [7, 9, 15, 17]; the problem arises how large the displacement of the node from the corner should be. In [15] it was proposed to take a distance of 1/4 and 1/6 of the element length for linear and quadratic elements, respectively, but this was not theoretically justified.

The aim of this work is to construct a model with optimal elements denoted by $M_{\mathcal{P};O-N}$, i.e. optimal in the distribution of the nodes on each element. This was achieved by applying the zeros of the Tchebycheff's polynomial as the nodes; an idea of such elements may be found in [3, 4, 5]. The Tchebycheff's zeros are exactly distributed. Such a model consists of a set of discontinuous elements. The new model turned out to be better quality than other known models. To confirm this conclusion, the following quantities have been calculated: the error of the models, their directivity functions and the acoustic pressure near the boundary.

Two comparative models were taken into account: a one-element model of higher degree and a multi-elements continuous model with evenly spaced nodes on each element.

For simplicity of the calculations, a plane axisymmetric membrane has been chosen as the source.

2. Interpolation theory

Let $f(x)$ be any given function. It is required to construct an interpolating function, $\widetilde{f}(x)$, which satisfies any (here Lagrange's) interpolation condition, i.e. $f(\text{nodes}) = \widetilde{f}(\text{nodes})$.

In this paper two forms of $\widetilde{f}(x)$ are presented:

- a polynomial form; $\widetilde{f}(x) \equiv \mathcal{W}(x)$,
- a piecewise polynomial form; $\widetilde{f}(x) \equiv \mathcal{P}(x)$.

The $\mathcal{W}(x)$ and $\mathcal{P}(x)$ are two standard models for the $f(x)$ function.

2.1. Polynomial interpolation

Let Δ be any partition of the interval $[a, b]$, such that

$$\Delta: \quad a = x_0 < x_1 < \cdots < x_{i-1} < x_i \cdots x_n = b \tag{2.1}$$

and the set of nodal values is $\{f(x_i)\}_0^n \equiv \{f_i\}_0^n$.

One desires to find a q-degree polynomial $\mathcal{W}_q(x)$ which satisfies the condition:

$$f(x_i) = \mathcal{W}_q(x_i), \qquad q = n. \tag{2.2}$$

There are several ways to represent an interpolating polynomial. It seems that the Newton form is the most efficient one [1] p. 3,

$$\mathcal{W}_q(x) = \sum_{i=0}^{n} f_{0..i} P_i(x). \tag{2.3}$$

The interpolating polynomial $\mathcal{W}_q(x)$, among the nodes x_i, is not identical with the function $f(x)$. Therefore, one defines the error of interpolation as follows:

$$E_{\mathcal{W};n+1}(x) = f(x) - \mathcal{W}_q(x). \tag{2.4}$$

This error could be exactly expressed by one of the three formulas, [11] p. 118, but the most known one is

$$E_{\mathcal{W};n+1}(x) = \frac{f^{(n+1)}(x_c)}{(n+1)!} P_{n+1}(x), \qquad x_c \in \operatorname{int}(x, x_0, x_1, \ldots, x_n). \tag{2.5}$$

The value $E_{\mathcal{W};n+1}(x)$ cannot be calculated because $f^{(n+1)}(x_c)$ is unknown. Therefore two estimations of $E_{\mathcal{W};n+1}(x)$ are used. The first one is the estimation at the point x and the second one the estimation over the interval $[a, b]$. They are given respectively by

$$\|E_{\mathcal{W};n+1}(x)\|_{\infty,f} \leq \frac{\mathfrak{M}_{f,n+1}}{(n+1)!} |P_{n+1}(x)|, \tag{2.6}$$

where

$$\mathfrak{M}_{f,n+1} = \|f^{(n+1)}(x)\|_\infty = \sup_{x \in [a,b]} |f^{(n+1)}(x)|, \tag{2.7}$$

and

$$\mathfrak{E}_{\mathcal{W};n+1} \leq \frac{\mathfrak{M}_{f,n+1}}{(n+1)!} \mathfrak{M}_{P,n+1}, \tag{2.8}$$

where

$$\mathfrak{M}_{P,n+1} = \|P_{n+1}(x)\|_\infty = \sup_{x \in [a,b]} |P_{n+1}(x)|. \tag{2.9}$$

If the interpolation points are equi-spaced, $\mathfrak{M}_{P,n+1}$ can be computed by the closed formula, [10] p. 63:

$$\mathfrak{M}_{P,n+1} = \left(\frac{b-a}{n}\right)^{n+1} (n+1)!\,. \tag{2.10}$$

2.2. *Piecewise polynomial interpolation*

At first sight it would appear that by increasing the number of nodes, and hence the degree of the polynomial, better interpolations to the function $f(x)$ should be successively obtained. However, in practice, between the nodes at the ends of the interval $[a, b]$ the interpolating polynomial of higher degree may oscillate quite violently (see Runge's problem, [1] p. 22, [11] p. 96). Thus it may reflect not truly the behaviour of the function $f(x)$.

An alternative approach is to use piecewise polynomial interpolation. Instead of looking for a higher degree polynomial over all the interval $[a, b]$, a polynomial composed of a sequence of low degree polynomials is constructed that it is valid only locally.

Let Δ_μ be any partition of the interval $[a, b]$, i.e.,

$$\Delta_\mu : \quad a = \mu_0 < \mu_1 < \cdots < \mu_{j-1} < \mu_j < \cdots < \mu_{n_j} = b. \tag{2.11}$$

Furthermore, let Δ_ν be an arbitrary partition of the j-subinterval, $x \in [\mu_{j-1}, \mu_j)$, Fig. 1,

$$\Delta_\nu : \quad \mu_{j-1} \leq \nu_0 < \nu_1 < \cdots < \nu_{i-1} < \nu_i < \cdots < \nu_{n_{ij}} \leq \mu_j\,, \tag{2.12}$$

and the set of nodal values $\{f(\nu_i)\}_0^{n_{ij}} = \{f_i\}_0^{n_{ij}}$, $j = 1, 2, ..., n_j$, where n_{ij} may be different on each j-subinterval.

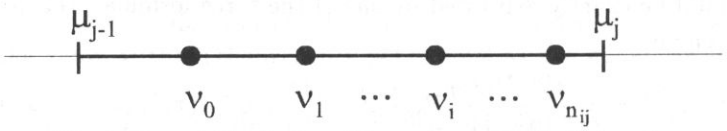

Fig. 1. General distribution of the nodes on the j-subinterval.

A q_j-degree polynomials $\mathcal{P}_{q_j}(x)$ and a q-degree piecewise polynomial $\mathcal{P}_q(x)$ are defined, on each j-subinterval and on the $[a, b]$ interval, respectively,

$$\mathcal{P}_{q_j}(x) \equiv \mathcal{W}_{q_j}(x), \qquad x \in [\mu_{j-1}, \mu_j), \quad q_j = n_{ij}\,, \tag{2.13}$$

$$\mathcal{P}_q(x) = \mathcal{P}_{q_j}(x), \qquad j = 1, 2, ..., n_j\,, \quad q = \max_j q_j\,, \tag{2.14}$$

The polynomial $\mathcal{P}_{q_j}(x)$ fulfils the interpolation condition

$$\widetilde{f}_{j,n_{ij}}(\nu_i) \equiv f(\nu_i) \equiv \mathcal{P}_{q_j}(\nu_i), \qquad \nu_i \in [\mu_{j-1}, \mu_j), \tag{2.15}$$

or in the $[a, b]$ interval

$$\widetilde{f}_{n_j,n_{ij}}(\nu_i) \equiv f(\nu_i) \equiv \mathcal{P}_q(\nu_i), \qquad \nu_i \in [a, b]. \tag{2.16}$$

The error of piecewise polynomial interpolation ought to be expressed similarly as pointed out above for polynomial interpolation. In this case, the error at every point of the j-subinterval and of the interval $[a, b]$ can be written respectively as follows

$$E_{\mathcal{P};j,n_{ij}+1}(x) = f(x) - \mathcal{P}_{q_j}(x), \qquad x \in [\mu_{j-1}, \mu_j), \tag{2.17}$$

$$E_{\mathcal{P};n_j,n_{ij}+1}(x) = f(x) - \mathcal{P}_q(x), \qquad x \in [a, b]. \tag{2.18}$$

Because of the reasons mentioned above, only the estimation of $E_{\mathcal{P};n_j,n_{ij}+1}(x)$ at the point x may be calculated, cf. Eq. (2.6),

$$\|E_{\mathcal{P};j,n_{ij}+1}(x)\|_{\infty,f} \leq \frac{\mathfrak{M}_{f,n_{ij}+1}}{(n_{ij}+1)!}|P_{n_{ij}+1}(x)|, \tag{2.19}$$

where

$$\mathfrak{M}_{f,n_{ij}+1} = \|f^{(n_{ij}+1)}(x)\|_\infty = \sup_{x\in[\mu_{j-1},\mu_j]} |f^{(n_{ij}+1)}(x)|, \tag{2.20}$$

$\|\cdots\|_\infty$ – norm of $C[\mu_{j-1},\mu_j]$ space (Tchebycheff norm).

In practice, however, it plays a minor part. Two estimations are more important: the estimation over the j-subinterval and that over interval the $[a,b]$,

$$\|E_{\mathcal{P};j,n_{ij}+1}\|_\infty = \frac{\mathfrak{M}_{f,n_{ij}+1}}{(n_{ij}+1)!}\mathfrak{M}_{P,n_{ij}+1}, \qquad x\in[\mu_{j-1},\mu_j), \tag{2.21}$$

$$\mathfrak{E}_{\mathcal{P};n_j,n_{ij}+1} = \max_j \|E_{\mathcal{P};j,n_{ij}+1}\|_\infty, \qquad x\in[a,b], \tag{2.22}$$

where

$$\mathfrak{M}_{P,n_{ij}+1} = \|P_{n_{ij}+1}(x)\|_\infty = \sup_{x\in[\mu_{j-1},\mu_j]} |P_{n_{ij}+1}(x)|. \tag{2.23}$$

For equi-spaced interpolation points on j-subintervals we have,

$$\mathfrak{M}_{P;n_{ij}+1} = \left(\frac{\mu_j-\mu_{j-1}}{n_{ij}}\right)(n_{ij}+1)!\,. \tag{2.24}$$

With regard to the distribution of the nodes on each j-subinterval, two cases should be considered: the first one, when two extreme nodes are placed at the ends of the j-subintervals; $\nu_0=\mu_{j-1}$, $\nu_{n_{ij}}=\mu_j$, and the second one, when these nodes are shifted inside; $\nu_0>\mu_{j-1}$, $\nu_{n_{ij}}<\mu_j$.

3. Models of the source

3.1. Acoustic source

For simplicity, let us consider the fully axisymmetric source, i.e. both the geometry and acoustic variables are independent of the angle of revolution. Here, the membrane placed in an infinite baffle is chosen as the source. In this case, the function $f(x)$ may be interpreted as a cross-section of the source, hence $a=0$, $b=x_b$.

An acoustic field of the source (exact acoustic field) has been described extensively in Refs. [16] p. 594, [18] p. 187 or [2, 6]; the final expressions for the directivity function and acoustic pressure near the source are given by,

$$Q(k,\gamma) = \int_0^{x_b} f(x)J_0(kx\sin\gamma)x\,dx, \tag{3.1}$$

$$p(k,H,x_P) = \int_0^{x_b} f(x)\left[\int_0^{2\pi} G(r)\,d\varphi\right]x\,dx, \tag{3.2}$$

respectively, where the geometric symbols are depicted in Fig. 2.

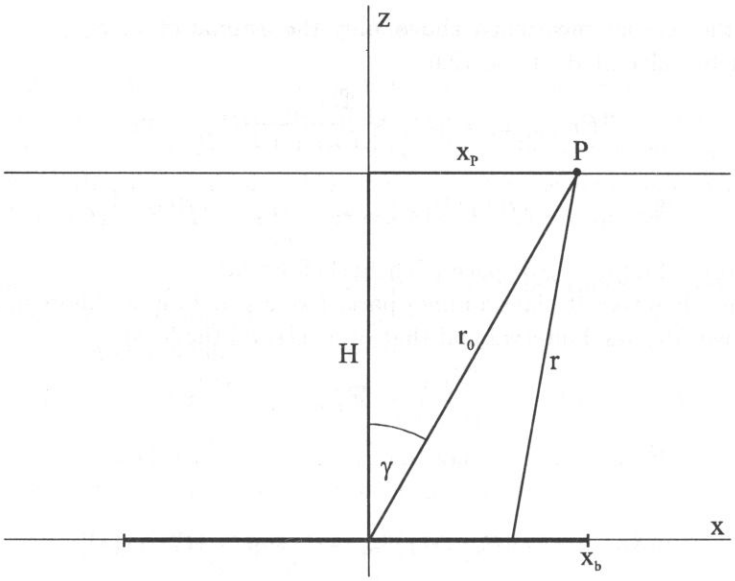

Fig. 2. Geometry of the problem.

3.2. Models of the source

Hereafter, the function $\widetilde{f}(x)$ ought to be interpreted as a cross-section of the model. The error of the model constitutes the error of interpolation, i.e. Eq. (2.4) or Eq. (2.18). Estimation of the model error on the interval $[a, b]$, Eq. (2.8) or Eq. (2.22), is assumed to be a direct measure of the quality of the model (see Sec. 5.1 below). However, in acoustics such a measure plays a minor part. It seems that the difference of the acoustic field may be more useful (indirect measure of the quality, see Sec. 5.2 below).

3.2.1. One-element model $M_{\mathcal{W}}$. Under the circumstances given above, the model $M_{\mathcal{W}}$ is given by Eq. (2.3): $M_{\mathcal{W}} \equiv \mathcal{W}_q(x) \equiv \widetilde{f}_n(x)$. If Eq. (2.3) is substituted into Eqs. (3.1) and (3.2), the acoustic field of $M_{\mathcal{W}}$ is obtained; it is denoted by $\widetilde{Q}_{\mathcal{W}}(k, \gamma)$, $\widetilde{p}_{\mathcal{W}}(k, H, x_P)$. The error of the model $M_{\mathcal{W}}$ is given by Eq. (2.4) and the direct measure of the quality by Eq. (2.8). In numerical calculations, the one-element model $M_{\mathcal{W}}$ with equi-spaced nodes $x_{e,i}$ is used as a comparative model. It is marked by $M_{\mathcal{W};R}$ and $x_{e,i}$ – ■ in Fig. 3. All the symbols ought to be completed by index $n+1$; e.g. $M_{\mathcal{W};R;n+1}$.

3.2.2. Multi-elements model $M_{\mathcal{P}}$. The model $M_{\mathcal{P}}$ is given by Eq. (2.14): $M_{\mathcal{P}} \equiv \mathcal{P}_q(x) \equiv \widetilde{f}_{n_j n_{ij}}(x)$. If Eq. (2.14) is substituted into Eqs. (3.1) and (3.2), the acoustic field of $M_{\mathcal{P}}$ is obtained; it is marked by $\widetilde{Q}_{\mathcal{P}}(k, \gamma)$, $\widetilde{p}_{\mathcal{P}}(k, H, x_P)$. The error of the model $M_{\mathcal{P}}$ is given by Eq. (2.18) and the direct measure of the quality by Eq. (2.22).

The multi-elements model $M_{\mathcal{P}}$ with equi-spaced break points $\mu_{e,j}$ (all elements have the same length) and equi-spaced nodes $\nu_{e,i}$ is called multi-elements regular model $M_{\mathcal{P};R}$ (in Fig. 3 $\mu_{e,j}$ – ∇ and $\nu_{e,i}$ – ■). It is a comparative model in numerical calculations.

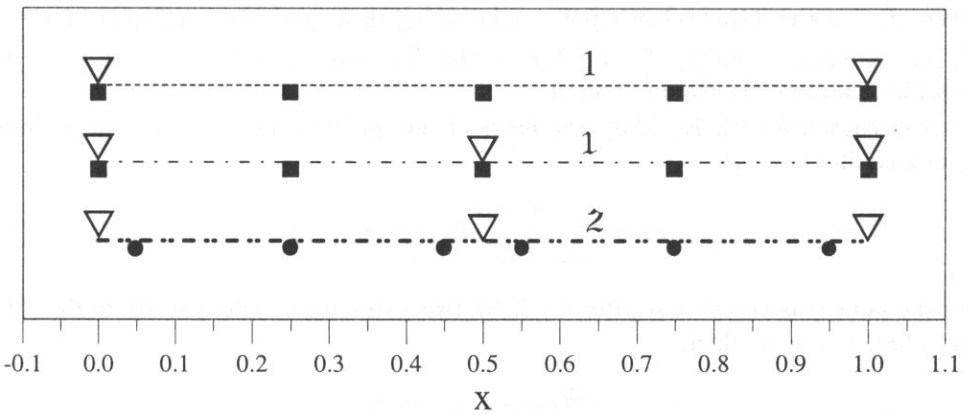

Fig. 3. Distribution of the nodes and break points: 1 – $M_{\mathcal{W};R;5}$, l – $M_{\mathcal{P};R;2,3}$, 2 – $M_{\mathcal{P};O-N;2,3}$.

Under conditions given above, instead of Eq. (2.3), Eqs. (2.13) and (2.14), $M_{\mathcal{P};R}$ may be expressed by a simpler formula,

$$\mathcal{P}_{q_j}(x) = \sum_{i=0}^{n_{ij}} f_{e,i}\mathfrak{N}_i(x), \qquad x \in [\mu_{j-1}, \mu_j), \tag{3.3}$$

where $f_{e,i} = f(\nu_{e,i})$ and $\mathfrak{N}_i(x)$ are the shape functions; they can be easily found elsewhere, [7] p. 71. Up to now, this is a fundamental equation applied in modelling the source in BEM. In this section the additional index n_j, $n_{ij} + 1$ has been dropped to simplify the notation; e.g. the full symbol is $M_{\mathcal{P};R;n_j,n_{ij}+1}$.

3.2.3. Multi-elements model with optimal elements $M_{\mathcal{P};O-N}$. The feature of $M_{\mathcal{P};O-N}$ are the equi-spaced break points $\mu_{e,j}$, but the nodes are the Tchebycheff's zeros.

Analysing formula (2.8), one can see that the error is a product of two factors. One of them, $\mathfrak{M}_{f,n+1}$, depends on the properties of the function $f(x)$ and is not amenable to regulation, while the other one $\mathfrak{M}_{P,n+1}$, is determined by the choice of the nodes x_i. Thus the question of an optimal choice of x_i arises so that $\mathfrak{M}_{P,n+1}$ deviates less than any other polynomial on interval $[a, b]$. This problem was solved by Tchebycheff, [3], [8] p. 540, who pointed out optimal nodes, here marked as $x_{T,i}$. Detailed discussions of the mathematical aspect of the nodes $x_{T,i}$ can be found in [3, 4, 5, 6]. In these papers, $x_{T,i}$ were applied to construct the one-element optimal model.

Hereafter the idea of $x_{T,i}$ is utilized to construct a multi-elements optimal model $M_{\mathcal{P};O-N}$ and $x_{T,i}$ ought to be replaced by $\nu_{T,i}$. Note, that the $\nu_{T,i}$ are non-uniformly spaced. Furthermore, the external $\nu_{T,i}$ are shifted from the borders of the j-subinterval and these displacements are mathematically proved.

In the case under consideration the interpolating polynomial can be expressed by Eq. (2.3). At such a particular distribution of the $\nu_{T,i}$, this formula takes a particular form of

$$\mathcal{P}_{q_j}(x) = \sum_{i=0}^{n_{ij}} f_{0..i}\widehat{T}_i(x), \qquad x \in [\mu_{j-1}, \mu_j), \tag{3.4}$$

where $\widehat{T}_{n_{ij}}$ is the Tchebycheff's polynomial of n_{ij}-th degree (the coefficient of $x^{n_{ij}}$ in $\widehat{T}_{n_{ij}}(x)$ is equal to unity); for further details, see Refs. [3] and [8] p. 540. Next, the Eqs. (2.13) and (2.14) should be used.

In accordance with Eq. (2.5), the error of interpolation by Eq. (3.4) can be found from a similar formula

$$E_{\mathcal{P};O-N;j,n_{ij}+1}(x) = \frac{f^{(n_{ij}+1)}(x)}{(n_{ij}+1)!}\widehat{T}_{n_{ij}+1}(x), \qquad x \in [\mu_{e,j-1}, \mu_{e,j}). \tag{3.5}$$

For the same reasons as those after Eq. (2.5), two estimations, quite parallel to Eqs. (2.6) and (2.8), can be applied,

$$\|E_{\mathcal{P};O-N;j,n_{ij}+1}(x)\|_{\infty,f} \leq \frac{\mathfrak{M}_{f,n_{ij}+1}}{(n_{ij}+1)!}\left|\widehat{T}_{n_{ij}}(x)\right|, \qquad x \in [\mu_{e,j-1}, \mu_{e,j}). \tag{3.6}$$

where $\mathfrak{M}_{f,n_{ij}+1}$ is expressed by formula (2.6) and

$$\|E_{\mathcal{P};O-N;j,n_{ij}+1}\|_{\infty} \leq \frac{\mathfrak{M}_{f,n_{ij}+1}}{(n_{ij}+1)!}\mathfrak{M}_{T,n_{ij}+1}, \qquad x \in [\mu_{e,j-1}, \mu_{e,j}). \tag{3.7}$$

The $\mathfrak{M}_{T,n_{ij}+1}$ can be calculated analytically [13], p. 94,

$$\mathfrak{M}_{T,n_{ij}+1} = (\mu_{e,j} - \mu_{e,j-1})^{n_{ij}+1}\, 2^{-(2n_{ij}+1)}. \tag{3.8}$$

The estimation of the error (3.5) over the $[a, b]$ interval can be written as

$$\mathfrak{E}_{\mathcal{P};O-N;n_j,n_{ij}+1} = \max_j \|E_{\mathcal{P};O-N;j,n_{ij}+1}\|_{\infty}, \qquad x \in [a, b]. \tag{3.9}$$

The $M_{\mathcal{P};O-N}$ model is given by Eq. (2.14) via (3.4): $M_{\mathcal{P};O-N} \equiv \mathcal{P}_q(x) \equiv \widetilde{f}_{n_j,n_{ij}}$. Note that this is a discontinuous model. If Eq. (3.4) is substituted into Eqs. (3.1), (3.2), an acoustic field of $M_{\mathcal{P};O-N}$ is obtained that is denoted by $\widetilde{Q}_{\mathcal{P};O-N}(k,\gamma), \widetilde{p}_{\mathcal{P};O-N}(k,H,x_P)$. The error of the $M_{\mathcal{P};O-N}$ model is given by Eq. (3.5) and a direct measure of the quality by Eq. (3.9).

The multi-elements model $M_{\mathcal{P}}$ with equi-spaced break points $\mu_{e,j}$ and nodes $\nu_{T,i}$ is called the multi-elements model with discontinuous optimal elements $M_{\mathcal{P};O-N}$ (in Fig. 3 $\mu_{e,j}$ - ∇ and $\nu_{T,i}$ - $\bullet$).

In this section all the symbols should be completed by an additional index $n_j, n_{ij}+1$; e.g. $M_{\mathcal{P};O-N;n_j,n_{ij}+1}$.

4. Numerical implementation

The aim of numerical calculations is to compare the quality of the new model $M_{\mathcal{P};O-N}$ with those of other models, i.e. with those of $M_{\mathcal{W};R}$ and $M_{\mathcal{P};R}$. To do this the same total

number of nodes and/or of the same degrees are assumed, see Fig. 3. To realise the task, one takes into account:

$M_{\mathcal{W};R;5}$ → 1-element regular model of degree 4 with 5 nodes; the graphs concerning this model are denoted by short dashed lines marked by 1,

$M_{\mathcal{P};R;2,3}$ → 2-element regular model of degree 2 with 3 nodes on each element; lines 1: short + long,

$M_{\mathcal{P};O-N;2,3}$ → 2-element model degree 2 with 3 nodes on each optimal element; lines 2: short + short + long (bolted).

In all the figures the same kind of lines relates to the same model.

5. Calculations, results, conclusions

As a preliminary check of the quality of the models, the cross-sections of the source and of the models are shown in Fig. 4; $x \in [0, x_b/4]$, where $x_b = 1$ is assumed. Inspection of the figure reveals two conclusions:

- *The model $M_{\mathcal{P};O-N}$ consists of discontinuous elements.*

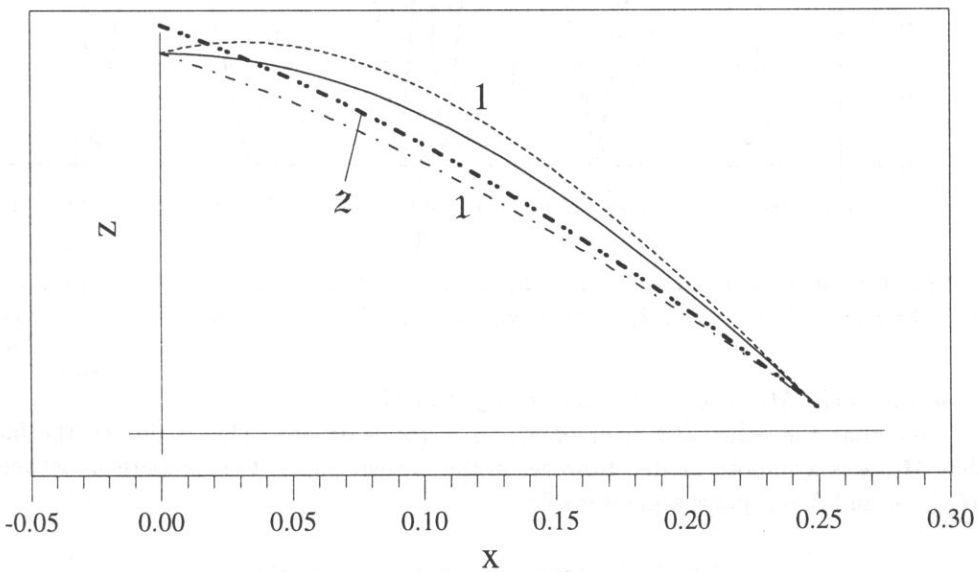

Fig. 4. Cross-sections of the source and the models: solid line – membrane, 1 – $M_{\mathcal{W};R;5}$, 1 – $M_{\mathcal{P};R;2,3}$, 2 – $M_{\mathcal{P};O-N;2,3}$.

Hereby it is quite suitable to modelling the boundary with singular points, see Ref. [7] p. 87, p. 237. Furthermore, the displacements of the nodes inside the element from singular points are exactly determined.

- *The model $M_{\mathcal{P};O-N}$ is more convergent to the source than the others are.*

In order to confirm this conclusion, two measures of the model quality are examined.

5.1. Direct measure of the model quality

As mentioned in Sec. 3.2, the estimation of the model error on the interval $[a, b]$ makes up a measure of the model quality, Eqs. (2.8) and (2.22). Here they are plotted in Fig. 5. As expected, the estimated error of $M_{\mathcal{P};O-N}$ is less than that of $M_{\mathcal{P};R}$. Because the error estimation on the $[a, b]$ interval is a direct measure of the model quality.

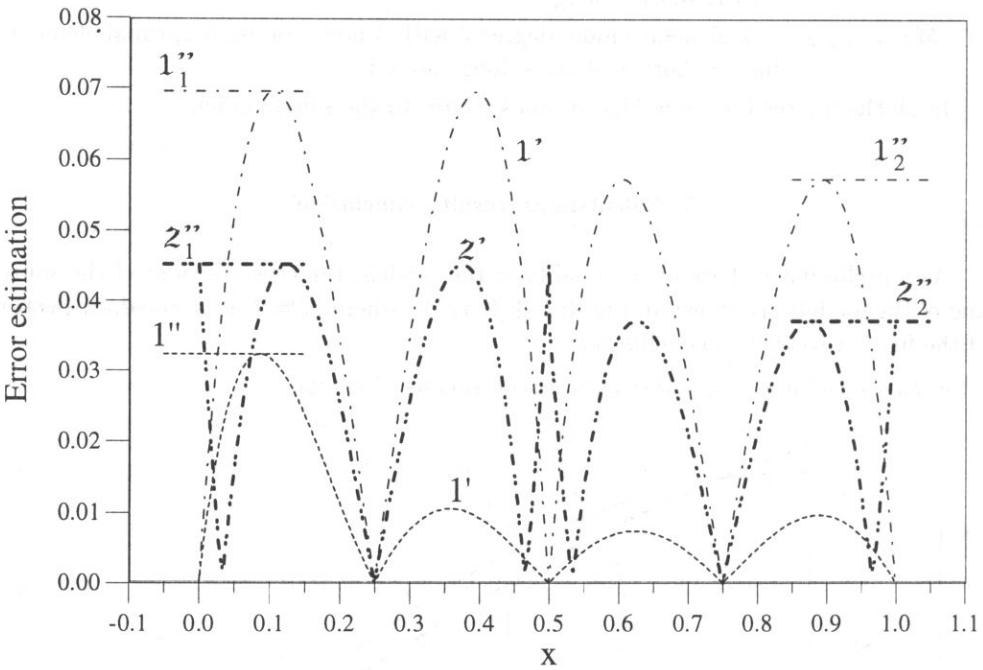

Fig. 5. Estimations of the errors: line $1' - \|E_{\mathcal{W};R;5}(x)\|_{\infty,f}$, $1'' \equiv \mathfrak{E}_{\mathcal{W};R;5}$, $1'_j - \|E_{\mathcal{P};R;j,3}(x)\|_{\infty,f}$, $1''_j - \|E_{\mathcal{P};R;j,3}\|_{\infty}$, $1''_1 \equiv \mathfrak{E}_{\mathcal{P};R;2,3}$, $2'_j - \|E_{\mathcal{P};O-N;j,3}(x)\|_{\infty,f}$, $2''_j - \|E_{\mathcal{P};O-N;j,3}\|_{\infty}$, $2''_1 \equiv \mathfrak{E}_{\mathcal{P};O-N;2,3}$.

- *The model $M_{\mathcal{P};O-N}$ is of better quality than $M_{\mathcal{P};R}$.*

Note that the estimated error of $M_{\mathcal{W};R}$ is the least one. This is due to the fact that $M_{\mathcal{W};R}$ is a smooth model. However in the present paper, the comparison between $M_{\mathcal{P};O-N}$ and $M_{\mathcal{P};R}$ plays a greater role.

5.2. Indirect measure of the model quality

To confirm the last conclusion, the models are compared in a different manner. For this purpose one defines:

- $\Delta Q(k, \gamma) = Q(k, \gamma) - \widetilde{Q}(k, \gamma)$,
- $\Delta p(k, H, x_P) = p(k, H, x_P) - \widetilde{p}(k, H, x_P)$.

These differences may be interpreted as indirect measures of the model quality.

The differences in the directivity functions are presented in Fig. 6. The results clearly confirm the last conclusion. For a comprehensive study, Figs. 7 and 8 show the differences

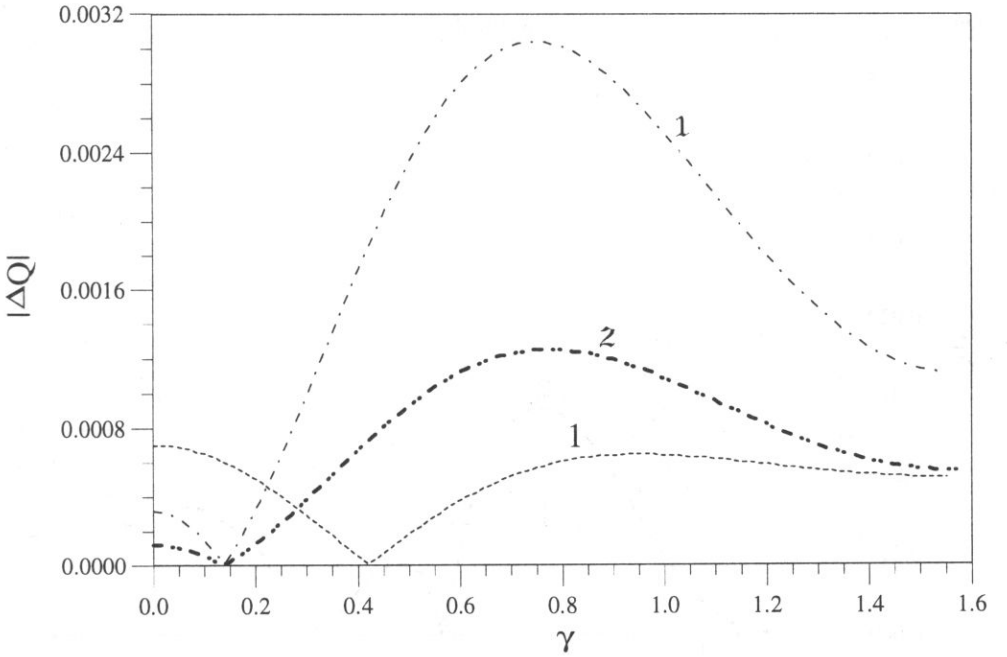

Fig. 6. Difference of the directivity functions $\Delta Q(k,\gamma)$, $k=5$; line 1 – $|\Delta Q_{\mathcal{W};R;5}|$, 1 – $|\Delta Q_{\mathcal{P};R;2,3}|$, 2 – $|\Delta Q_{\mathcal{P};O-N;2,3}|$.

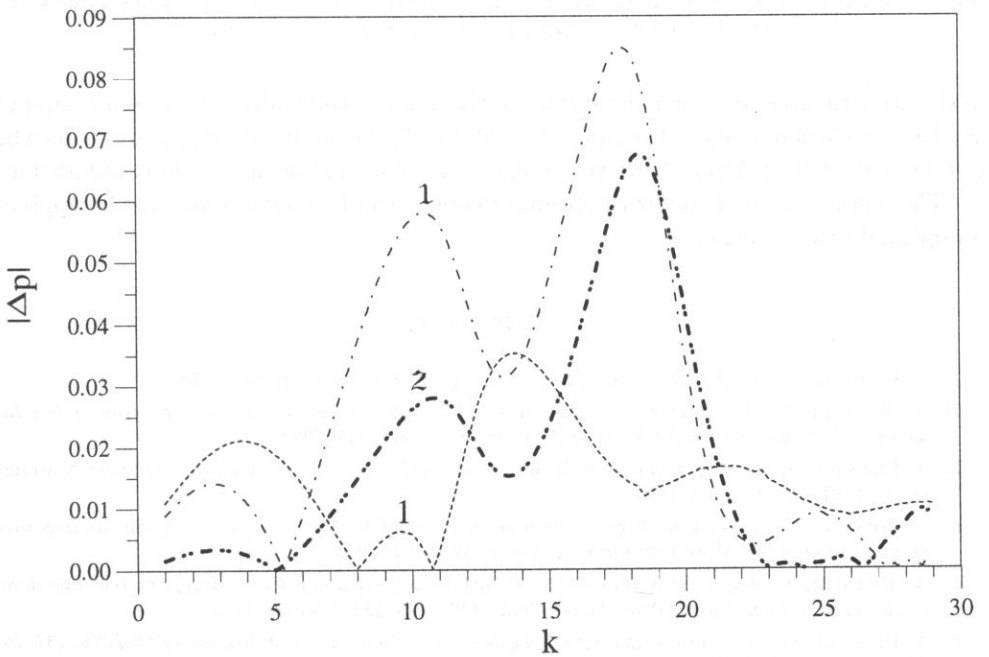

Fig. 7. Difference in the acoustic pressures $\Delta p(k,H,x_P)$ at the fixed point of the axis, $H=0.1x_b$, $k=5$; line 1 – $|\Delta p_{\mathcal{W};R;5}|$, 1 – $|\Delta p_{\mathcal{P};R;2,3}|$, 2 – $|\Delta p_{\mathcal{P};O-N;2,3}|$.

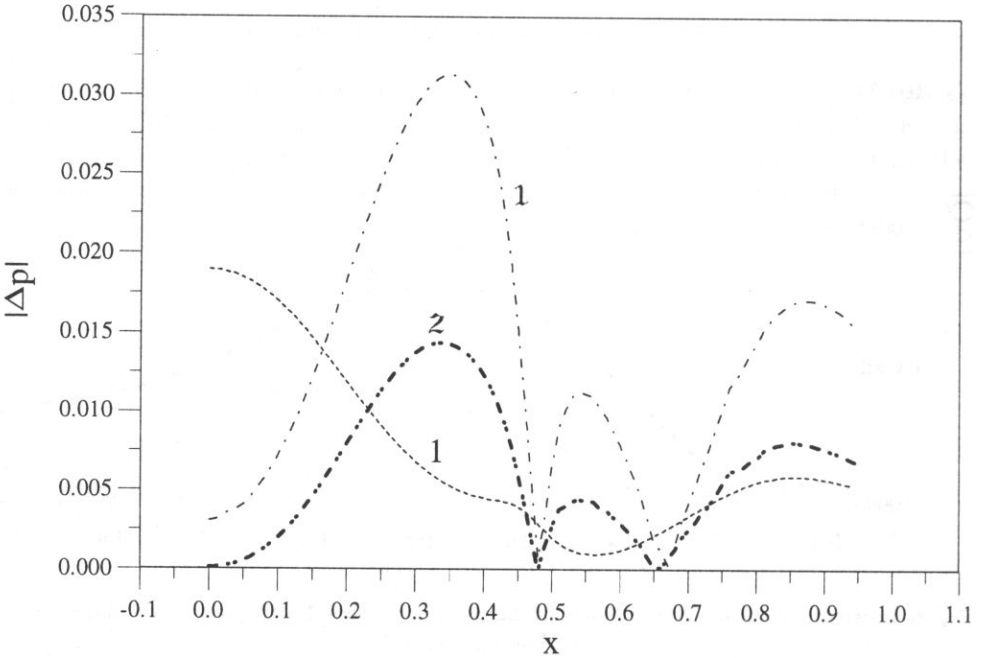

Fig. 8. Difference in the acoustic pressures $\Delta p(k, H, x_p)$ on the line parallel to the radius of the source, $H = 0.1x_b$, $k = 5$; line 1 – $|\Delta p_{\mathcal{W};R;5}|$, 1 – $|\Delta p_{\mathcal{P};R;2,3}|$, 2 – $|\Delta p_{\mathcal{P};O-N;2,3}|$.

of the acoustic pressures near the surface of the models. Generally, all the results support the last conclusion. Only in the range $k > 20$, Fig. 7, the quality of $M_{\mathcal{P};O-N}$ is somewhat poorer than that of $M_{\mathcal{P};R}$. However an explanation of this phenomenon is impossible.

The quality of the model with optimal elements can be further improved by applying an optimal discretization

References

[1] C. DE BOOR, *A practical guide to splines*, Springer-Verlag, N.Y., Berlin 1978.

[2] A. BRAŃSKI, M. RATUSZNIAK, *Modelowanie płaskiego źródła drgającego z prędkością bez linii węzłowych*, Materiały OSA'93, 107–110, Rzeszów – Polańczyk 1993.

[3] A. BRAŃSKI, *Optymalny, z punktu doboru węzłów, model akustyczny membrany kołowej*, Materiały OSA'94, 61–64, Wrocław 1994.

[4] A. BRAŃSKI, A. GRZEBYK, *Błędy optymalnego, z punktu doboru węzłów, modelu akustycznego membrany kołowej*, Materiały OSA'94, 65–68, Wrocław 1994.

[5] A. BRAŃSKI, *Optimal, from the choice of nodes, acoustical model of axisymmetric membrane vibrating with high modes*, Proc. Noise Control'95, 123–126, Warsaw 1995.

[6] A. BRAŃSKI, *Zastosowanie rozsuniętych węzłów Czebyszewa w BEM*, Materiały OSA'96, 137–142, Gliwice – Ustroń 1996.

[7] C.A. BREBBIA, J. DOMINGUEZ, *Boundary elements. An introductory course*, Comp. Mech. Publ., McGraw-Hill Book Company, Southampton 1992.

[8] C.F. GERALD, P.O. WHEATLEY, *Applied numerical analysis*, Addison-Wesley Publ. Comp., USA 1984.

[9] L.J. GRAY, E. LUTZ, *On the treatment of corners in the boundary element method*, J. Comput. Appl. Math., **32**, 369–386 (1990).

[10] J.M. JANKOWSCY, *Przegląd metod i algorytmów numerycznych*, WNT, Warszawa 1981.

[11] J.R. RICE, *Numerical methods, software, and analysis*, IMSL Refrence Edition, Mc Graw-Hill Book Company, N.Y. 1983.

[12] L.L. SCHUMAKER, *Splines functions: basic theory*, John Wiley & Sons, N.Y. 1981.

[13] B. SENDOW, Stare i nowe w metodach numerycznych, PWN, 1976.

[14] A.F. SEYBERT, C.Y.R. CHENG, *Application of the boundary element method to acoustic cavity response and muffler analysis*, ASME Trans., 1988, private communication.

[15] J.J. DO REGO SILVA, *Acoustic and elastic wave scattering using boundary elements*, Computational Mechanics Publications, Southampton – Boston 1994.

[16] E. SKUDRZYK, *The foundations of acoustics*, Springer-Verlag, Wien – New York 1971.

[17] W. WANG *et al.*, *A boundary integral approach for acoustic radiation of axisymmetric bodies with arbitrary boundary conditions valid for all wave number*, J.A.S.A., **101**, 3, 1468–1478 (1997).

[18] R. WYRZYKOWSKI, *Liniowa teoria pola akustycznego ośrodków gazowych*, WSP, Rzeszów 1972.

ARCHIVES OF ACOUSTICS
22, 4, 397–410 (1997)

THEORETICAL AND EXPERIMENTAL ANALYSIS OF THE BAND NOISE RADIATED FROM A HARD-WALLED CYLINDRICAL DUCT

A. SNAKOWSKA

Institute of Physics, Pedagogical University
(34-310 Rzeszów, Rejtana 16a, Poland)

H. IDCZAK

Institute of Telecommunication and Acoustics,
Wrocław Technical University,
(50-370 Wrocław, Wybrzeże Wyspiańskiego 27, Poland)

The paper presents, basing on the results obtained for the single tone and multitone excitations, the theory of the white noise propagation in and radiation from a cylindrical duct. The duct is assumed to be semi-infinite and hard walled, the excitation axisymmetrical and with no mean flow.

Solution of the wave equation with adequate boundary condition constitutes a base of the carried out analysis. It allows for propagation of certain number of wave modes, which cut-on frequencies are below the excitation frequency. Anyhow, when more than one mode are present the analysis of the sound field complicates, as it requires the knowledge of modes complex amplitudes.

To make any quantitative comparison between the theory and experiment possible two extra assumptions are incorporated into the theory: on the equipartition of the density of energy between all modes admissible at a given frequency and on their random phase. The second assumption results in the necessity of describing the acoustical field by means of the expected value, the variance and the standard deviation of the pressure, the intensity, the power output etc.

The paper contains the directivity characteristics of the pressure and the intensity and evaluation of the power output for the one third octave (tierce) band white noise.

1. Introduction

The aim of the presented paper is to extend the theory of sound wave propagating in and radiating from a circular duct on a case of narrow-band white noise excitation.

The theory of propagation of acoustic waves in a semi-infinite duct predicts that at a given frequency only some waves can propagate without damping [2, 3, 15]. The quantity which is the most convenient for investigations on this problem is the non-dimensional wavenumber, ka, being a product of the wave number k and the duct radius a, and so combining the wave frequency with the duct size. Apart from the plane wave which

propagates at any ka the occurrence of any higher mode is specified by the so-called cut-on frequency. Propagation of the plane wave or single higher mode, in a duct excited with a single tone signal has been considered by many authors, who applied the so-called time independent form of the velocity potential [11, 25, 26, 6, 8, 9, 13, 14, 22].

In the following we consider a case in which the duct is excited with a narrow-band white noise. That means that the velocity potential has to be written as a sum over all allowed modes and an integral over frequencies.

The theory of sound field inside and outside the duct has been a subject of our interest since long. Especially, we have analysed the far field of a single higher mode by means of the directivity patterns (pressure, intensity, power-gain function) [17]. Next step has been to derive the directivity characteristics for an arbitrary superposition of modes, what has led to a conclusion that directivity strongly depends on complex amplitudes i.e. on the modulae and phases of the excited modes [18].

That means that a set of numbers representing the modulae and phases has to be inserted into mathematical formulae to make any predictions about the radiation characteristics, the power output etc., or comparison with the experimental data possible.

To deal with these drawbacks the model composed of two assumptions [21] is proposed

— the total energy is shared in equal parts between all excited modes,

— phases are independent random variables with the uniform distribution in the range $[0, 2\pi]$.

The first assumption, often called "equal energy per mode" has been successfully applied by many authors [1, 14, 19, 21], the second assumption seems to be well physically justified – if there is no knowledge what exactly the phases are the best solution is to assume them being random [21].

2. Analysis technique and results

2.1. Mathematical background. Solution of the wave equation for the single tone excitation

Mathematical tools applied to obtain a solution of the problem are rather complicated and include the theory of two-valued analytical functions, application of the Green function in the cylindrical coordinates, the solution of the Wiener-Hopf integral equations by means of the factorisation method, the saddle point method etc., so there will be reminded only in short.

Consider the wave equation for the acoustic potential $\Delta\Phi(\mathbf{r}, t) = c^{-2}\partial_{tt}\Phi(\mathbf{r}, t)$, with adequate boundary condition given on the duct surface (Fig. 1) $v_{\mathrm{n}} = -\partial_{\mathrm{n}}\Phi|_{\Sigma} = 0$, and assume an axisymmetrical harmonic excitation of given frequency ω.

First, the solution of the wave equation for a single l mode propagating towards the outlet will be reminded – in cylindrical coordinates ϱ, φ, z, for inside of the duct [26]

$$\Phi_l(\omega, \varrho, z, t) = \left[\frac{J_0(\mu_l \varrho/a)}{J_0(\mu_l)} e^{-i\gamma_l z} + \sum_{n=0}^{N} R_{ln} \frac{J_0(\mu_n \varrho/a)}{J_0(\mu_n)} e^{i\gamma_n z}\right] e^{-i\omega t}, \tag{2.1}$$

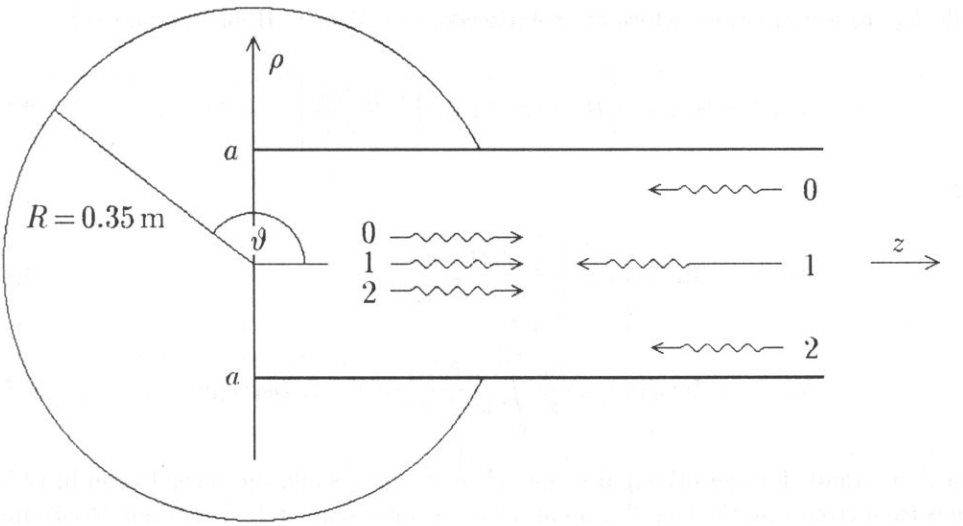

Fig. 1. Geometry of the problem.

and in spherical coordinates R, ϑ, φ, in the far field outside the duct [17]

$$\Phi_l(\omega, R, \vartheta, t) = d_l(\vartheta)\frac{e^{i(kR-\omega t)}}{R}. \tag{2.2}$$

The incident wave, l radial mode, described by the first factor in (2.1), propagates with the radial wave number $\gamma_l = \sqrt{(ka)^2 - \mu_l^2}/a$, where μ_l is the l-th zero of the Bessel function J_1. Terms under the summation sign represent waves appearing due to diffraction at the outlet, where R_{ln} is the reflection/transformation coefficient. The number of admissible modes depends on the dimensionless parameter ka, called also the non-dimensional wavenumber. The index of the highest mode, which propagates without attenuation fulfils the condition $\mu_N < ka < \mu_{N+1}$. For a duct of radius a the cut-on frequencies ω_l are equal to $\omega_l = c_0\mu_l/a$, where c_0 is the sound speed.

In the far field outside the duct the incident lth mode propagates as a spherical wave modified by the directivity function d_l, which in general is a function of R, ϑ. In the following we will concentrate on the infinite distance approximation ($kR \to \infty$), when the directivity function, derived by means of the saddle point method, is a function of only the angle ϑ [17] (Fig. 1)

$$d_l(\vartheta) = \frac{1}{2}ka\sin\vartheta J_1(ka\sin\vartheta)F_l(ka\cos\vartheta). \tag{2.3}$$

The method itself, successfully applied to many acoustical problems, is described in [12]. Mathematical considerations leading to (2.3), reported in [17, 22], especially deriving the $F_l(w)$ function, which in fact is the Fourier transform of the discontinuity of potential $\Phi(\varrho, z)|_{\varrho\to a+} - \Phi(\varrho, z)|_{\varrho\to a-}$ at the duct wall, are rather complicated.

Assuming a unit amplitude of the incident wave we obtain [17]

$$F_l(w) = \frac{L_+(\gamma_l)}{i(w+\gamma_l)L_-(w)}, \tag{2.4}$$

while $L_{\pm}(w)$ are functions which are solutions of the Wiener - Hopf equation [12]

$$L_{\pm}(w) = (k \pm w)\left[H_1^{(1)}(va)J_1(va)\prod_{i=1}^{N}\frac{\gamma_i \pm w}{\gamma_i \mp w}\right]^{1/2} e^{\pm\frac{1}{2}S(w)}, \tag{2.5}$$

and

$$\mathrm{X}(w) = \mathrm{Re}\,S(w) = \frac{1}{\pi}\mathrm{P}\int_{-k}^{k}\frac{\Omega(v'a)}{w'-w}\,dw', \tag{2.6}$$

$$\mathrm{Y}(w) = \mathrm{Im}\,S(w) = \frac{2w}{\pi}\int_{0}^{i\infty}\frac{\omega(v'a)}{w^2-w'^2}dw' + i\omega(va)\mathrm{sign}w. \tag{2.7}$$

P in (2.6) stands for the principal value, $w^2 + v^2 = k^2$, while the second term in (2.5) comes from circuiting the singular point $w' = \pm w$ on a semicircle. Functions $\Omega(va)$ and $\omega(va)$ are equal to

$$\Omega(va) = \arg H_1^{(1)}(va) + \pi/2\,, \tag{2.8}$$

$$\omega(va) = \Omega(va) - \Omega(\mu_n), \qquad \mu_n < va < \mu_{n+1}\,. \tag{2.9}$$

The $L_+(w)$ function for $w = \gamma_n$ exists only as a limited value for $w \to \gamma_n$ and is equal to

$$L_+(\gamma_l) = \begin{cases} 2k\left(\dfrac{-i}{\pi}\displaystyle\prod_{i=1}^{N}\frac{\gamma_i + k}{\gamma_i - k}\right)^{1/2} e^{\frac{1}{2}S(k)}, & l = 0, \\ \dfrac{2(k+\gamma_l)\gamma_l a}{\mu_l}\left(\dfrac{-i}{\pi}\displaystyle\prod_{\substack{l=1\\ i\neq l}}^{N}\frac{\gamma_i + \gamma_l}{\gamma_i - \gamma_l}\right)^{1/2} e^{\frac{1}{2}S(\gamma_l)}, & l \neq 0, \end{cases} \tag{2.10}$$

where $\gamma_0 = k$.

Because of mathematical complexity of the problem a set of numerical programs has been derived, which enables us to present the reflection coefficients, the directivity functions etc. graphically and to carry out a thorough analysis of the sound field of interest.

Previously we assumed a unit amplitude incident wave. As was mentioned before, the theory foresees and the experiments, in which the power spectra density [1] and the directivity characteristics [21] were measured, confirm excitation of all admissible modes. If N indicates the highest Bessel mode and A_l is a complex amplitude, we can write the potential in the form

$$\Phi = \sum_{l=0}^{N} A_l \Phi_l\,. \tag{2.11}$$

2.2. *The white noise excitation*

Basing on the results obtained for excitation with a fixed frequency [21] we will extend the formulae for the potential, the mean pressure and the intensity on the case of continues spectrum of frequencies.

For the white noise we obtain

$$\phi(\bar{r},t) = \int\limits_{\omega\in B} \phi(\omega,\bar{r},t)\,\varrho(\omega)\,d\omega\,, \tag{2.12}$$

where $\varrho(\omega)$ is the spectral density of energy and B is the band width. In the following we assume constant spectral density $\varrho(\omega) = 1$.

Thus, the acoustic pressure, $p = \varrho_0 \partial_t \Phi$, can be expressed as

$$p(\bar{r},t) = \int\limits_{\omega\in B} p(\omega,\bar{r},t)\,d\omega\,, \tag{2.13}$$

where

$$p(\omega,R,\vartheta,t) = \varrho_0\omega \sum_{l=0}^{N} A_l(\omega) d_l(\omega,R,\vartheta)\frac{e^{i(kR-\omega t-\pi/2)}}{R} = \sum_{l=0}^{N} P_l(\omega,R,\vartheta)e^{i(-\omega t+\theta_l)}\,, \tag{2.14}$$

is an extension of the formula for a single tone excitation [21].

The pressure real amplitude P_l and phase θ_l were expressed by the modulus and phase of the complex amplitude $A_l = |A_l|e^{i\phi_l}$:

$$P_l(\omega,R,\vartheta) = \frac{\varrho_0}{R}\omega|A_l(\omega)|d_l(\omega,R,\vartheta), \qquad \theta_l = kR + \phi_l - \pi/2\,. \tag{2.15}$$

According to the first assumption, for each frequency ω the modulae of amplitudes are related as follows

$$\left|\frac{A_m(\omega)}{A_l(\omega)}\right| = \sqrt{\frac{\gamma_l(\omega)}{\gamma_m(\omega)}}\,. \tag{2.16}$$

According to the second assumption, for each frequency, phases are stochastically independent random variables.

Below presented formulae are valid in an infinite distance approximation ($kR \to \infty$). To indicate this the variable R is omitted and we write, for example, $I(\vartheta)$ instead of $I(R,\vartheta)$

$$I(\vartheta) = \frac{1}{2\varrho_0 c}\int\limits_{\omega\in B}\left[\sum_{l=0}^{N(\omega)} P_l^2 + 2\sum_{\substack{l,m\\ l<m}}^{N(\omega)} P_l\,P_m\cos(\phi_l-\phi_m)\right]d\omega\,. \tag{2.17}$$

Note that the intensity depends on the phase differences between modes of the same frequency ω.

Note that the same results can be achieved exchanging operation of summation over some discrete frequencies [20] for integration over a certain frequency band.

For constant power spectral density, choosing the amplitude of the principal mode (plane wave, $m = 0$) at the mid-frequency ω_0 as the reference amplitude we obtain

$$|A_0(\omega)|^2 = \frac{N(\omega_0)+1}{N(\omega)+1}\left(\frac{\omega_0}{\omega}\right)^2 |A_0(\omega_0)|^2. \tag{2.18}$$

As was mentioned before, the second assumption on the random phase results in the necessity of carrying out the field analysis by means of the expected value $E(\,)$, the standard deviation $\varepsilon(\,)$ etc. Below, their final formulae for the intensity $I(\vartheta)$, the intensity directivity function $s^I(\vartheta)$ and the power output $\mathcal{P}$, calculated basing on the results obtained for multifrequency excitation [20] are presented.

The expected value and the variance [10] of the sound intensity are equal to, respectively

$$E(I(\vartheta)) = \frac{1}{2\varrho_0 c}\int\limits_{\omega\in B}\sum_{l=0}^{N(\omega)} P_l^2\, d\omega \tag{2.19}$$

and

$$\operatorname{var}(I(\vartheta)) = \frac{1}{2(\varrho_0 c)^2}\int\limits_{\omega\in B}\sum_{\substack{l,m\\ l<m}}^{N(\omega)} (P_l\, P_m)^2\, d\omega\,. \tag{2.20}$$

Theoretical results were compared with experimental data for the one third octave (tierce) white noise with the mid-frequencies $f_0 = 8\,\mathrm{kHz}$ and $f_0 = 10\,\mathrm{kHz}$.

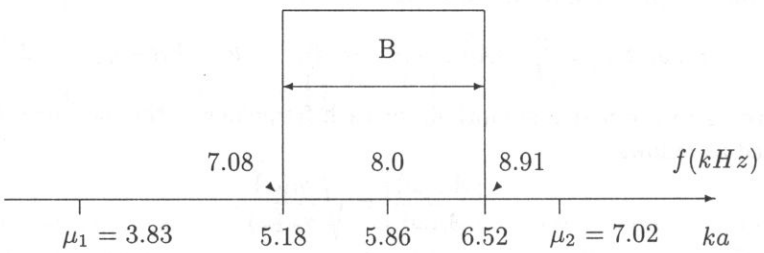

Fig. 2. Third-octave passband in the first experiment. Note constant density of energy distribution.

The first band, Fig. 2, covers the range of frequencies from 7.08 kHz to 8.91 kHz, which for considered duct 0.04 m in radius corresponds to the values of the dimensionless wavenumber ka from 5.18 to 6.52, so the number of modes remains constant, $N(\omega) = 2$, in the whole band. The second band, Fig. 3, lowest and uppest frequencies are equal to 8.91 kHz and 11.2 kHz, so the ka parameter changes within the range $[6.52 \div 8.22]$, crossing the third root, $\mu_2 = 7.02$, of he Bessel function J_1. Thus, the number of modes excited in the duct changes within the band being equal $N(\omega) = 2$ for $ka \leq \mu_2$ and $N(\omega) = 3$ for $ka > \mu_2$.

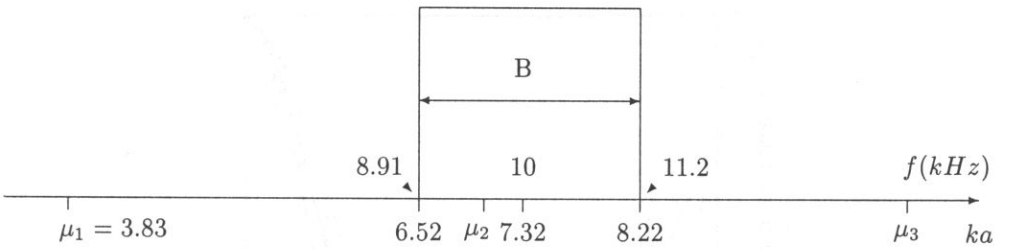

Fig. 3. Third-octave passband in the second experiment.

3. Physical quantities describing the far field

3.1. The intensity and the pressure directivity characteristics

The relative intensity directivity function was defined [20] as the intensity in a given direction referred to its expected value on the axis (the forward radiation) $s^I(\vartheta) = I(\vartheta)/E(I(\pi))$.

The next two formulae present its expected value and the standard deviation [10, 21]

$$E(s^I(\vartheta)) = \frac{E(I(\vartheta))}{E(I(\pi))} = \frac{\int\limits_{\omega\in B} \sum\limits_{l=0}^{N(\omega)} P_l^2(\omega,\vartheta)\, d\omega}{\int\limits_{\omega\in B} \sum\limits_{l=0}^{N(\omega)} P_l^2(\omega,\pi)\, d\omega}, \tag{3.1}$$

$$\varepsilon(s^I(\vartheta)) = \frac{\sqrt{\mathrm{var}(I(\vartheta))}}{E(I(\vartheta))} = \frac{\sqrt{2\int\limits_{\omega\in B} \sum\limits_{\substack{l,m \\ l<m}}^{N(\omega)} (P_l\, P_m)^2\, d\omega}}{\int\limits_{\omega\in B} \sum\limits_{l=0}^{N(\omega)} P_l^2\, d\omega}. \tag{3.2}$$

Defining the pressure directivity function as the pressure in a given direction referred to its expected value on the axis (the forward radiation) $s^p(\vartheta) = p_{rms}(\vartheta)/E(p_{rms}(\pi))$, and basing on considerations enclosed in [21] we obtain

$$E(s^p(\vartheta)) \cong \sqrt{E(s^I(\vartheta))}, \tag{3.3}$$

$$\varepsilon(s^p(\vartheta)) \cong \frac{1}{2}\varepsilon(s^I(\vartheta)). \tag{3.4}$$

Theoretical results, calculated with the help of the presented model assuming additionally equipartition of energy between the modes composing the incident wave, and their phases constituting, for each frequency, a set of mutually independent random variables, compared with experimental data are presented on graphs.

Analysing Figs. 4–7 one sees that the accordance between theory and experiment is quite good for the forward radiation, when rays bent from the axis of no more than 30 deg

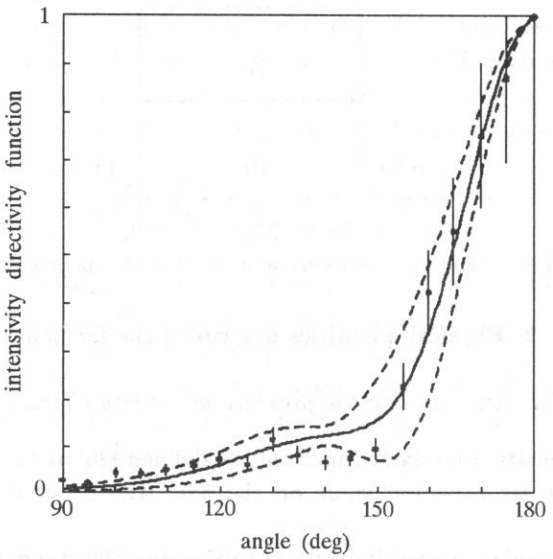

Fig. 4. Relative intensity directivity function $s^I(\vartheta)$ for the third-octave white noise band excitation with nominal centre frequency $f_0 = 8\,\text{kHz}$). The expected value $E(s^I(\vartheta))$ (continuous line), values of $E(s^I(\vartheta))(1 \pm \varepsilon)$, (dashed lines) ε being the standard deviation. Stars indicate the experimental data and bars the measurement errors.

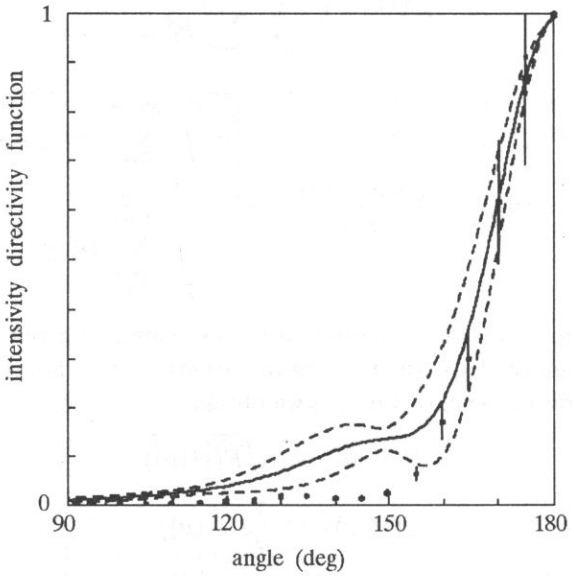

Fig. 5. Same as Fig. 4, but for centre frequency $f_0 = 10\,\text{kHz}$.

are considered (range 150 – 180 deg on drawings, note that angle 180 deg corresponds to the forward radiation) and deteriorates for smaller angles. The last effect is especially visible on Figs. 5 and 7, that is for the band with the centre frequency equal to 10 kHz,

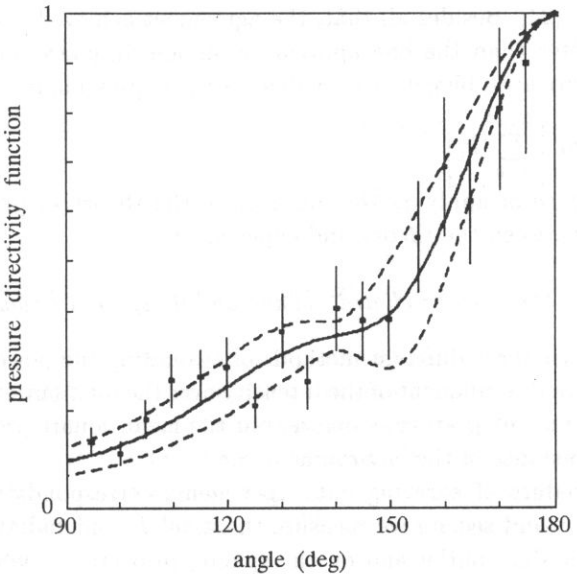

Fig. 6. Relative pressure directivity function $s^p(\vartheta)$ for the third-octave white noise band excitation with nominal centre frequency $f_0 = 10\,\text{kHz}$. The expected value $E(s^p(\vartheta))$ (continuous line), values of $E(s^p(\vartheta))(1 \pm \varepsilon)$, (dashed lines) ε being the standard deviation. Stars indicate the experimental data and bars the measurement errors.

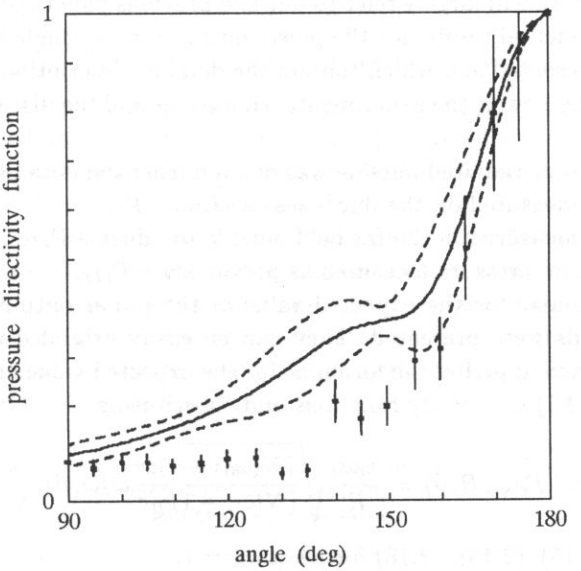

Fig. 7. Same as Fig. 6, but for centre frequency $f_0 = 10\,\text{kHz}$.

theoretical predictions exceeding experimental data. It may stem from the tendency of the physical system to occupy the state of the lowest possible energy and the fact, that the directivity characteristic representing the most probable state lies below the line of

the expected value [24]. Besides all that, the agreement achieved assuming the random phase is much better than the one applying all-modes-in-phase model, for which the theoretical values are even bigger. It is evident as the expression in bracket in Eq. (2.17) takes then the form $\left[\sum_{l=0}^{N(\omega)} P_l\right]^2$.

The inconvenience of applying the methods of the theory of probability results in better agreement between the theory and experiment.

3.2. The power radiated outside and its space distribution

There are at least three different methods of evaluating the power radiated outside: integrating the normal component of the intensity over the duct outlet or over a sphere in the far field outside or integrating as before, but the mean square pressure p_{rms}^2 divided by the specific impedance of the environment $\varrho_0 c$.

A certain procedure of carrying out experiments corresponds to each theoretical method. In the first and second we measure the axial I_z and radial I_R components of the intensity on the duct outlet and on the sphere, respectively, while in the third we measure the mean pressure p_{rms} on the sphere in the far field.

Because of assumed random phases we should compare the experimental data with the expected value of the power output and the measurement error with the standard deviation.

In the following we will largely refer to our two previous papers [19, 20] in which theoretical and experimental results for the power output for the single tone and multitone excitations were presented and which contain the detailed description of the three methods of evaluating the power, the experimental conditions and the discussion of measuring errors.

In short, the power radiated outside was derived from the data of
- the intensity measured on the duct cross-section – $\mathcal{P}_I$,
- the intensity measured in the far field outside the duct – $\mathcal{P}_{II}$,
- the mean square pressure measured as previously – $\mathcal{P}_{III}$.

In [20] the formulae for the expected value of the power output corresponding to these three methods were presented. They can be easily extended on the case of the white noise excitation applying the formulae for the expected value of the pressure (3.3) and the intensity (3.1) directivity functions and substituting

$$P_l(\omega, R, \vartheta) = \frac{\varrho_0 \omega_0}{R} \sqrt{\frac{(N(\omega_0)+1)\omega}{(N(\omega)+1)\gamma_l c}}\, d_l(\omega, \vartheta), \tag{3.5}$$

calculated from (2.15)–(2.16), (2.18) for $|A_0(\omega_0)| = 1$.

Focusing on methods applying the far–field relations, which are of our main interest, two formulae for deriving the power output will be reminded

$$E(\mathcal{P}_{II}) = 2\pi R^2 E(I(\pi)) \int_0^{\pi} E(s^{(I)}(\vartheta)) \sin\vartheta \, d\vartheta\,, \tag{3.6}$$

$$E(\mathcal{P}_{III}) = \frac{2\pi R^2}{\varrho_0 c} E(p^2_{rms}(\pi)) \int_0^{\pi} E(s^{(p)}(\vartheta))^2 \sin\vartheta \, d\vartheta \,. \tag{3.7}$$

The standard deviation is calculated according to formula $\varepsilon(\mathcal{P}) = \sqrt{\mathrm{var}\mathcal{P}}/E(\mathcal{P})$, where

$$\mathrm{var}(\mathcal{P}) = E(\mathcal{P}^2) - E^2(\mathcal{P}) = 2\left(\frac{\pi R^2}{\varrho_0 c}\right)^2 \int_{\omega\in B} \sum_{\substack{l,m \\ l<m}}^{N(\omega)} \left(\int_0^{\pi} P_l \, P_m \sin\vartheta \, d\vartheta \right)^2 , \tag{3.8}$$

exchanging in the expression for the variance [20] summation for integration over frequencies.

Another difficulty which arises when comparing theory with experiment comes from the fact that the assumptions of the model allow only for determining the relative amplitudes of modes and thus we have to incorporate one experimental data into the theoretical formulae to derive the so-called scale factor. In the presented analysis a point on the axis ($\vartheta = 180°$) served as a scaling point, so we substituted theoretical value $E(I(\pi))$ by $\widetilde{I}(\pi)$ and $E(p^2_{rms}(\pi))$ by $\widetilde{p}^2_{rms}(\pi)$. Tilde over a symbol means, in this paper, the experimental value.

Discussion of errors carried in [19, 20], which results are valid also in the considered case, led to expressions for the measuring error and the method uncertainty (the last stemmed from the assumption on random phase) and allowed for deriving a criterion of correctness of the proposed model [19]

$$\Delta L_{\mathcal{P}} \leq L_{\delta} \,, \tag{3.9}$$

where $\Delta L_{\mathcal{P}} = \left| 10 \log E(\mathcal{P}')/\widetilde{\mathcal{P}} \right|$ is the method uncertainty, while the total error of the experiment, in decibels, is equal to $L_{\delta} = -10\log(1 - \delta - \delta_{\Delta S}/1 + \varepsilon_{\mathcal{P}} + \delta)$, where $E(\mathcal{P}')$ denotes the expected value of the power obtained by replacing the theoretical value $E(I(\pi))$ by the adequate experimental data $\widetilde{I}(\pi)$, $\widetilde{\mathcal{P}}$ denotes measured power, δ – error in the intensity or the mean square pressure data, while $\delta_{\Delta S}$ denotes error in surface estimation when approximating the integral by a finite sum. The relative error in the pressure and the intensity measuring data is assumed to be the same in all measuring data, not exceeding 0.2, same as the maximum of the surface error.

The experimental results for the power radiated outside, for the third-octave white noiseband with nominal centre frequency $f_0 = 8\,\mathrm{kHz}$ and $f_0 = 10\,\mathrm{kHz}$, obtained by means of three methods are depicted in Table 1.

Table 1. Values of the sound power level $L_{\mathcal{P}}$ measured by means of the three methods, estimated from the theory $L_{E(\mathcal{P}')}$, the uncertainty $\Delta L_{\mathcal{P}'}$ resulting from the applied theoretical model and the measuring error L_{δ}.

nominal centre frequency	experimental			theoretical		uncertainty		error
f_0 (kHz)	$L_{\mathcal{P}_I}$ (dB)	$L_{\mathcal{P}_{II}}$ (dB)	$L_{\mathcal{P}_{III}}$ (dB)	$L_{E(\mathcal{P}'_{II})}$ (dB)	$L_{E(\mathcal{P}'_{III})}$ (dB)	$\Delta L_{\mathcal{P}_{II}}$ (dB)	$\Delta L_{\mathcal{P}_{III}}$ (dB)	$L_{\delta_{II,III}}$ (dB)
8.0	78.9	80.0	77.6	80.1	77.2	0.1	0.4	4.1
10.0	81.0	80.1	76.7	83.5	80.2	3.4	3.5	4.0

The Table includes only the method uncertainty $\Delta L_{\mathcal{P}}$ and the measuring error L_δ for measurements taken in the far field because the upper frequencies became too big for the used microphone probe (the two 1/2 inches microphone sound intensity probe type face to face with the 6 mm spacer in between) what affected the experimental error.

From the results presented in the above table we conclude that the relation $\Delta L_{\mathcal{P}} \leq L_\delta$ is fulfilled for both tierces and for all measuring methods. As the experimental data fulfil the criterion of correctness we can say that at least they do not contradict the assumptions. Similar results were obtained for the single tone [19] and the multitone [20] excitation.

Many applications demand the knowledge of the space distributions of the energy radiated from the duct outlet, which is described by the power-gain function, $\mathcal{G}(\vartheta, \phi)$, referring the amount of energy radiated into a certain solid angle to the total energy radiated outside.

For axisymmetrical excitation, according to the definition, we obtain

$$\mathcal{G}(\vartheta) = 4\pi R^2 \frac{I(\vartheta)}{\mathcal{P}(\text{rad})}. \tag{3.10}$$

Experimental results versus the angle ϑ are presented in Table 2, pointing at a strong radiation in the vicinity of the axis.

Table 2. Experimental results for the power-gain function versus angle ϑ on a front hemisphere, as data for backward radiation were negligible small.

angle deg	nominal centre frequency $f_0 = 8$ kHz	nominal centre frequency $f_0 = 10$ kHz
ϑ	$\mathcal{G}$	$\mathcal{G}$
90	0.50	0.26
95	0.43	0.15
100	0.81	0.18
105	0.81	0.17
110	0.96	0.17
115	1.08	0.24
120	1.38	0.38
125	1.17	0.49
130	2.15	0.96
135	1.54	1.01
140	1.23	0.80
145	1.43	0.81
150	1.78	1.34
155	4.23	3.36
160	7.84	8.67
165	10.22	15.06
170	13.95	30.86
175	16.19	43.41
180	18.59	49.84

The integrand of $\mathcal{G}(\vartheta, \phi)$ over the entire solid angle is equal to 4π, so the integrand of (3.7) over the angle ϑ is equal to 2. The results obtained from the experimental data, when replacing integration by summation, are presented in Table 3 and show very good agreement with the theory. If the experimental data fulfil this condition we can say that they do not contradict the assumptions.

Table 3. Experimental results for the power-gain function, when the theory predicts the value equal to 2.

nominal centre frequency f_0 [kHz]	$\sum G_I(\vartheta) \sin\vartheta \, \Delta\vartheta$
8.0	1.983
10.0	1.953

4. Conclusions and possible applications

The paper presents a certain model for qualitative and also quantitative description of the narrow band sound field radiated from axially excited cylindrical duct in the absence of the mean flow. The last two assumptions were set because of some limitations of the experimental set-up to make comparison with the experiment possible. Nevertheless the results can be generalised by solving the wave equation with sources. The starting formulae were derived for the semi-infinite duct and take into account diffraction phenomena at the open end. Thus they are valid for the duct long in comparison to the wave length and with only one outlet – provided at the other end with sound absorbing material. These features are found in many duct-like devices, to mention only heating and ventilation systems, cars and planes exhausts, factory chimneys etc., what makes investigation on the problem interesting from both, theoretical and practical, points of view. In the light of the above we expect many potential applications in problems requiring the knowledge of the directivity characteristics or the power output.

The experimental results presented in the paper show that good agreement between the theory and experiment has been obtained, what in a way verifies the model we proposed. Considering the directivity characteristics, the random phase assumption approaches theoretical predictions to measurement data much better than commonly used all-modes-in-phase assumption.

Especially good agreement was obtained for the power output, which we found very promising in applying the circular duct as a reference source. As was shown in Table 1 the power estimated by means of the model and single measurement on the axis in the far field differs from the one calculated following one of the well known procedures described above less than the experimental error. There from origins the idea to estimate the power output basing at only one measurement on the axis.

The paper is considered to be a step forward in deriving a procedure of evaluating, or at least estimating, the power radiated outside measuring the pressure or the intensity in only one point. It needs preparation of a set of numerical programs computing the expected value and the standard deviation along the formulae (3.6), (3.8), (2.15), but we hope to present it in the next paper.

References

[1] U. BOLLETER, M.J. CROCKER, *Theory and measurement of modal spectra in hard-walled cylindrical duct*, J. Acoust. Soc. Am., **51**, 1439–1447 (1972).

[2] P.E. DOAK, *Excitation, transmission and radiation of sound from source distributions in hard-walled ducts of finite length. I. The effects of duct cross-section geometry and source distribution space-time pattern*, J. Sound Vib., **31**, 1, 1–72 (1973).

[3] P.E. DOAK, *Excitation, transmission and radiation of sound from source distributions in hard-walled ducts of finite length. II. The effects of duct length*, J. Sound Vib., **31**, 2, 137–174 (1973).

[4] DUHAMEL, *Improvement of noise barrier efficiency by active control*, Acta Acustica, **3**, 1, 25–35 (1995).

[5] S.J. ELLIOT, P. JOSEPH, P.A. NELSON, M.E. JOHNSON, *Power output minimization and power absorption in the active control of sound*, J. Acoust. Soc. Am., **90**, 5, 2501–2512 (1991).

[6] G.F. HOMICZ, J.A. LORDI, *A note on the radiative directivity patterns of duct acoustic modes*, J. Sound and Vib., **41**, 283–290 (1975).

[7] M.E. JOHNSON, S.J. ELLIOT, *Measurement of acoustic power output in the active control of sound*, J. Acoust. Soc. Am., **93**, 1453–1459 (1993).

[8] G.W. JOHNSTON, K. OGIMOTO, *Sound radiation from a finite length unflanged circular duct with uniform axial flow. I. Theoretical analysis*, J. Acoust. Soc. Am., **68**, 1858–1870 (1980).

[9] G.W. JOHNSTON, K. OGIMOTO, *Sound radiation from a finite length unflanged circular duct with uniform axial flow. II. Computed radiation characteristics*, J. Acoust. Soc. Am., **68**, 1871–1883 (1980).

[10] W. LEDERMANN, *Handbook of applicable mathematics*, Wiley & Sons, N. York 1980.

[11] H. LEVINE, J. SCHWINGER, *On the radiation of sound from an unflanged circular pipe*, Phys. Rev., **73**, 383–406 (1948).

[12] B. NOBLE, *Methods based on the Wiener–Hopf technique for the solution of partial differential equations*, Pergamon Press, London – New York 1958.

[13] A.D. RAWLINS, *Radiation of sound from an unflanged rigid cylindrical duct with an acoustically absorbing internal surface*, Proc. R. Soc. London, **A 361**, 65–91 (1978).

[14] E.J. RICE, *Multi-modal far-field acoustic radiation pattern using mode cut-off ratio*, AIAA Journal, **16**, 906–911 (1978).

[15] E. SKUDRZYK, *The foundations of acoustics*, Springer-Verlag, Wien–New York 1971.

[16] M.A. SWINBANKS, *The active control of sound propagation in long ducts*, J. Sound Vib., **27**, 3, 411–436 (1973).

[17] A. SNAKOWSKA, *The acoustic far field of an arbitrary Bessel mode radiating from a semi-infinite unflanged cylindrical wave-guide*, Acustica, **77**, 53–62 (1992).

[18] A. SNAKOWSKA, *Directivity patterns of the acoustic field radiated from a semi-infinite unflanged hard walled circular duct*, Journal de Physique III, 2, C1-653–656 (1992).

[19] A. SNAKOWSKA, H. IDCZAK, *The acoustic power radiated from the outlet of a hard-walled circular duct – theory and measurement*, Acta Acustica, **3**, 119–128 (1995).

[20] A. SNAKOWSKA, H. IDCZAK, *Prediction of multitone sound radiation from a circular duct*, Acustica-Acta Acustica, **83**, 955–962 (1997).

[21] A. SNAKOWSKA, H. IDCZAK, B. BOGUSZ, *Modal anlysis of the acoustic field radiated from an unflanged cylindrical duct – theory and measurement*, Acustica-Acta Acustica, **82**, 2, (1996).

[22] A. SNAKOWSKA, R. WYRZYKOWSKI, *Calculation of the acoustical field of a semi-infinite cylindrical wave-guide by means of the Green function expressed in cylindrical coordinates*, Archives of Acoustics, **11**, 261–285 (1986).

[23] A. SNAKOWSKA, R. WYRZYKOWSKI, *Impedance of the semi-infinite unbaffled cylindrical waves quide outlet*, Archives of Acoustics, **13**, 1-2 (1988).

[24] J.K. SNAKOWSKI, *Private communication.*

[25] L.A. VAJNSHTEJN, *The theory of sound waves in open tubes*, Res. Rep. No. EM– 63, Inst. Math. Sci., N. Y. U., 87–116 (1954).

[26] L.A. WEINSTEIN, *The theory of diffraction and the factorization method (Generalised Wiener-Hopf technique)*, Golem Press, Boulder, Colorado 1969.

[27] A.C. ZANDER, C.H. HANSEN, *Active control of higher-order acoustic modes in ducts*, J. Acoust. Soc. Am., **92**, 244–257 (1992).

ARCHIVES OF ACOUSTICS
22, 4, 411–421 (1997)

PROPAGATION OF SOUND WAVES OF FINITE AMPLITUDE IN A HORN AT FREQUENCIES BELOW THE CUT-OFF FREQUENCY

T. ZAMORSKI

Institute of Physics, Pedagogical University of Rzeszów,
Department of Acoustics
(35-310 Rzeszów, ul. Rejtana 16a, Poland)

An investigation of the wave of finite amplitude in hyperbolic horn with annular cross-section is described. The fluid in the horn is assumed to be nondissipative. The equation of the sound wave propagation in the horn is solved for the case of frequencies below the cut-off frequency. The analysis is qiven in Lagrangian coordinates.

1. Introduction

The problem of propagation of sound waves with finite amplitude in horns at frequencies above the cut-off frequency was described in the papers [4, 10]. In this work the case where the input wave has a frequency below the cut-off frequency but her harmonics have frequencies above that of cut-off is discussed. Harmonics waves are then favoured in propagation with respect to the fundamental and they can be amplified. This problem is considered for hyperbolic horns with annular cross-section which are frequently applied [2, 5–8, 10].

2. Analysis of the propagation equation of wave with finite amplitude for excitation frequencies below the cut-off frequency

The equation of propagation of a wave with finite amplitude in a horn with arbitrary shape has the following form [4]:

$$\ddot{\xi} = \frac{c^2}{\left[\dfrac{S(x)}{S(a)}\right]^{\gamma-1}(1+\xi')^{\gamma}} \left\{ \frac{\dfrac{\partial}{\partial a}\left[\dfrac{S(x)}{S(a)}\right]}{\dfrac{S(x)}{S(a)}} + \frac{\xi''}{1+\xi'} \right\}, \tag{2.1}$$

where ξ is the displacement of the acoustic particle, S is the cross-sectional area of the horn, c is the sound velocity for small amplitudes, a is Lagrangian coordinate, γ is the adiabatic exponent, $x = a + \xi$ is Eulerian coordinate. Dots and commas in equation

(2.1) denote differentiation with respect to time and to the coordinate a, respectively. Equation (2.1) was formulated under the assumption that the horn is filled by a lossless gaseous medium. In the derivation of equation (2.1) the nonlinearity of the equation of continuity, Euler's equation and adiabate equation was taken into account [4].

The following dependence between the cross-sectional area and position of the horn's axis determines the family of hyperbolic horns with annular cross-section [8]:

$$S = \frac{S_0}{\cosh \varepsilon} \cdot \cosh(mx + \varepsilon), \tag{2.2}$$

where $S_0 = \pi d_0 h_0$ (Fig. 1) is the area at the throat, m is the coefficient of flare of the horn and ε is the coefficient of shape of the walls; $\varepsilon \in [0, \infty)$.

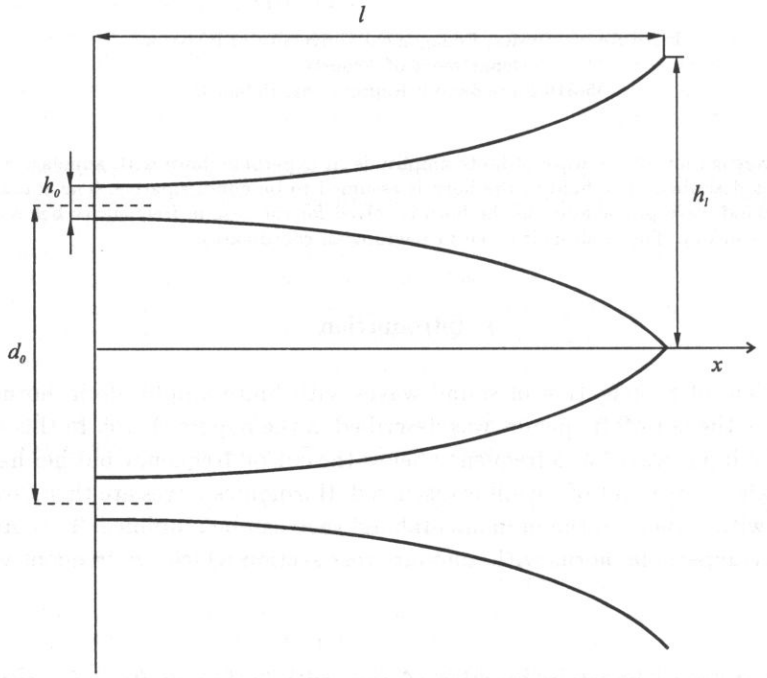

Fig. 1. The longitudinal section of a horn defined by (2.2).

Let us assume that there are no refflection at the mouth of a horn and that a hypothetical annular piston vibrating with harmonical motion is the source of waves at the throat $a = 0$:

$$\xi(0, t) = k^{-1} A \cos \omega t, \tag{2.3}$$

where k is the wave number, ω is the pulsation and t is time. The dimensionless amplitude $A = 2\pi M$, where M is the Mach acoustic number [11].

It is known [10, 11] that even for relatively high intensity of the sound we have $A \ll 1$. Therefore the displacement ξ of the acoustic particle has the form of a power series of the amplitude A:

$$\xi(a, t) = k^{-1} \left[A \cdot \varphi_1(a, t) + A^2 \cdot \varphi_2(a, t) + \ldots \right], \tag{2.4}$$

where $\varphi_1(a,t)$, $\varphi_2(a,t),\ldots$ corresponds to succesive harmonics. The functions $\varphi_1(a,t)$, $\varphi_2(a,t),\ldots$ must reduce for $a=0$ to

$$\begin{aligned}\varphi_1(0,t) &= \text{const},\\ \varphi_2(0,t) &= \varphi_3(0,t)=\ldots=0.\end{aligned} \tag{2.5}$$

In the case of hyperbolic horns with annular cross-section the functions $\varphi_1(a,t)$, $\varphi_2(a,t)$ fulfil the following equations [10]:

$$\varphi_1'' + m\left[\operatorname{tgh}(ma+\varepsilon)\right]\varphi_1' + m^2\left[1-\operatorname{tgh}^2(ma+\varepsilon)\right]\varphi_1 - \frac{1}{c^2}\ddot{\varphi}_1 = 0, \tag{2.6}$$

$$\varphi_2'' + m\left[\operatorname{tgh}(ma+\varepsilon)\right]\varphi_2' + m^2\left[1-\operatorname{tgh}^2(ma+\varepsilon)\right]\varphi_2 - \frac{1}{c^2}\ddot{\varphi}_2 = \psi(a,t), \tag{2.7}$$

where

$$\begin{aligned}\psi(a,t) = \varphi_1\ddot{\varphi}_1\frac{m(\gamma-1)}{kc^2}\operatorname{tgh}(ma+\varepsilon) + \varphi_1'\ddot{\varphi}_1\frac{\gamma}{kc^2} + \frac{\varphi_1'\varphi_1''}{k}\\ + \varphi_1^2\frac{m^3\operatorname{tgh}(ma+\varepsilon)\left[1-\operatorname{tgh}^2(ma+\varepsilon)\right]}{k}\\ - \varphi_1\varphi_1'\frac{m^2\left[1-\operatorname{tgh}^2(ma+\varepsilon)\right]}{k}.\end{aligned} \tag{2.8}$$

Substituting to equation (2.6)

$$\varphi_1(a,t) = \phi_1(a)\cdot e^{i\omega t} \tag{2.9}$$

we obtain the equation of the first harmonic wave:

$$\phi_1'' + m\left[\operatorname{tgh}(ma+\varepsilon)\right]\phi_1' + \left[\frac{m^2}{\cosh^2(ma+\varepsilon)} + k^2\right]\phi_1 = 0. \tag{2.10}$$

For frequencies above the cut-off frequency the solution of this equation is [10]:

$$\phi_1(a)\frac{B_1}{\sqrt{\cosh(ma+\varepsilon)}}e^{i\overline{K}(ma+\varepsilon)} + \frac{B_2}{\sqrt{\cosh(ma+\varepsilon)}}e^{-i\overline{K}(ma+\varepsilon)}, \tag{2.11}$$

where B_1 and B_2 are constants. $\overline{K}$ can be presented in the following form:

$$\overline{K} = \left\{k^2m^{-2} - \frac{1}{4} + \frac{3}{ml}\left[\operatorname{tgh}\varepsilon - \operatorname{tgh}(ml+\varepsilon)\right]\right\}^{1/2}. \tag{2.12}$$

Here l is the length of the horn (Fig. 1).

In the case of frequencies below the cut-off frequency $\overline{K} = -i\bar{\chi}$ [9] and the solution of equation (2.10) can be presented in the form

$$\phi_1(a) = \frac{B_1}{\sqrt{\cosh(ma+\varepsilon)}}e^{\bar{\chi}(ma+\varepsilon)} + \frac{B_2}{\sqrt{\cosh(ma+\varepsilon)}}e^{-\bar{\chi}(ma+\varepsilon)}, \tag{2.13}$$

where

$$\bar{\chi} = \left\{\frac{1}{4} - k^2m^{-2} - \frac{3}{4ml}\left[\operatorname{tgh}\varepsilon - \operatorname{tgh}(ml+\varepsilon)\right]\right\}^{1/2}. \tag{2.14}$$

Subsequently, taking into account the formula (2.9) and considering only the real part of the solution, the following equation can be obtained for the wave propagating from the inlet to the outlet:

$$\varphi_1(a,t) = \frac{B_3 e^{-\bar{\chi}(ma+\varepsilon)}}{\sqrt{\cosh(ma+\varepsilon)}} \cos\omega t - \frac{B_4 e^{-\bar{\chi}(ma+\varepsilon)}}{\sqrt{\cosh(ma+\varepsilon)}} \sin\omega t . \tag{2.15}$$

The constants B_3 and B_4 can be determined from the boundary condition (2.5):

$$B_3 = \sqrt{\cosh\varepsilon}\, e^{\bar{\chi}\varepsilon} , \qquad B_4 = 0 \tag{2.16}$$

and the formula (2.15) may now be written

$$\varphi_1(a,t) = \sqrt{\frac{\cosh\varepsilon}{\cosh(ma+\varepsilon)}} \cdot e^{-\bar{\chi}ma} \cdot \cos\omega t . \tag{2.17}$$

With the help of (2.17), the right-hand side of (2.7) can be presented as follows:

$$\psi = \sigma(a)\,[1 + \cos 2\omega t] , \tag{2.18}$$

where

$$\sigma(a) = \frac{e^{-2\bar{\chi}ma}\cosh\varepsilon}{4\cosh(ma+\varepsilon)} \Big[D_1 \operatorname{tgh}^3(ma+\varepsilon) + D_2 \operatorname{tgh}^2(ma+\varepsilon) + D_3 \operatorname{tgh}(ma+\varepsilon) + D_4 \Big] \tag{2.19}$$

while

$$\begin{aligned} D_1 &= -\frac{15m^3}{4k} , \qquad D_2 = -\frac{9\bar{\chi}m^3}{2k} , \\ D_3 &= \frac{m^3(7-6\bar{\chi}^2)}{2k} - mk(\gamma-2), \\ D_4 &= 2m\gamma k\bar{\chi} + \frac{m^3(3\bar{\chi}-2\bar{\chi}^3)}{k} . \end{aligned} \tag{2.20}$$

The term $\psi(a,t)$ is a periodical function of time with pulsation 2ω. Therefore the function $\varphi_2(a,t)$, as an integral of equation (2.7), has also pulsation 2ω. The function $\varphi_2(a,t)$, which corresponds to second harmonic is a sum [3]:

$$\varphi_2(a,t) = \varphi_{21}(a,t) + \varphi_{22}(a,t). \tag{2.21}$$

The component $\varphi_{21}(a,t)$ is the general solution of a homogeneous equation coupled with equation (2.7). In the case where the frequency of the second-order harmonic is above the cut-off frequency, the function $\varphi_{21}(a,t)$ has a form similar to (2.11):

$$\varphi_{21} = \frac{C_1}{\sqrt{\cosh(ma+\varepsilon)}} \cos\left[2\omega t - \overline{K}_1(ma+\varepsilon)\right] - \frac{C_2}{\sqrt{\cosh(ma+\varepsilon)}} \sin\left[2\omega t - \overline{K}_1(ma+\varepsilon)\right] , \tag{2.22}$$

where

$$\overline{K}_1 = \left\{ 4k^2 m^{-2} - \frac{1}{4} + \frac{3}{4ml} \left[\operatorname{tgh} \varepsilon - \operatorname{tgh}(ml + \varepsilon) \right] \right\}^{1/2} . \tag{2.23}$$

The component $\varphi_{22}(a,t)$ is the particular solution of the equation (2.7) and has a form similar to the term $\psi(a,t)$ (2.18):

$$\varphi_{22}(a,t) = g(a) + f(a) \cos 2\omega t . \tag{2.24}$$

Introducing (2.24) into equation (2.7) we obtain equations for the functions $g(a)$ and $f(a)$:

$$g''(a) + m \left[\operatorname{tgh}(ma + \varepsilon) \right] g'(a) + \frac{m^2}{\cosh^2(ma + \varepsilon)} g(a) = \sigma(a), \tag{2.25}$$

$$f''(a) + m \left[\operatorname{tgh}(ma + \varepsilon) \right] f'(a) + \left[\frac{m^2}{\cosh^2(ma + \varepsilon)} + 4k^2 \right] f(a) = \sigma(a). \tag{2.26}$$

The solution of the equation (2.25) can be presented in the following form [3]:

$$g(a) = g_2(a) \int \sigma(a)\, da - \frac{1}{m} g_1(a) \int \sigma(a) \cdot \sinh(ma + \varepsilon)\, da + C_1 g_1(a) + C_2 g_2(a) , \tag{2.27}$$

where

$$g_1(a) = \frac{1}{\cosh(ma + \varepsilon)} , \tag{2.28}$$

$$g_2(a) = \frac{1}{m} \operatorname{tgh}(ma + \varepsilon). \tag{2.29}$$

The solution of the equation (2.26) is expressed by

$$f(a) = f_2(a) \int \frac{f_1(a)\sigma(a)}{W(a)}\, da - f_1(a) \int \frac{f_2(a)\sigma(a)}{W(a)}\, da + C_1 f_1(a) + C_2 f_2(a) , \tag{2.30}$$

where

$$f_1(a) = \frac{\cos\left[\overline{K}_1 (ma + \varepsilon) \right]}{\sqrt{\cosh(ma + \varepsilon)}} , \tag{2.31}$$

$$f_2(a) = \frac{\sin\left[\overline{K}_1 (ma + \varepsilon) \right]}{\sqrt{\cosh(ma + \varepsilon)}} , \tag{2.32}$$

$$W(a) = \frac{m \overline{K}_1}{\cosh(ma + \varepsilon)} . \tag{2.33}$$

Finally the displacement of the acoustic particle in the hyperbolic horn with annular cross-section, for frequencies below the cut-off frequency, can be presented as follows:

$$\xi(a,t) = k^{-1} A \varphi_1(a,t) + k^{-1} A^2 \left[\varphi_{21}(a,t) + g(a) + f(a) \cos 2\omega t \right] , \tag{2.34}$$

where $\varphi_1(a,t)$, $\varphi_{21}(a,t)$, $g(a)$ and $f(a)$ are expressed by formulas (2.17), (2.22), (2.27) and (2.30), respectively. The constants C_1, C_2 can be determined from the condition (2.5).

3. The exponential horn with annular cross section

In this important particular case $\varepsilon \to \infty$ and the formula (2.2) has the following form:

$$S = S_0 e^{mx}. \tag{3.1}$$

The cut-off frequency for the exponential horn is [4]

$$f_c = \frac{mc}{4\pi}. \tag{3.2}$$

The solution (2.17) of equation (2.6) for the frequencies below the cut-off frequency is simplified to the form

$$\varphi_1(a,t) = e^{-\left(\frac{m}{2}+\sqrt{\frac{m^2}{4}-k^2}\right)a} \cos \omega t. \tag{3.3}$$

The equation (2.7) for the second harmonic is

$$\varphi_2'' + m\varphi_2' - \frac{1}{c^2}\ddot{\varphi}_2 = \psi(a,t), \tag{3.4}$$

where the right-hand side of this equation has the following form:

$$\psi(a,t) = \left\{N\left[(\gamma+1)k - \frac{m^2}{k}\right] + \frac{m}{2}\left[(5-\gamma)k - \frac{m^2}{k}\right]\right\} e^{-(m+2N)a}\frac{1+\cos 2\omega t}{2}. \tag{3.5}$$

Here

$$N = m \lim_{\varepsilon\to\infty} \bar{\chi} = \sqrt{\frac{m^2}{4} - k^2}. \tag{3.6}$$

The particular solution of equation (3.4) can be presented in the following form:

$$\varphi_{22}(a,t) = [C + D\cos 2\omega t]\, e^{-(m+2N)a}. \tag{3.7}$$

The coefficients C and D can be found by introducing $\varphi_{22}(a,t)$ into equation (3.4):

$$C = \frac{\frac{1}{2}N\left[(\gamma+1)\omega^2 c - m^2c^3\right] + mc\left(\frac{5-\gamma}{4}\omega^2 - \frac{m^2c^2}{4}\right)}{2m\omega c^2 N + m^2\omega c^2 - 4\omega^3}, \tag{3.8}$$

$$D = \frac{\frac{1}{2}N\left[(\gamma+1)\omega^2 c - m^2c^3\right] + mc\left(\frac{5-\gamma}{4}\omega^2 - \frac{m^2c^2}{4}\right)}{2m\omega c^2 N + m^2\omega c^2}. \tag{3.9}$$

Note that for a frequency $f \ll f_c$

$$C \simeq D \simeq -\frac{m}{4k}. \tag{3.10}$$

In the case where the frequency of the second harmonic is above the cut-off frequency, the general solution of a homogeneous equation coupled with equation (3.4) has the following form:

$$\varphi_{21}(a,t) = Pe^{-ma} + Qe^{-ma/2}\cos(2\omega t - N_1 a), \tag{3.11}$$

where

$$N_1 = m \lim_{\varepsilon \to \infty} \overline{K}_1 = \sqrt{4k^2 - \frac{m^2}{4}}\,. \tag{3.12}$$

The sum of (3.7) and (3.11) represents a solution of equation (3.4). Next, from the boundary condition (2.5), the constants P and Q can be found. Thus at $a = 0$

$$\varphi_{21}(0,t) + \varphi_{22}(0,t) = P + Q\cos 2\omega t + C + D\cos 2\omega t = 0. \tag{3.13}$$

This condition is fulfiled at all times when

$$P = -C, \qquad Q = -D. \tag{3.14}$$

Finally, for excitation frequencies below the cut-off frequency, the displacement of the acoustic particle in the exponential horn takes in the second approximation following form:

$$\xi(a,t) = k^{-1}Ae^{-(\frac{m}{2}+N)a}\cos\omega t + k^{-1}A^2\Big\{Ce^{-ma}\left(e^{-2Na}-1\right) - De^{-\frac{m}{2}a}\left[\cos\left(2\omega t - N_1 a\right) - e^{-(\frac{m}{2}+2N)a}\cos 2\omega t\right]\Big\}. \tag{3.15}$$

It can be noticed that in above formula the term

$$k^{-1}A^2C\,e^{-ma}\left(e^{-2Na}-1\right) \tag{3.16}$$

occurs. This term is independent of time and signifies that during the acoustic motion, a layer of air inside the horn oscillates about a mean position which is not its position of rest but is displaced in the direction of propagation of the wave.

By differentiating equation (3.15) with respect to time the vibration velocity of a particle can be obtained. The vibration velocity is a sum of two components: the first one is the term with pulsation ω (first harmonic):

$$v_1 = -Ace^{(\frac{m}{2}+N)a}\sin\omega t\,. \tag{3.17}$$

The second component with pulsation 2ω (second harmonic) can be presented as follows:

$$v_2 = 2cA^2De^{-\frac{m}{2}a}\left[\sin(2\omega t - N_1 a) - e^{-(\frac{m}{2}+2N)a}\sin 2\omega t\right]. \tag{3.18}$$

When the distance from the source at the throat is big enough that

$$e^{-(\frac{m}{2}+2N)a} \ll 1 \tag{3.19}$$

and the only important part of the second harmonic wave in formula (3.18) is

$$v_2 \simeq 2cA^2De^{-\frac{m}{2}a}\sin(2\omega t - N_1 a). \tag{3.20}$$

In this case the ratio of the amplitudes of vibration velocities of both harmonics is equal to

$$\eta = \frac{2cA^2|D|e^{-\frac{m}{2}a}}{Ace^{-(\frac{m}{2}+N)a}} = 2A|D|e^{Na}\,. \tag{3.21}$$

The square of this ratio gives the ratio of the radiated powers.

At the end the exponential horns with the same dimensions of the throat and of the mouth but with different lengths are taken into account in the numerical example:

— width of the channel at the inlet $h_0 = 1.5 \cdot 10^{-3}\,\mathrm{m}$,

— diameter of the annular channel $d_0 = 10^{-1}\,\mathrm{m}$,

— width of the channel at the outlet $h_l = 10^{-1}\,\mathrm{m}$,

— lengths (coefficients of flare, cut-off frequencies):

$$
\begin{aligned}
l_1 &= 60 \cdot 10^{-2}\mathrm{m} \quad \left(m_1 = 7\frac{1}{\mathrm{m}}, \quad f_{c_1} = 190\,\mathrm{Hz}\right),\\
l_2 &= 42 \cdot 10^{-2}\mathrm{m} \quad \left(m_2 = 10\frac{1}{\mathrm{m}}, \quad f_{c_2} = 270\,\mathrm{Hz}\right),\\
l_3 &= 28 \cdot 10^{-2}\mathrm{m} \quad \left(m_3 = 15\frac{1}{\mathrm{m}}, \quad f_{c_3} = 406\,\mathrm{Hz}\right),\\
l_4 &= 21 \cdot 10^{-2}\mathrm{m} \quad \left(m_4 = 20\frac{1}{\mathrm{m}}, \quad f_{c_4} = 540\,\mathrm{Hz}\right),\\
l_5 &= 15 \cdot 10^{-2}\mathrm{m} \quad \left(m_5 = 28\frac{1}{\mathrm{m}}, \quad f_{c_5} = 760\,\mathrm{Hz}\right).
\end{aligned}
$$

For the acoustic particles at the mouth of the horn the termin the formula (3.19) can be written as follows:

$$\delta = e^{-\left(\frac{m}{2}+2N\right)l}. \tag{3.22}$$

In Fig. 2 δ as a function of frequency for expotential horns with the above dimensions is shown. We can see that practically $\delta \ll 1$. Thus, the ratio of the amplitudes of vibration velocities of both harmonics can be calculated from formula (3.21) which can now be presented in the form

$$\eta = 4\pi M |D| e^{Nl}. \tag{3.23}$$

The relation between the ratio η and the vibration frequency of the piston at the throat, in the range of frequency $\frac{1}{2}f_c < f < f_c$, for the horn with length $l = 0.6\,\mathrm{m}$ is presented in Fig. 3. The five curves in Fig. 3 correspond to five values of the Mach number, from $M = 0.002$ (intensity of sound level at the throat $J_0 = 156\,\mathrm{dB}$) to $M = 0.015$ ($J_0 = 173\,\mathrm{dB}$). The relation $\eta = \eta(f)$ for the horn with length $l = 0.15\,\mathrm{m}$ is presented in Fig. 4. The graphs of the functions $\eta = \eta(f)$ for horns with another lengths resemble the graphs in Fig. 3 and Fig. 4, and therefore they are not presented here.

It is shown in Fig. 3 and Fig. 4 that, for frequencies below the cut-off frequency, the amplitude of vibration velocity of the second harmonic increases in comparison with that of the first one when the frequency decreases. This increase is faster when the amplitude of the piston which initiates the wave is greater.

It can be seen comparing these results with the results of the [10], that for frequencies below the cut-off frequency the second harmonic is more amplified than for the frequencies above the cut-off. Assume e.q. that the length of the horn is $0.15\,\mathrm{m}$ ($f_c = 760\,\mathrm{Hz}$) and Mach acoustic number is 0.01 ($J_0 = 170\,\mathrm{dB}$). In this case for frequency $f = \frac{1}{2}f_c$ from the (Fig. 4) we obtain $\eta \simeq 60\%$, but for frequency $f = 2f_c$ we have $\eta \simeq 5\%$ (see [10]).

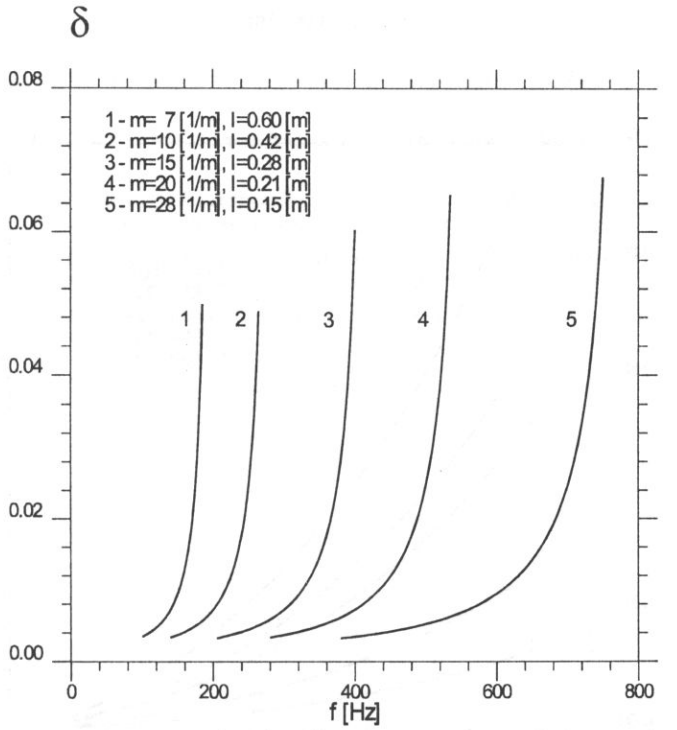

Fig. 2. The coefficient δ [see (3.22)] for the horns with different lengths.

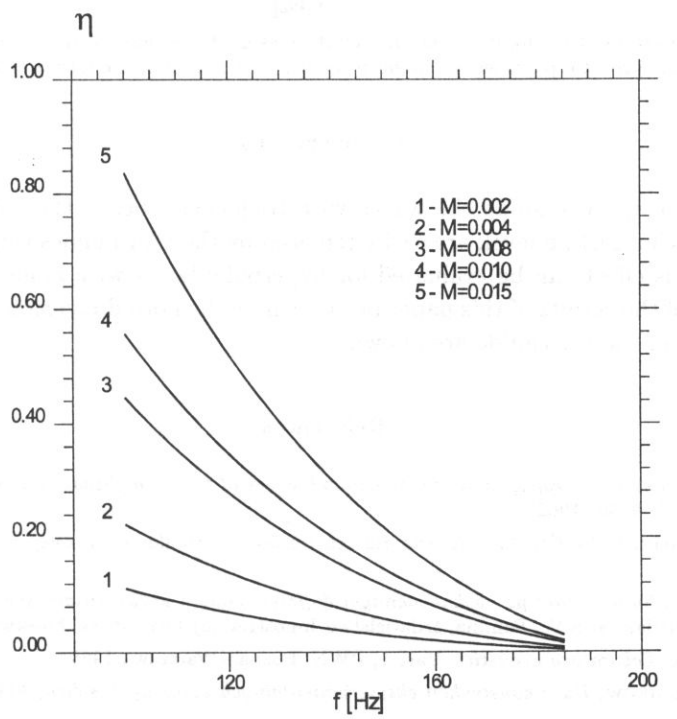

Fig. 3. The ratio of the vibration velocity amplitudes of the second harmonic to the first one for the acoustic particles at the horn mouth. The length of the horn $l = 0.6$ m.

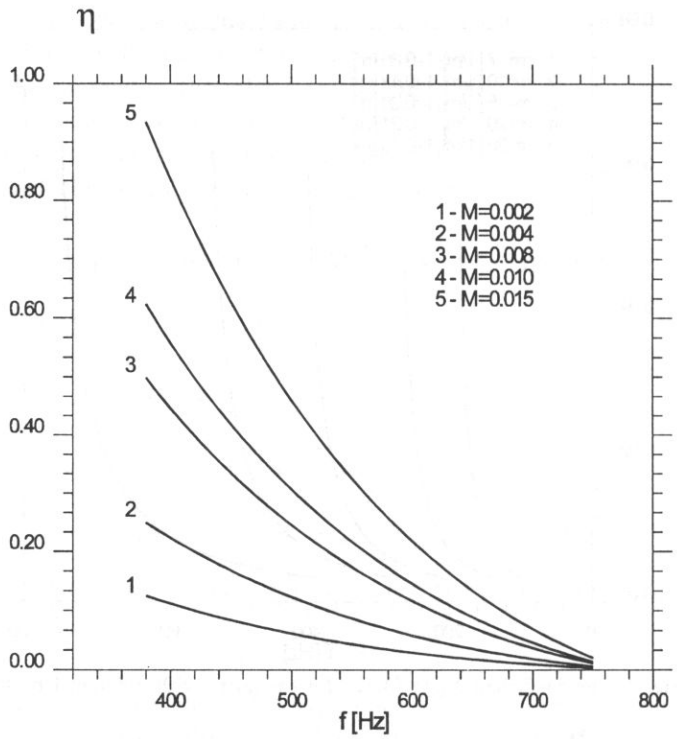

Fig. 4. The ratio of the vibration velocity amplitudes of the second harmonic to the first one for the acoustic particles at the horn mouth. The length of the horn $l = 0.15$ m.

4. Conclusions

In the acoustic waveguide the waves with frequencies below the cut-off frequency, once they reach a certain level, are easily replaced by their harmonics which are strongly amplified. This effect can be evaluated for hyperbolic horns with annular cross-section on the basis of the results of this paper in case where the horn dimensions and amplitude at the throat of the waveguide are known.

References

[1] D.T. BLACKSTOCK, *Propagation of plane sound waves of finite amplitude in nondissipative fluids*, JASA, **34**, 1, 9–30 (1962).

[2] S.A. CIEBILIN, W.M. CIETLIN, *Siriena dla akusticzieskoj koagulacji aerozolej*, Akust. Ż, **7**, 1, 78–86 (1961).

[3] E. KAMKE, *Sprawocznik po obyknowiennym dyfferencjalnym urawnieniam*, pieriewod s niemieckowo pod riedakciej S.W. Fomina, Izdatielstwo Innostrannoj Litieratury, Moskwa 1951.

[4] M. KWIEK, *Laboratory acoustics*, Part 1, PWN, Poznań-Warszawa 1968.

[5] E.P. MIEDNIKOW, *Dwie konstrukcji ekspierymientalnych zwukowych sirien*, Akust. Ż., **4**, 1, 59–63 (1958).

[6] A. PUCH, *Generalized model of axial dynamic generator*, Archives of Acoustics, **13**, 1, 17–34 (1978).

[7] R. WYRZYKOWSKI, R. HNATKÓW, *Sirene mit hoher akustischer Leistung*, Acustica, **59**, 225–229 (1986).

[8] T. ZAMORSKI, R. WYRZYKOWSKI, *Hyperbolic horns of annular cross-section* [in Polish], Prace XXV OSA, 367–370.

[9] T. ZAMORSKI, R. WYRZYKOWSKI, *Approximate methods for the solution of the equation of acoustic wave propagation in horns*, Archives of Acoustics, **6**, 3, 237–285 (1981).

[10] T. ZAMORSKI, *Simple waves with finite amplitude in axially - symmetrical chanels with annular cross-section*, Archives of Acoustics, **19**, 3, 405–418 (1994).

[11] L.K. ZARIEMBO, W.A. KRASILNIKOW, *Vvedenije w nieliniejnuju akustiku*, Izd. Nauka, Moskwa 1966.

ARCHIVES OF ACOUSTICS
22, 4, 423–435 (1997)

ACOUSTIC POWER OF FLUID-LOADED CIRCULAR PLATE LOCATED IN FINITE BAFFLE

L. LENIOWSKA

Institute of Technology, Pedagogical University
(35-310 Rzeszów, ul. Rejtana 16a, Poland)

The oblate spheroidal coordinate system was used for calculation of the acoustic power radiated by a thin circular plate located in a finite baffle. It was assumed that the plate was clamped at the circumference of the planar limited baffle and radiated into lossless homogeneous liquid medium. The vibrations of the plate were forced by time harmonic external pressure. The damping effects caused by internal friction in the plate material as well as dynamic influence of the waves emitted by the plate were taken into consideration. The formula for the acoustic power was derived by the application of properties of eigenfunctions of plate equation of motion.

Notations

a plate radius,
A_l expansion coefficients,
B bending stiffness,
b baffle radius,
c propagation velocity of a wave in fluid,
c_m, c_n expansion coefficients,
E Young's modulus,
f surface density of the force exciting vibrations,
f_n expansion coefficients,
F time dependent surface density of the force exciting vibrations,
F_0 time independent constant,
h_η, h_ξ, h_φ components of measurement tensor,
h acoustic parameter, $h = k_0 a(b/a)$,
H plate thickness,
J_m m-order Bessel functions,
I_m m-order modified Bessel functions,
k_0 wave number,
k_p structural wavenumber,
m mass of the plate per surface unit,
n normal component,
N acoustic power radiated by the plate,
N' normalised acoustic power radiated by the plate,
N^∞ norm factor,
N_l Flammer norm factor,
p sound presure,
r radial variable in polar coordinates,
R coefficient of internal damping,

$R_{0l}^{(3)}(-ih,,i\xi)$ radial spheroidal function of the third kind, l-order,
$S_{0l}^{(1)}(-ih,\eta)$ angular spheroidal function of the first kind, l-order,
ν Poisson's ratio,
v normal component of the vibration velocity of points on the surface of the plate,
v_n vibration velocity of points on the surface of the plate for mode $(0,n)$,
v_{0n} normalised coefficient of the vibration velocity,
w transverse dislocation of points on the surface of the plate,
W time dependent transverse dislocation of points on the surface of the plate,
W_{nl} characteristic function,
ε_1 fluid-loading parameter,
ε_2 parameter of the plate damping,
γ_n $= k_n a$ is solution of the homogeneous plate equation of motion,
χ_l mutual impedance,
η spheroidal coordinate,
λ length of acoustic wave in fluid,
σ area of the plate with baffle,
ξ spheroidal coordinate,
ζ_{mn} mutual impedance,
ψ acoustic potential,
Ψ time dependent acoustic potential,
ω angular frequency of the force exciting vibrations,
ϱ density of the plate material,
ϱ_0 density of the fluid.

1. Introduction

The problem of radiation of acoustic waves by circular planar sources located in a limited baffle caught the attention of acoustic researches in the thirties [3]. It is well known that for waves longer than the dimensions of the considered sources the obtained results do not fully tally with characteristics calculated for the sources with infinite baffle and Huygens - Rayleigh integral applied [1, 2, 4]. Detailed analytical investigations have been made for the piston with uniform and parabolic velocity distribution [1,2,11] and also for a freely vibrating membrane [12].

Most papers dealing with the influence of a finite baffle apply properties of the oblate spheroidal coordinates system [1 - 4, 11]. Interest in acoustic radiation from sources on oblate spheroidal baffles results primarily from the reparability of the scalar wave equation in coordinates in question and the wide variety of useful shapes that are natural to this systems. For a circular plate supplied with a finite rigid baffle the oblate spheroid is also particularly suited to the study of sound radiation, so the basic quantities that characterise an acoustic field were calculated by the author in a similar way [6, 7, 8]. Spheroidal geometry offers a convenient system in which the curvature of the radiating surface may be varied and the relative size of the vibrating surface to the baffle surface may be changed. Of particular interest is the case in which the spheroid reduces to a flat circular source (plate) in the xy plane. In this way the sound field around the plate in question can be obtained by solving the separable Helmholtz wave equation in the oblate spheroidal coordinates with Neuman's boundary condition.

Properties of the oblate spheroidal coordinate system have been used to calculate the acoustic pressure for the freely vibrating plate [8] and for the fluid-loaded plate excited harmonically at low frequencies [7]. This paper gives formulae for the acoustic power

of the plate clamped at a finite baffle and excited to vibrate by an external force. The mathematical model of the plate includes internal dissipation and interaction with fluid.

2. Assumption of the analysis

Consider the fluid-plate configuration as illustrated in Fig. 1.

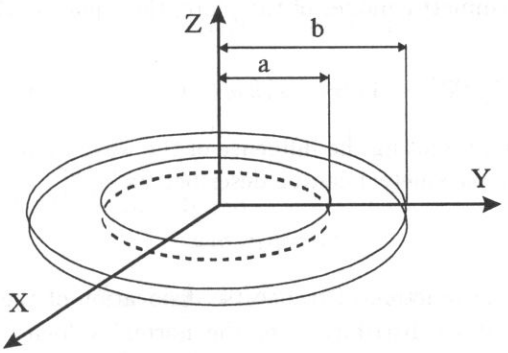

Fig. 1. A circular plate in a rigid baffle with radius b.

A circular thin plate with radius a and thickness H is surrounded by an ideal liquid medium with the static density ϱ_0. It is assumed that the plate is made of a homogeneous isotropic material with density ϱ, Poisson's ratio ν, Young's modulus E. The plate is clamped in a flat, rigid and finite baffle with radius b and is excited to vibration by an external time-harmonic force:

$$F(r,\phi,t) = f(r,\phi)e^{-i\omega t} = F_0 e^{-i\omega t}, \tag{2.1}$$

where $F_0 = \text{const}$ for $0 < r < a$.

Taking into account only linear, harmonic and axially-symmetric vibrations of the plate in a steady state, as well as the influence of a radiated wave on vibrations of the plate and an internal damping inside the plate's material, the plate differential equation of motion can be described as follows [5, 9, 10]:

$$B\nabla^4 W(r,\phi,t) + m\frac{\partial^2 W(r,\phi,t)}{\partial t^2} + R\frac{\partial}{\partial t}\left[\nabla^4 W(r,\phi,t)\right] = R(r,\phi,t) - \varrho_0 \frac{\partial \Psi(r,\phi,0,t)}{\partial t}, \tag{2.2}$$

where $B = EH^3/12(1-\nu^2)$ is the bending stiffness, $W(r,\phi,t) = w(r,\phi)e^{-i\omega t}$ – transverse dislocation of points on the surface of the plate, m – mass of the plate per surface unit, R – coefficient of internal damping, $\Psi(r,\phi,0,t)$ – acoustic potential on the surface of the plate, related to the acoustic pressure p in the fluid by the equation [15]

$$p = -\varrho_0 i\omega \Psi(r,\phi,z) \tag{2.3}$$

and satisfies the Helmholtz equation

$$\left(\nabla^2 + k_0^2\right)\Psi = 0, \tag{2.4}$$

with the condition

$$\left.\frac{\partial \Psi}{\partial n}\right|_{z=0} = -v(r,\phi) = i\omega w(r,\phi), \tag{2.5}$$

k_0 denotes the acoustic wavenumber at the frequency ω, $v(r,\phi)$ – amplitude of surface velocity distribution on the plate.

Using well-known formulae appropriate for harmonic phenomena and taking into account only axially-symmetric modes of the plate, the equation (2.2) can be expressed as [5, 9, 10]:

$$\left(k_p^{-4}\nabla^4 - 1\right) v(r) - \varepsilon_1 k_0 \psi(r,0) = -\frac{i}{\omega m} f(r). \tag{2.6}$$

The parameter ε_1 representing the influence of the wave radiated by the plate on its vibration (fluid-loading parameter) can be described as [5, 7]:

$$\varepsilon_1 = \varrho_0 c/m\omega\,. \tag{2.7}$$

In the equation (2.6) the function of transverse dislocation of the plate $w(r)$ has been replaced by wanted surface distribution of the normal velocity $v(r)$. The structural wavenumber k_p in the vacuum at frequency ω is defined by

$$k_p^4 = m\omega^2/\overline{B}, \tag{2.8}$$

where $\overline{B}$ is the complex rigidity

$$\overline{B} = B - i\omega R = B(1 - i\varepsilon_2) \tag{2.9}$$

and parameter ε_2

$$\varepsilon_2 = \omega R/B \tag{2.10}$$

is a measure of the plate damping.

3. Solution of the Helmholtz equation

For the plate located in a finite baffle, the problem of determining the far-field acoustic pressure cannot be treated with the well known Rayleigh's formula. In this paper the solution of Eq. (2.4) in conjunction with (2.5) has been obtain by the use of the method of separation of variables in the oblate spheroidal coordinate system (OSCS) [6]. Due to symmetry of radiated waves with respect to z axis, the following equation for outgoing waves has been obtained [14]:

$$\psi(\eta,\xi) = \sum_{l}^{\infty} A_l S_{0l}^{(1)}(-ih,\eta) R_{0l}^{(3)}(-ih,i\xi), \tag{3.1}$$

where $S_{0l}^{(1)}(-ih,\eta)$ denotes angular spheroidal function of the first kind, $R_{0l}^{(3)}(-ih,i\xi)$ – radial spheroidal function of the third kind, $h = k_0 b$ and A_l – the expansion coefficients.

The coefficients can be derived from Neuman's boundary condition (2.5) which in oblate spheroidal system has the form

$$\frac{\partial \Psi}{\partial n} = \frac{1}{h_\xi}\frac{\partial \Psi}{\partial \xi}\bigg|_{\xi=\xi_0} = \begin{cases} -v(\xi_0,\eta), & \eta_0 \le \eta \le 1, \\ 0, & \eta_0 \ge \eta \ge -\eta_0, \\ v(\xi_0,\eta), & -1 \le \eta \le -\eta_0. \end{cases} \tag{3.2}$$

Applying the orthogonal property of angular spheroidal functions [14], we finally obtain [8]:

$$A_l = -\frac{bW_{nl}}{\dfrac{\partial R_{0l}^{(3)}(-ih,i0)}{\partial \xi} N_l}, \tag{3.3}$$

where N_l denotes the norm factor [14] and

$$W_{nl} = \int_{\eta_0}^{1} v(\eta) S_{0l}(-ih,\eta)\eta \, d\eta \tag{3.4}$$

is the characteristic function in OSCS. The vibration velocity distribution in the oblate spheroidal coordinate system $v(\eta)$ is an unknown function. It will be determined by applying the orthogonal series method.

4. Solution of the plate equation of motion

By applying the well known eigenfunction expansion theorem, one can derive the solution of Eq. (2.7). In order to do it the vibration velocity distribution $v(r)$ and the external force $f(r)$ will be expressed as the infinite series of eigenfunctions of the homogeneous plate equation

$$v(r) = \sum_n^\infty c_n v_n(r), \tag{4.1}$$

$$f(r) = \sum_n^\infty f_n v_n(r). \tag{4.2}$$

The quantity c_n denotes unknown expansion coefficients, while f_n can be determined by means of the orthonormal property

$$f(r) = \int_0^a f(r) v_n^*(r) r \, dr. \tag{4.3}$$

For the clamped circular plate the eigenfunctions $v_n(r)$ take the form [5, 9]:

$$v_n(r) = v_{0n}\left[J_0(\gamma_n r/a) - \frac{J_0(\gamma_n)}{I_0(\gamma_n)} I_0(\gamma_n r/a)\right], \tag{4.4}$$

where $\gamma_n = k_n a$ is solution of the equation $J_0(\gamma_n)I_1(\gamma_n) + J_1(\gamma_n)I_0(\gamma_n) = 0$, $n = 1, 2, \ldots$ and have an orthonormal property if

$$v_{0n} = 1/\left(aJ_0(k_n a)\right). \tag{4.5}$$

Regarding the following equation

$$\nabla^4 v_n(r) = k_n^4 v_n(r) \tag{4.6}$$

as a result we obtain

$$\sum_n c_n \left(k_p^{-4} k_n^4 - 1\right) v_n(r) - \varepsilon_1 k_0 \psi(r, 0) = -\frac{i}{\omega m} \sum_m f_n v_n(r). \tag{4.7}$$

The equation (4.7) is now expressed in the oblate spheroidal coordinate system (OSCS) with the use of the following transformation [14]

$$r = b\left[(1-\eta^2)(\xi_0^2 + 1)\right]^{1/2}. \tag{4.8}$$

Using properties of OSCS and assuming $\xi_0 = 0$, $r = b(1-\eta^2)$, the obtained expressions become appropriate for the plate in the finite baffle. The eigenfunctions are

$$v_n(\eta) = v_{0n}\left[J_0\left(\gamma_n \frac{b}{a}\sqrt{1-\eta^2}\right) - \frac{J_0(\gamma_n)}{I_0(\gamma_n)} I_0\left(\gamma_n \frac{b}{a}\sqrt{1-\eta^2}\right)\right] \tag{4.9}$$

and they remain orthonormal if

$$v_{0n} = b/(aJ_0(k_n a)). \tag{4.10}$$

In turn, Eq. (4.7) is multiplied by the orthonormal function $v_m^*(\xi_0, \eta)$ and integrated on the surface of the spheroid. Denoting the components of the left side of Eq. (4.7) as L_1 and L_2 and its right side as L_3, the following integrals are obtained:

$$\begin{aligned} L_1 &= \iint_\sigma \sum_n c_n \left(k_p^{-4} k_n^4 - 1\right) v_n(\xi_0, \eta) v_m^*(\xi_0, \eta)\, d\sigma, \\ L_2 &= -\varepsilon_1 k_0 \iint_\sigma \psi(\xi_0, \eta) v_m^*(\xi_0, \eta)\, d\sigma, \\ L_3 &= -\frac{1}{\omega \varrho h} \iint_\sigma \sum_n f_n v_n(\xi_0, \eta) v_m^*(\xi_0, \eta)\, d\sigma\,. \end{aligned} \tag{4.11}$$

In order to find the solutions of the above integrals we must take into account that the element of spheroid surface $d\sigma$ is equal to

$$d\sigma = h_\eta h_\varphi\, d\eta\, d\varphi, \tag{4.12}$$

where h_η, h_φ denotes the scaling factors (components of measurement tensor) [14]:

$$\begin{aligned} h_\eta &= b\sqrt{\frac{\xi_0^2 + \eta^2}{1-\eta^2}}, \\ h_\varphi &= b\sqrt{(1-\eta^2)(1+\xi_0^2)}. \end{aligned} \tag{4.13}$$

As a result of this calculation, the previous equation (4.7) turns into a system of linear algebraic equations [7, 9]

$$c_m\left(\frac{k_m^4}{k_p^4}-1\right)-\varepsilon_1\sum_n^{\infty} i\zeta_{mn}c_n = f_m\,, \tag{4.14}$$

where

$$f_m = -\frac{2i}{\omega m\gamma_m b^2}v_{0n}F_0a^2J_1(\gamma_m) \tag{4.15}$$

is the expansion coefficient of the external excitation into the Fourier series which has been obtained according to expression (4.3) and quantity

$$\zeta_{mn} = \sum_l \frac{W_{nl}W_{ml}}{N_l} ih\frac{R_{0l}^{(3)}(-ih,i0)}{\partial R_{0l}^{(3)}(-ih,i0)/\partial\xi} \tag{4.16}$$

means normalised impedance of the plate [7].

The solution of the system (4.14) is possible with the application of numerical methods. In order to determine expansion coefficients c_n the system (4.14) has been solved using Crout algorithm, which enables us to find the velocity distribution on the surface of the plate, in accordance with the analysed case.

5. Calculation of the acoustic power

The total acoustic power of the vibrating plate is calculated according to the definition [15]

$$N = \frac{1}{2}\iint_\sigma pv^*\,d\sigma, \tag{5.1}$$

where p is the acoustic pressure and v^* denotes the amplitude of vibration velocity distribution, which is coupled with the velocity of the considered source.

In the case of flat circular sources vibrating in a finite baffle, the total acoustic power can be calculated by the application of Eq. (5.1) in oblate spheroidal coordinate. In this case the surrounded spheroidal surface $\sigma = \sigma_0$ becomes the surface of a considered vibrator system, including the baffle. In the oblate spheroidal coordinate system the definition (5.1) can be expressed as

$$N = \pi b^2\int_{-1}^{1} p(0,\eta)v^*(\eta)\eta\,d\eta\,. \tag{5.2}$$

The quantities that appear in the integrand function can be described as follows:

$$v^*(\eta) = \sum_n^{\infty} c_n^* v_n(\eta). \tag{5.3}$$

where c_n^* denotes complex coefficients coupled with c_n obtained above.

Basing our calculations on the relation (2.3) and expression (2.6) together with (2.7) and (2.8), the formula of the acoustic pressure of the circular plate with the finite baffle takes the form [7]

$$p(0,\eta) = -2i\varrho_0 hc \sum_{n=1}^{\infty} c_n \sum_{l=1}^{\infty}{}' \frac{W_{nl}}{N_l \partial R_{0l}^{(3)}(-ih,i0)/d\xi} S_{0l}(-ih,\eta) R_{0l}^{(3)}(-ih,i0). \tag{5.4}$$

Symbol "/" in the second sum is associated with the manner in which the waves are emitted by a system with the plate as a vibration source. In our analysis the acoustic field is radiated by both upper and lower surfaces of the plate, so in the expression (5.4) only odd index of l can be taken into account.

Introducing the transfer impedance [11]

$$\chi_l(-ih) = -ih \frac{R_{0l}^{(3)}(-ih,i0)}{R_{0l}^{(3)\prime}(-ih,i0)}, \tag{5.5}$$

where $R_{0l}^{(3)\prime}(-ih,i0)$ denotes $\partial R_{0l}^{(3)}(-ih,i0)/\partial\xi$, the acoustic pressure takes the simpler form

$$p(0,\eta) = 2\varrho_0 c \sum_{n=1}^{\infty} c_n \sum_{l=1}^{\infty}{}' \frac{W_{nl}}{N_l} S_{0l}(-ih,\eta)\chi_l(-ih). \tag{5.6}$$

In order to obtain the pattern for the acoustic power radiated by a plate let us replace the above quantities into definition (5.2)

$$N = 2\pi b^2 \varrho_0 c \sum_{n=1}^{\infty} c_n \sum_{l=1}^{\infty}{}' \frac{W_{nl}}{N_l} \chi_l(-ih) \int_{-1}^{1} v^*(\eta) S_{0l}(-ih,\eta)\eta\, d\eta. \tag{5.7}$$

Regarding expression (5.3), we obtain

$$N = 2\pi b^2 \varrho_0 c \sum_{n=1}^{\infty} c_n \sum_{l=1}^{\infty}{}' \frac{W_{nl}}{N_l} \chi_l(-ih) \sum_m c_m^* \int_{-1}^{1} v_m(\eta) S_{0l}(-ih,\eta)\eta\, d\eta. \tag{5.8}$$

The integral that appears in the above relation can be separated into two parts, according to the boundary condition (3.2)

$$N = 2\pi b^2 \varrho_0 c \sum_{n=1}^{\infty} c_n \sum_{l=1}^{\infty}{}' \frac{W_{nl}}{N_l} \chi_l(-ih) \sum_m c_m^* \times \left[\int_{-1}^{-\eta_0} v_m(\eta) S_{0l}(-ih,\eta)\eta\, d\eta + \int_{\eta_0}^{1} v_m(\eta) S_{0l}(-ih,\eta)\eta\, d\eta \right] \tag{5.9}$$

which leads to the change of integration limits after applying the following property of angle oblate spheroidal functions [14]

$$S_{0l}(-ih,\eta) = (-1)^l S_{0l}(-ih,-\eta). \tag{5.10}$$

The calculations explained above result in:

$$N = 2\pi b^2 \varrho_0 c \sum_{n=1}^{\infty} \sum_{m=1}^{\infty} c_m^* c_n \sum_{l=1}^{\infty}{}' \frac{W_{nl} W_{ml}}{N_l} \chi_l(-ih). \tag{5.11}$$

In this way the final formula for the total acoustic power radiated by the plate located in a finite baffle has been derived. It can easily be separated into real and imaginary part because there is only one complex quantity $\chi_l(-ih)$ inside:

$$\begin{aligned} \mathrm{Re}(N) &= 2\pi b^2 \varrho_0 c \sum_{n=1}^{\infty} \sum_{m=1}^{\infty} c_m^* c_n \sum_{l=1}^{\infty}{}' \frac{W_{nl} W_{ml}}{N_l} \mathrm{Re}[\chi_l(-ih)], \\ \mathrm{Im}(N) &= 2\pi b^2 \varrho_0 c \sum_{n=1}^{\infty} \sum_{m=1}^{\infty} c_m^* c_n \sum_{l=1}^{\infty}{}' \frac{W_{nl} W_{ml}}{N_l} \mathrm{Im}[\chi_l(-ih)], \end{aligned} \tag{5.12}$$

where

$$\begin{aligned} \mathrm{Re}[\chi_l(-ih)] &= \frac{1}{\left[R_{0l}^{(1)\prime}(-ih, i0)\right]^2 + \left[R_{0l}^{(2)\prime}(-ih, i0)\right]^2}, \\ \mathrm{Im}[\chi_l(-ih)] &= \frac{R_{0l}^{(2)}(-ih, i0) R_{0l}^{(2)\prime}(-ih, i0)}{\left[R_{0l}^{(1)\prime}(-ih, i0)\right]^2 + \left[R_{0l}^{(2)\prime}(-ih, i0)\right]^2}. \end{aligned} \tag{5.13}$$

6. Figures and conclusions

It is convenient for calculations to introduce the normalised factor N^{∞}, described as the acoustic resistance when wavenumber $k_0 \to \infty$ [13]

$$N^{\infty} = \lim_{k_0 \to \infty} N = 2\pi b^2 \varrho_0 c \sum_{n=1}^{\infty} c_n c_n^*. \tag{6.1}$$

Then the normalised acoustic power can be calculated as follows:

$$N' = \frac{N}{N^{\infty}} = \frac{\displaystyle\sum_{n=1}^{\infty} \sum_{m=1}^{\infty} c_m^* c_n \sum_{l=1}^{\infty}{}' \frac{W_{nl} W_{ml}}{N_l} \chi_l(-ih)}{\displaystyle\sum_{n=1}^{\infty} c_n c_n^*}. \tag{6.2}$$

On the basis of the above formula the real and imaginary part of the total acoustic power radiated by the plate in question has been calculated. Since the series in the formula (6.2) are infinite, the number of terms ensuring adequate accuracy of results have been numerically determined.

The largest considered value of h was 15, for which it was found that the series with index l converged in approximately 30 terms. The number of terms required for convergence of this series was always greater for the real part than for the imaginary

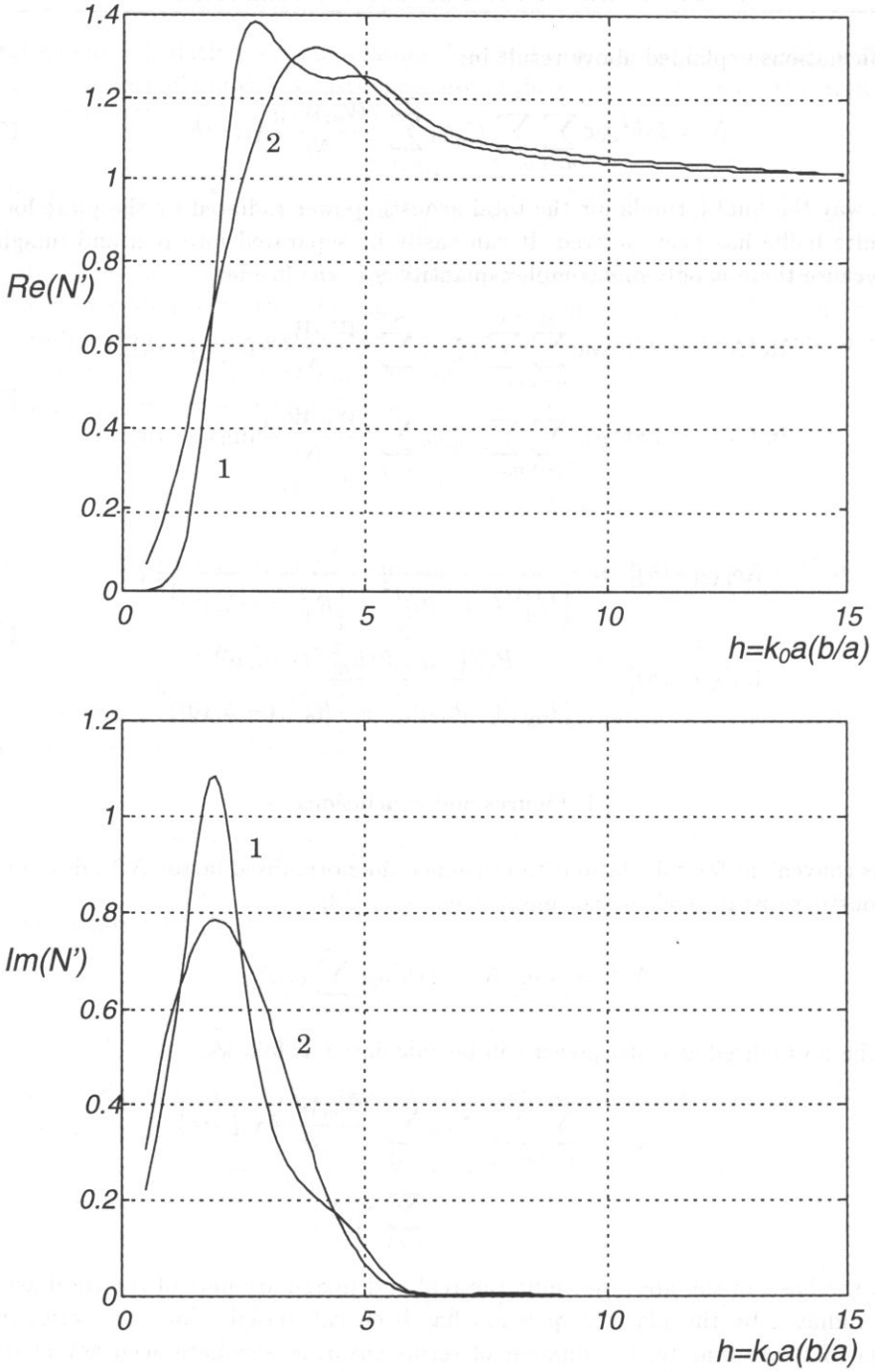

Fig. 2. Acoustic power radiated by the circular plate in terms of the acoustic parameter $h = k_0 b$. 1 – plate without the baffle, $a/b = 1$, $H/2a = 0.08$; 2 – plate with the unlimited baffle – the curve was calculated from formula (11′) in [9], $H/2a = 0.08$.

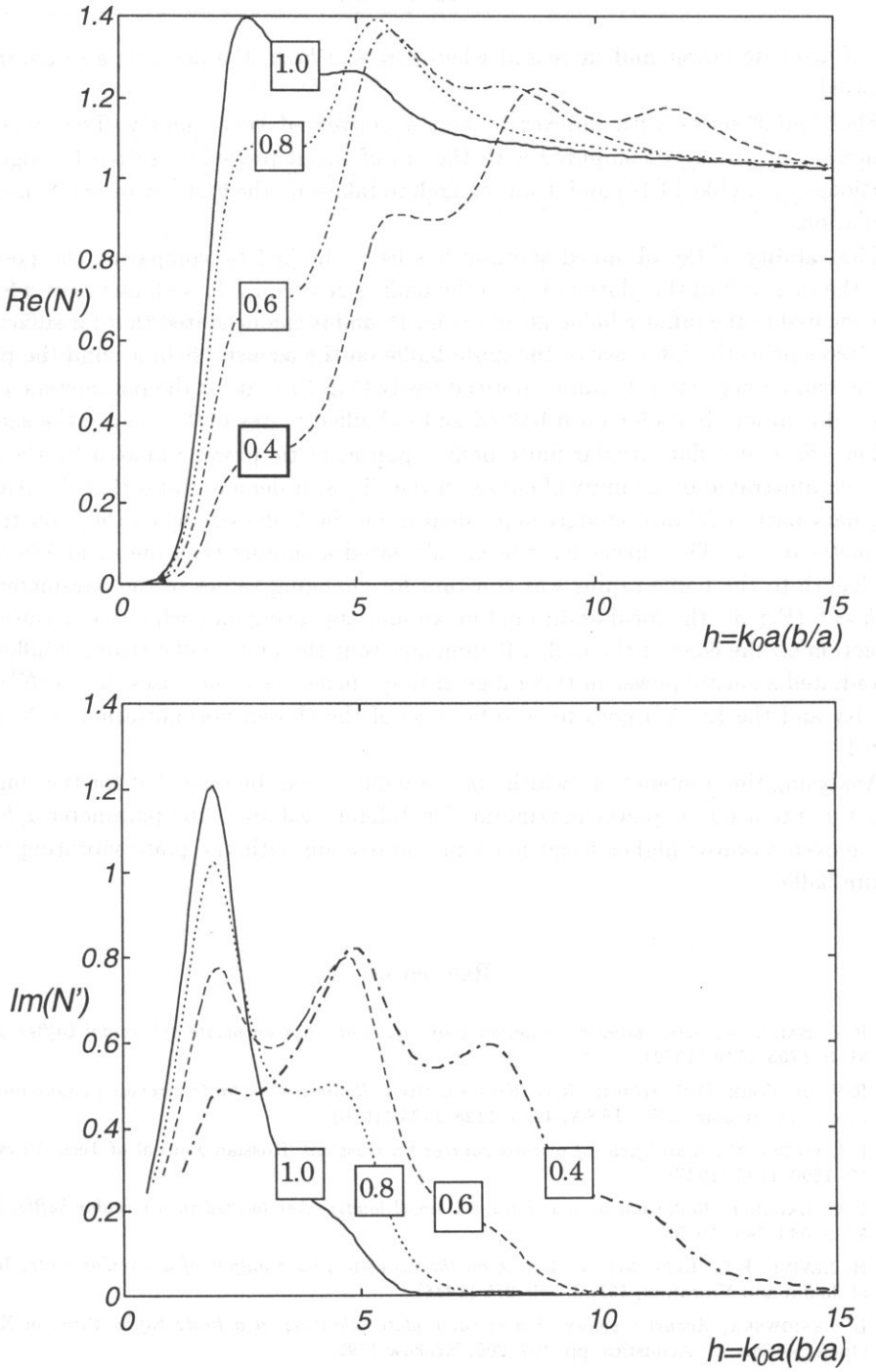

Fig. 3. Acoustic power radiated by the circular plate in terms of acoustic the parameter $h = k_0 b$, $H/2a = 0.08$. The numbers on the curves denote the values of the ratio a/b of the plate radius to the baffle size.

part of acoustic power and increased when $h = k_0 a(b/a)$, the acoustic size parameter increased.

The double series with indexes m and n converged very quickly. The expansion coefficients c_n, c_m were computed with the aid of Crout procedure suited for algebraic equations system like (4.14) and it was enough to take only the first few terms in practical calculations.

The validity of the obtained solution has been checked by comparing the no-baffle case (the ratio a/b of the plate radius to the baffle size is equal 1) with plots given for the plate located in the infinite baffle [9, 10], (Fig. 2), and it can be stated that for sufficiently high frequencies the influence of the finite baffle on the acoustic field around the planar sources can be neglected. It can be noticed easily (Fig. 2) that for the parameters $h > 10$ obtained characteristics for both baffled and unbaffled plates ($a/b = 1$) are the same.

The effect of a flat circular finite baffle upon acoustic power radiated by the plate has been illustrated by a family of curves in the Fig. 3. It demonstrates that the real and imaginary part of N' are strongly dependent upon the baffle size when the acoustic size parameter $h < 7$. The curves have been calculated assuming that the ratio λ/b of the wavelength to the baffle radius was constant for changing values of the parameter a/b. For $h \approx 6$ (Fig. 3), the local additional maximum appearing on each curve is caused by diffraction on the edge of the baffle. It indicates that the finite baffle strongly influences the radiated acoustic power in this range of frequencies. As h increases the $\mathrm{Re}(N')$ goes to unity and the $\mathrm{Im}(N')$ goes to zero because of the chosen normalisation of N' given by (6.1).

Analysing the influence of "width" of the baffle, it can be seen that for the constant ratio λ/b, the acoustic power maximums for different values of the parameter a/b have been moved towards higher frequencies in comparison with the plate vibrating in the infinite baffle.

References

[1] R.V. BAIER, *Acoustic radiation impedance of caps and rings on oblate spheroidal baffles*, JASA, **51**, 5, 1705–1716 (1972).

[2] R.V. DE VORE, D.B. HODGE, R.G. KOUYOUMJIAN, *Radiation by finite circular pistons imbedded in a rigid circular baffle*, JASA, **48**, 5, 1128–1134 (1970).

[3] L.J. GUTIN, *On sound field of pistons sources* [in Russian], Russian Journal of Tech. Physics, **7**, 10, 1096–1106 (1937).

[4] G.C. LAUCHLE, *Radiation of sound from a small loudspeaker located in a circular baffle*, JASA, **57**, 3, 543–549 (1975).

[5] H. LEVINE, F.G. LEPPINGTON, *A note on the acoustic power output of a circular plate*, Journal of Sound and Vibration, **121**, 2, 269–275 (1988).

[6] L. LENIOWSKA, *Acoustic power of a circular plate vibrating in a finite baffle*, Proc. of XXXIX Open Seminar on Acoustics, pp. 197–200, Kraków 1992.

[7] L. LENIOWSKA, *Acoustic pressure of a circular plate vibrating in a finite baffle with fluid loading*, Proc. of International Symp. on Hydroacoustics and Ultrasonics, pp. 311–316, Jurata 1977.

[8] L. LENIOWSKA, W. RDZANEK, *Acoustic pressure of a freely vibrating circular plate without a baffle*, Archives of Acoustics, **17**, 3, 413–432 (1992).

[9] W. RDZANEK, *Acoustic radiation of circular plate including the attenuation effect and influence of surroundings*, Archives of Acoustic, **16**, 3-4, 581–590 (1991).

[10] W. RDZANEK, *Acoustic power of radiation of a circular plate fixed on the rim and vibrating under external pressure*, Archives of Acoustics, **17**, 2, 321–333 (1992).

[11] A. SILBIGER, *Radiation from circular pistons of elliptical profile*, JASA, **33**, 11, 1515–1522 (1961).

[12] E.L. SZENDEROW, *Radiation of sound by oscillating disk without a baffle*, Russian Journal of Acoustics, **34**, 2, 326–335 (1988).

[13] R. WYRZYKOWSKI *et al., Chosen issues of the theory of acoustic field* [in Polish], FOSZE, Rzeszów 1994.

[14] C. FLAMMER, *Spheroidal wave functions*, Stanford University Press, 1957.

[15] E. SKUDRZYK, *The foundations of acoustics*, Springer-Verlag, Wien 1971.

ARCHIVES OF ACOUSTICS
22, 4, 437–444 (1997)

ON THE RELATION BETWEEN THE INERTIAL COAGULATION AND THE AMPLITUDAL EFFECT

H. CZYŻ

Institute of Physics, Pedagogical University of Rzeszów
(35-310 Rzeszów, Rejtana 16a, Poland)
e-mail: hczyz@atena.univ.rzeszow.pl

The phenomenon of drift of small particles suspended in a gaseous medium in which the acoustic wave propagates, is known since long. In the present work, which refers to [7], we present an outline of a theory allowing for full interrelation of all quantities characterizing the particle, the medium and the acoustic field.

1. Introduction

In the paper published in 1963 by ROMAN WYRZYKOWSKI [7] there is at the beginning a serious printing fault, which spuriously could missinterprete the results. The theory of sound coagulations of aerosols, formulated by Roman Wyrzykowski allows to obtain formulae, which give mutual dependance between the acoustical data and the data of the aerosol. In this paper we present this theory in new shape, of course with the assistance of the author.

The coagulating action of the acoustic wave on aerosols is known since long [1], as well as theories explaining partially this phenomenon [2–5].

We will assume in the following that the coagulation occurs always in the polydispersion aerosols, as even monodispersion aerosols become polydispersional as a result of heat motions. Particles of greater dimensions vibrate in the acoustic field with smaller amplitudes, while smaller particles amplitudes are greater. As a result, relative velocities occur which in turn result in collision of particles (if only the amplitude of vibration is sufficiently great; a problem which will be discussed in the following) and in the so-called inertial sedimentation (coagulation) of small particles on bigger ones.

In practice, sedimentation of aerosols takes place in a settling tank, which is a tower long enough to assure that the dusted gas, turning round along helical lines, spends necessarily long time (3 to 5 seconds) in the acoustic field, produced by a generator located at the top of the purifier [6, 8].

2. The amplitude effect, or proper acoustic coagulation

In the present section we will deal with the problem of selection of acoustic field parameters such that for a given aerosol one would obtain amplitude of vibration great enough for occurrence of the acoustic coagulation.

The average distance between aerosol particles may be estimated temporarily as

$$l_0 = \frac{1}{\sqrt[3]{n_0}}, \tag{2.1}$$

where n_0 is the number of particles in 1 cubic centimeter of the gas.

In reality, we deal with some statistical distribution in both mutual distances and velocities of particles. We assume that in unit volume of the gas, the number of particles which are able to get in contact with each other is expressed by the integral

$$\int_0^A n(l)\, dl, \tag{2.2}$$

where $n(l)$ is the distribution function, and A is the amplitude of particle vibrations:

$$\int_0^\infty n(l)\, dl = n_0. \tag{2.3}$$

The aerosols conform themselves in general to the Gauss type distribution, therefore we apply

$$n(l) = n_m e^{-\left(\frac{l-l_0}{L}\right)^2}. \tag{2.4}$$

The efficiency of the dust removal process as an result of what we call here the amplitude effect, may be described as

$$\eta_A = \frac{\int_0^A n(l)\, dl}{\int_0^\infty n(l)\, dl}. \tag{2.5}$$

By substitution of Eq. (2.4) into (2.5), the constant n_m is being reduced, and the L constant will be determined from experimental data.

Making use of definition of the error function:

$$\mathrm{Erf}(x) = \frac{2}{\sqrt{\pi}} \int_0^x e^{-t^2}\, dt \tag{2.6}$$

we may write

$$\eta_A = \frac{\mathrm{Erf}\left(\frac{l_0}{L}\right) + \mathrm{Erf}\left[\frac{l_0}{L}(\psi - 1)\right]}{\mathrm{Erf}\left(\frac{l_0}{L}\right) - 1}, \tag{2.7}$$

where ψ denotes the relative amplitude of particle vibrations:

$$\psi = \frac{A}{l_0}. \tag{2.8}$$

We calculate the value of the L constant by means of the following consideration: it is known from experiment [6, 7] that even at $\psi = 1.5$, the efficiency of acoustic purification is very high. Therefore, adopting arbitrarily the value $\eta_A = 0.99$ we obtain, by means of numerical solution of Eq. (2.7),

$$\frac{l_0}{L} = 3.3 \tag{2.9}$$

and

$$\eta_A = \frac{1}{2}\{1 + \mathrm{Erf}[3.3(\psi - 1)]\}. \tag{2.10}$$

Equation (2.10) is an estimation formula, but one thing is for sure: the efficiency of acoustic dedusting depends on relative amplitude (2.8), therefore it is worthwhile to calculate this quantity here.

The vibration maximum velocity amplitude of an aerosol particle in the acoustic field v_0 is expressed with the so-called drag coefficient μ and with the vibration velocity amplitude of the medium U_0 by means of a simple formula [5]:

$$v_0 = \mu U_0, \tag{2.11}$$

where

$$\mu = \frac{1}{\sqrt{1 + (\omega\tau)^2}} \tag{2.12}$$

ω is the angular frequency of vibrations, τ is the particle relaxation time given by (assumed applicability of the Stokes law):

$$\tau = \frac{2\varrho_p r^2}{9\eta}. \tag{2.13}$$

ϱ_p is the density of the aerosol particle, being r its radius and η the medium viscosity.

In dust removing devices we use in practice the plane wave, the intensity I of which is expressed by means of the formula [3]:

$$I = \frac{1}{2}\varrho_0 c_0 U_0^2, \tag{2.14}$$

where ϱ_0 is the rest density of the medium, c_0 is the acoustic wave velocity in this medium. Therefore, assuming that in practice the wave intensity is given, we have for the value of the medium vibration velocity amplitude:

$$U_0 = \sqrt{\frac{2I}{\varrho_0 c_0}}. \tag{2.15}$$

By Eqs. (2.11) and (2.15), the maximum amplitude of particle vibration is:

$$A = \frac{1}{\omega}\sqrt{\frac{2I}{\varrho_0 c_0}}\,\mu \tag{2.16}$$

and the dimensionless relative maximum amplitude ψ (2.11), (2.8):

$$\psi = \frac{\mu}{\omega}\sqrt{\frac{2I}{\varrho_0 c_0}}\sqrt[3]{n_0}\,. \tag{2.17}$$

In practice, we define usually the mass concentration of an aerosol s as the mass of dust particles contained in unit volume. We have obviously

$$n_0 = \frac{3}{4}\frac{s}{\pi r^3 \varrho_p}\,. \tag{2.18}$$

Substituting (2.18) to (2.17), we obtain the relative amplitude in its final form:

$$\psi = \frac{\mu}{r\omega}\sqrt{\frac{2I}{\varrho_0 c_0}}\sqrt[3]{\frac{3s}{4\pi\varrho_p}}\,. \tag{2.19}$$

During the process of dust removal, the above value should remain constant. For given acoustic wave, parameters μ and ω are defined, therefore we have a condition:

$$I \cdot s^{2/3} = \text{const}\,. \tag{2.20}$$

Thus, greater concentrations require smaller intensities and *vice versa*, which was confirmed by numerous experiments [7]. On the other hand, establishing all parameters except for the angular frequency ω, or frequency of vibrations ν, substituting Eq. (2.19) into (2.10) we obtain the dependence $\eta_A(\nu)$.

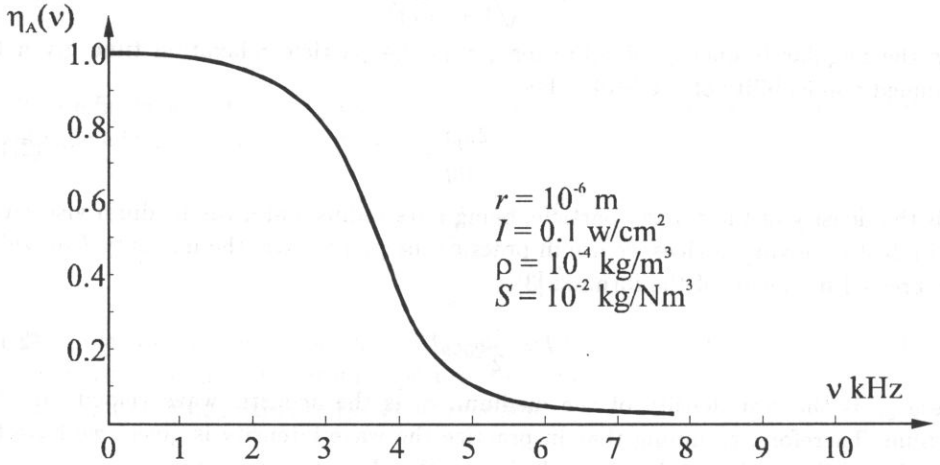

Fig. 1. An example of dependence $\eta_A(\nu)$ for conditions typical for acoustic dust removal process, described in the legend of the graph.

Figure 1 represents an example of this dependence for conditions typical for acoustic dust removal process, described in the legend of the graph. One can see that η_A is practically equal to unity up to several kHz and then rapidly falls to zero. This phenomenon is also well known from experiment [7]. From Eqs. (2.19) and (2.10), we may calculate a maximum value of the wave frequency which gives the value of η_A yet close to unity.

3. The inertial coagulation

Presently we proceed with consideration concerning the second factor influencing the overall efficiency of the acoustic coagulation the efficiency of the process of inertial sedimentation of smaller particles on bigger ones. Denoting this efficiency by η_i we may write the overall efficiency of the process η as

$$\eta = \eta_i \cdot \eta_A \,. \tag{3.1}$$

Numerous examinations show [1] that the quantity η_i is a function of the so called Stokes number, which for bigger particle of radius R is given by

$$n_{\mathrm{St}} = \frac{\tau v_w}{2R}\,, \tag{3.2}$$

where τ is the relaxation time of the settled (smaller) particle, v_w being the maximum amplitude of relative velocity of particles.

The problem of the $\eta_i(n_{\mathrm{St}})$ dependence has been discussed in numerous experimental and theoretical papers, based on assumption of potential flow-around and viscous flow-around [5]. In any case, this is a function growing from 0 to 1, however it reaches the upper value for $n_{\mathrm{St}} \approx 1$ according to experimental data, and 2–3 at theoretical curves. Therefore, in practice the problem is reduced to the value of the Stokes number, Eq. (3.2). We start form an analysis of relative velocity amplitude v_w as a function of angular frequency ω. From Eqs. (2.11) and (2.12) we see instantly that the function has to have a maximum – for $\omega = 0$ any particle, small or big, has the same velocity amplitude U_0, while the relative velocity is zero. At $\omega \to \infty$, the velocities of both particles tend to zero, and therefore the relative velocity is equal to zero also in this case.

For simplification of the following calculations, we assume that the relaxation time of the bigger particle is expressed by:

$$\tau_1 = \alpha\tau, \tag{3.3}$$

where obviously $\alpha > 1$.

Based on Eq. (3.4), we write formula for vibration velocity amplitude of the bigger particle:

$$v_{01} = \frac{U_0}{\sqrt{1+\omega^2\alpha^2\tau^2}} \tag{3.4}$$

and of the smaller one:

$$v_{02} = \frac{U_0}{\sqrt{1+\omega^2\tau^2}}\,. \tag{3.5}$$

The amplitude v_{01} is shifted in phase with respect to U_0 by an angle φ_1 defined by equation:

$$\varphi_1 = \tan^{-1}(\omega\alpha\tau) \tag{3.6}$$

and amplitude v_{02} is shifted by an angle

$$\varphi_2 = \tan^{-1}(\omega\tau). \tag{3.7}$$

Obviously, the relative velocity of both particles is shifted in phase by an angle φ:

$$\varphi = \varphi_1 - \varphi_2 , \tag{3.8}$$

or by an angle, tangent of which is equal to:

$$\tan\varphi = \frac{\omega\tau(\alpha-1)}{1+\omega^2\tau^2\alpha^2} . \tag{3.9}$$

The velocities v_{01} and v_{02} should be subtracted geometrically (because of the phase shift), therefore, introducing the relative drag coefficient μ_w

$$\mu_w = \frac{v_w}{U_0} \tag{3.10}$$

we may calculate it out from equation

$$\mu_w^2 = \frac{1}{1+\omega^2\alpha^2\tau^2} + \frac{1}{1+\omega^2\tau^2} - \frac{2\cos\varphi}{\sqrt{1+\omega^2\alpha^2\tau^2}\sqrt{1+\omega^2\tau^2}} \tag{3.11}$$

$\mu_w(\omega\tau)$ has, as one can easily prove, a maximum for the same value for which the function $\tan\varphi(\omega\tau)$ has its maximum, which makes the following calculations much easier. Namely, we have a condition:

$$\frac{d}{d(\omega\tau)}\tan\varphi = \frac{(\alpha-1)(1+\omega^2\tau^2\alpha) - 2\omega^2\tau^2\alpha(\alpha-1)}{(1+\omega^2\tau^2\alpha)^2} = 0, \tag{3.12}$$

or, after performing elementary calculations, we have from (2.13)

$$\omega\tau = \frac{1}{\sqrt{\alpha}} = \frac{r}{R} . \tag{3.13}$$

This value of $\omega\tau$ refers to

$$(\tan\varphi)_{\max} = \frac{1}{2}\frac{\alpha-1}{\sqrt{\alpha}} , \tag{3.14}$$

$$(\cos\varphi)_{\max} = \frac{2\sqrt{\alpha}}{\alpha+1} , \tag{3.15}$$

and

$$\mu_{w\ \max} = \frac{\alpha-1}{\alpha+1} . \tag{3.16}$$

For value $\omega\tau$ given by Eq. (3.13) we have the Stokes number equal to (3.13):

$$n_{\mathrm{St}} = \frac{\tau U_0}{2r} f(\alpha), \tag{3.17}$$

where

$$f(\alpha) = \frac{\alpha-1}{(\alpha+1)\sqrt{\alpha}} . \tag{3.18}$$

Figure 2 represents the dependence $\eta_A(\nu)$. The function has a maximum, which we presently calculate form the condition

$$\frac{df(\alpha)}{d\alpha} = 0, \tag{3.19}$$

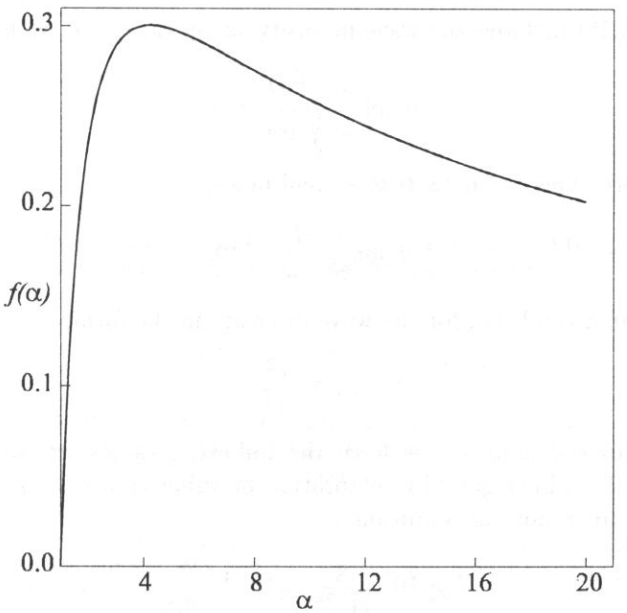

Fig. 2. The dependence $f(\alpha)$.

or

$$\frac{(\alpha+1)\sqrt{\alpha}-(\alpha-1)\sqrt{\alpha}-(\alpha-1)(\alpha+1)\dfrac{1}{2\sqrt{\alpha}}}{(\alpha+1)^2\alpha}=0. \tag{3.20}$$

We adopt here

$$\alpha_{\text{extr}}=2+\sqrt{5}=4.236 \tag{3.21}$$

as the other solution would be negative, which makes no sense. Therefore, the maximum value of $f_{\max}(\alpha)$ is equal to (3.18):

$$f_{\max}(\alpha)=0.305 \tag{3.22}$$

and the respective value $\omega\tau$ (3.13), referring to the maximum of relative velocity, is

$$\omega\tau=\frac{1}{\sqrt{2+\sqrt{5}}}=0.493 \tag{3.23}$$

and

$$\mu_{w\ \max}=0.618\,. \tag{3.24}$$

Taking into account that the real processes are realized statistically, one should assume that the inertial coagulation $\alpha<\alpha_{\text{extr}}$ (3.21) is very little probable. At the value of α_{extr} we have an optimum course of the process. At $\alpha>\alpha_{\text{extr}}$, as can be seen from Fig. 2, function $f(\alpha)$ decreases very slowly. The condition $n_{\text{St}}>1$ now takes the form:

$$\frac{\tau U_0}{2r}\cdot 0.305>1. \tag{3.25}$$

The condition (3.25) includes the wave intensity, as by Eq. (2.15) we have

$$0.305\frac{\tau}{2r}\sqrt{\frac{2I}{\varrho_0 c}} > 1, \tag{3.26}$$

or, by raising both sides of Eq. (2.2) to second power,

$$0.465\frac{\tau^2}{r^2}\frac{I}{\varrho_0 c} > 10. \tag{3.27}$$

Finally, we obtain a condition for the wave intensity in the form:

$$I > 21.5 \cdot \frac{r^2}{\tau^2}\varrho_0 c\,. \tag{3.28}$$

For average industrial aerosols we have the following values: $r^2 \approx 10^{-8}$ [cm^2] and $\tau^2 \approx 10^{-8}$ [s^2] [7], which give, by adaptation of value of $\varrho_0 c = 42$ [g/cm^{2}s] (corresponding to the air in normal conditions):

$$I \geq 10^3 \frac{\text{g}}{\text{cm}^2\text{s}} = 10^{-4}\frac{\text{W}}{\text{cm}^2}\,. \tag{3.29}$$

The calculated intensity value is tens thousand times weaker than the intensity required for occurrence of proper acoustical coagulation, i.e. related to the amplitude effect.

4. Conclusions

The described phenomenon is fully "responsible" for coagulating action of the acoustic field, and provides, with great excess, conditions in which the efficiency of the inertial coagulation may be considered as equal to unity.

References

[1] H. CZYŻ, *On the concentration of aerosol particles by means of drift forces in a standing wave field*, Acustica, **70**, 23–28 (1990).

[2] N.A. FUCHS, *The mechanics of aerosols*, Pergamon Press, London 1964.

[3] L.V. KING, *On the acoustic radiation on spheres*, Proc. Roy. Soc., **A 147**, 212–241 (1934).

[4] I. MALECKI, *Theory of acoustic waves and systems* [in Polish], PWN, Warszawa 1964.

[5] E.P. MEDNIKOV, *Acoustic coagulation and precipitation of aerosols*, Consultants Bureau, New York 1966.

[6] R. WYRZYKOWSKI, *Analysis of the possibility of increasing of sirens efficiency*, part II [in Polish], Technical University, **95**, 59–71, Wrocław (1964).

[7] R. WYRZYKOWSKI, *Comparative criteria and bases of calculatings of dust collectors* [in Polish], Technical University of Wrocław, **80**, 79–103, Wrocław (1963).

[8] R. WYRZYKOWSKI, *A theory of acoustic coagulation* [in Polish], University of Rzeszów, **1**, 125–135, Rzeszów (1969).

ARCHIVES OF ACOUSTICS
22, 4, 445–454 (1997)

THE MOTION OF GAS BUBBLES IN A LIQUID UNDER THE INFLUENCE OF ACOUSTICAL STANDING WAVE

H. CZYŻ and W. ŚCIUK

Institute of Physics, Pedagogical University of Rzeszów
(Rejtana 16a, 35-310 Rzeszów, Poland)
e-mail: hczyz@atena.univ.rzeszow.pl

This paper comprise the results of theoretical analysis of the problem of the forces influencing the gas bubbles in a liquid in a stationary wave field. The problem of the motion of small particles suspended in the gaseous medium (aerosols and fumes) has been studied intensively starting from the forties of our century in connection with the technical application of the acoustic coagulation for the precipitation of gases. This paper considers the equation of the motion of a gas bubble in a standing wave field under the influence of the drift and the resistance forces in the Stokes and Oseen approximation. We take into account the drift related to the radiation pressure, periodic viscosity changes and the asymmetry of motion of gas bubble vibrating in a standing wave field. This study considers an estimation of the intensity of the drift forces of types R, L and A as a function of the bubble radius at 10 – 100 kHz frequency of the wave. We give the general properties of the solutions of the motion equation of the gas bubble in the case of large attenuation constants, corresponding for typical values of the drift forces.

Notations

F_D – drift force,
A_D – drift intensity amplitude,
m_p – gas bubble mass,
r – gas bubble radius,
μ_g – gas bubble flow-around coefficient,
μ_p – gas bubble entrainment coefficient,
E – acoustic wave energy density,
k – wave number,
x – gas bubble position,
η – medium viscosity,
ω – angular frequency,
f – frequency,
t – time,
ϱ_g – medium density,
ϱ_p – gas bubble density.

1. Introduction

The drift forces, a consequence of interaction between the gas bubble and the vibrating medium, result from such phenomena as the radiation pressures, the asymmetric

vibration motion of the gas bubble or periodic changes in the viscosity of the liquid. The first mechanism of the drift has been presented by KING [6] and is called the radiation drift, the R – type drift in short. It is connected with the radiation pressure acting on the gas bubble as the result of momentum carried out by acoustic wave diffracted on the particle. This type of drift is important for large gas bubbles.

For small gas bubbles of radii of order of microns, authors introduced different mechanisms [7]. The most important models concern the effect of variations of viscosity in the wave field caused by local changes of the temperature during periodical compressions and decompressions of the medium [7]. This type of drift is called the viscosity drift, and the L – type drift in short.

Another type of drift is characteristics only of a standing wave. It results from the fact that in such a wave the vibration amplitude of the medium depends on position being greater in the area of loops. In view of their inertia, gas bubbles do not keep pace with the motion of the medium and are affected by variable forces over the time of their oscillation. Asymmetry drift is the most natural one and its mechanism is physically the most fundamental, it is called the A – type drift in short [2].

Different kinds of drift have a common property: the forces applied on the gas bubble depend in the same way on its position with respect to the loops and nodes of the standing wave and are proportional to the density of the wave energy. The drift forces depend strongly on the gas bubble size [4]. Below, consideration is given only to the problem of the motion of a single gas bubble. This means that the effect of interaction of gas bubbles is neglected, i.e., the process leading to augmentation itself, namely the fact that smaller gas bubbles link to form larger aggregates. Causing gas bubbles to gather near points of stable equilibrium (minima of the potential of the drift forces), the phenomena caused by the drift forces assist in a way the elementary acts of augmentation by increasing the concentration of gas bubbles near the nodes or loops of the standing wave.

2. Analysis of the equation of motion

It appears that, irrespective of the mechanism of the occurrence of drift forces, they can be described by the formula [1]

$$F_D(x) = F_0 \sin(2kx), \tag{2.1}$$

where F_0, constant, denotes the value of the drift force amplitude. The forces of this type are called the drift forces. The position of the potential minima

$$U_D(x) = F_0(2k)^{-1} \cos(2kx) + \text{const} \tag{2.2}$$

depends on the sign of the constant describing the maximum value of drift force. It is clear, that the sign of the constant has no effect on the kinetics of the process of gas bubble transport.

The equation of motion of the average position of the gas bubble is [1]

$$m_p \frac{d^2x}{dt^2} = -C_{\mathrm{St}} \frac{dx}{dt} - C_{\mathrm{Os}} \frac{dx}{dt} \left| \frac{dx}{dt} \right| + F_0 \sin(2kx) \tag{2.3}$$

or

$$m_p \frac{d^2x}{dt^2} = -6\pi\eta r \frac{dx}{dt} - \frac{9}{4}\pi r^2 \varrho_p \frac{dx}{dt}\left|\frac{dx}{dt}\right| + F_0 \sin(2kx). \tag{2.4}$$

The first term on the right side of the equation represents the Stokes force, the second one represents the nonlinear Oseen correction which is significant for large Reynolds numbers. This equation is nonlinear in view of the last two terms. The above simple differential equation has no elementary solution. To estimate on the character of the solution, let us reduce to a minimum the number of constants in the equation (2.5) by replacing the position and time by the nondimensional variables

$$y = \pi - 2kx \qquad \theta = (2kA_D)^{1/2}, \tag{2.5}$$

where the quantity $A_D = F_0/m_p$ which by analogy to other interactions, can be called the intensity of the drift force field.

On the basis of the formulae for the radiation drift [2]

$$F_R = \frac{8}{3}\pi k r^3 \mu_g^2 E \sin(2kx) \tag{2.6}$$

the asymmetry drift [2]

$$F_A = -\frac{1}{2} m_p \varrho_g^{-1} k \mu_p^2 \sin(2kx) \tag{2.7}$$

and the viscosity drift [2]

$$F_L = 3\pi(\kappa - 3) r \mu_g^2 \eta (\varrho_g c)^{-1} E \sin(2kx) \tag{2.8}$$

we obtain the amplitudes of the drift intensity A_{DR}, A_{DA}, A_{DL} (the symbols R, L, A distinguish the considered types of the drift).

$$A_{DR} = 2\varrho_p^{-1} k \mu_g^2 E, \tag{2.9}$$

$$A_{DA} = -\frac{1}{2}\varrho_g^{-1} k \mu_p^2 E, \tag{2.10}$$

$$A_{DL} = \frac{9}{4}(\kappa - 3)\eta r^{-2} (\varrho_p \varrho_g c)^{-1} \mu_g^2 E. \tag{2.11}$$

The amplitudes of the drift intensity are proportional to the wave number k and to the wave energy density E.

In calculating the numerical values it is assumed that the density of acoustic wave $E = 100\ \mathrm{J/m^3}$, $c = 1500\ \mathrm{m/s}$, $\varrho_p = 1.249 \cdot 10^3\ \mathrm{kg/m^3}$, $\varrho_g = 1000\ \mathrm{kg/m^3}$, $\eta = 1.8 \cdot 10^{-3}\ \mathrm{N\,s/m^2}$.

Figures 1 a, b, c, d, e, f show plots of the intensity of the field of the drift forces of types R, L and A as a function of the gas bubble radius. The horizontal dashed line represents the acceleration of gravity. The plots made on a double logarithmic scale. This makes it easy to read the values of intensity for a density of the wave energy other than the given one, since the quantities represented in plots depend on E in a linear way and an increase or decrease in this value by one order of magnitude causes the same change in the value of the intensity drift fields.

Analysis of the plots indicates that particular kinds of drift dominate various intervals of variation of the particle radius.

a)

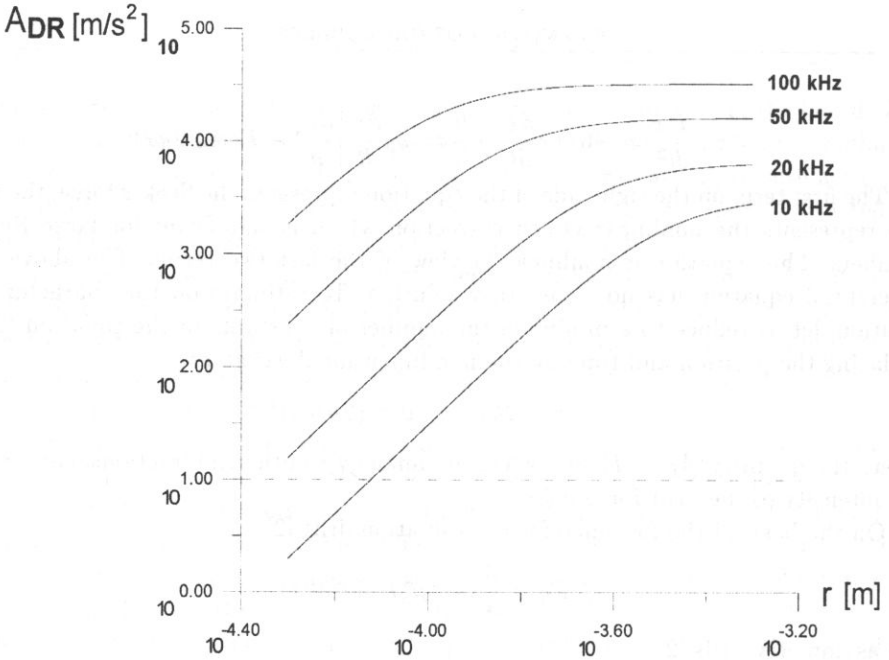
A_{DR} [m/s^2]
$10^{5.00}$
$10^{4.00}$
$10^{3.00}$
$10^{2.00}$
$10^{1.00}$
$10^{0.00}$
100 kHz
50 kHz
20 kHz
10 kHz
r [m]
$10^{-4.40}$
$10^{-4.00}$
$10^{-3.60}$
$10^{-3.20}$

b)

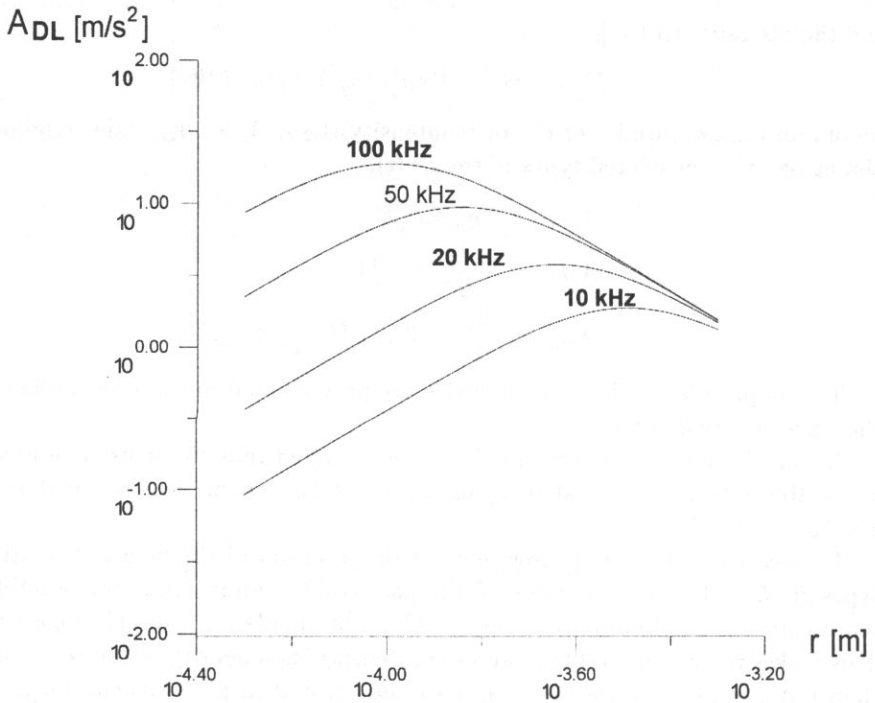
A_{DL} [m/s^2]
$10^{2.00}$
$10^{1.00}$
$10^{0.00}$
$10^{-1.00}$
$10^{-2.00}$
100 kHz
50 kHz
20 kHz
10 kHz
r [m]
$10^{-4.40}$
$10^{-4.00}$
$10^{-3.60}$
$10^{-3.20}$

[FIG. 1 a, b]

c)

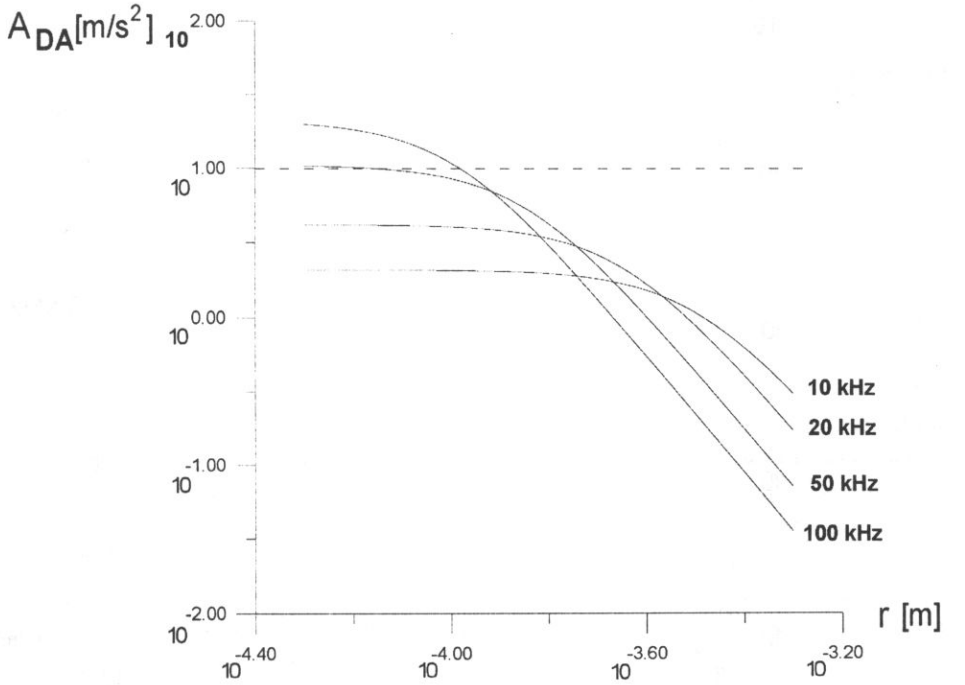
$A_{DA}[m/s^2]$
$10^{2.00}$
$10^{1.00}$
$10^{0.00}$
$10^{-1.00}$
$10^{-2.00}$
10 kHz
20 kHz
50 kHz
100 kHz
r [m]
$10^{-4.40}$
$10^{-4.00}$
$10^{-3.60}$
$10^{-3.20}$

d)

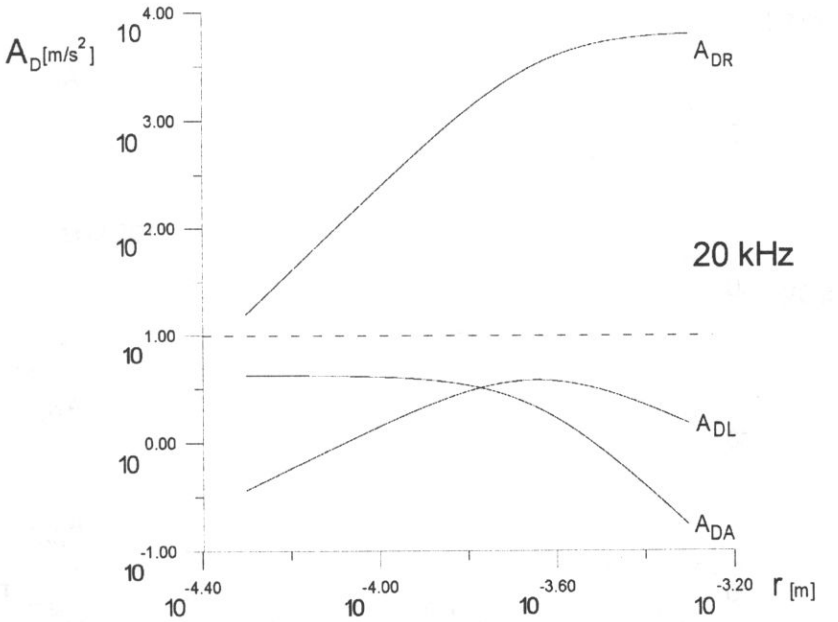
$A_{D[m/s^2]}$
$10^{4.00}$
$10^{3.00}$
$10^{2.00}$
$10^{1.00}$
$10^{0.00}$
$10^{-1.00}$
A_{DR}
20 kHz
A_{DL}
A_{DA}
$10^{-4.40}$
$10^{-4.00}$
$10^{-3.60}$
$10^{-3.20}$
r [m]

[FIG. 1 c, d]

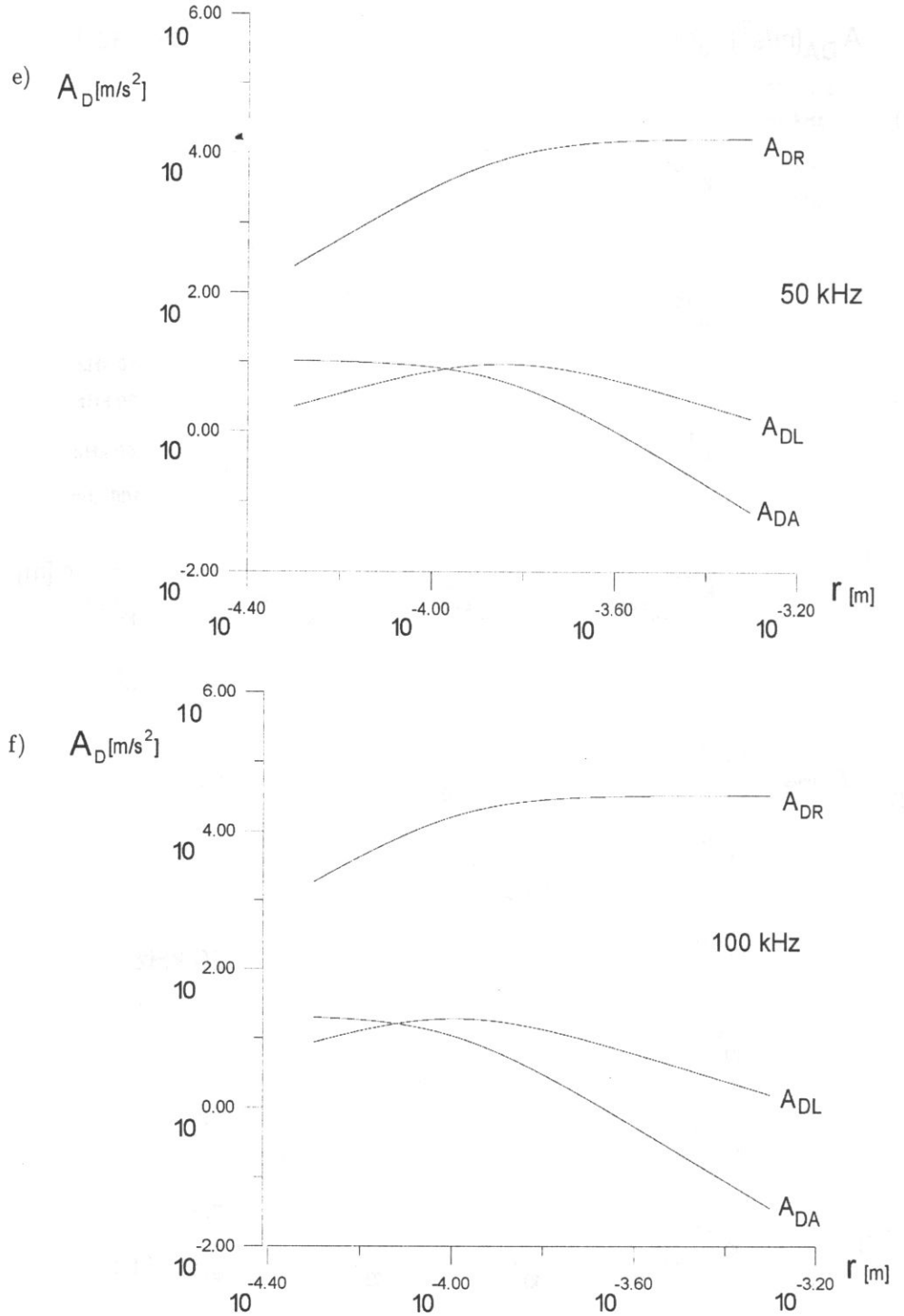

Fig. 1. Plots of the intensity of the field of the drift forces a) of type – R, b) of type – L, c) of type – A, as a function of the gas bubble radius, at 20 kHz, 50 kHz, 100 kHz, and of types R, L and A as a function of the gas bubble radius d) at 20 kHz, e) at 50 kHz, f) at 100 kHz. The horizontal dashed line represents the acceleration of gravity.

The equation of motion becomes

$$\frac{d^2y}{d\theta^2} + \alpha\frac{dy}{d\theta} + \beta\frac{dy}{d\theta}\left|\frac{dy}{d\theta}\right| + \sin(y) = 0, \tag{2.12}$$

where the following was introduced

$$\alpha = \tau^{-1}(2kA_D)^{-1/2}, \tag{2.13}$$

$$\beta = \frac{27\varrho_g}{32kr\varrho_p}. \tag{2.14}$$

The equation of motion in this form (2.12) contains only two constant, whereas the initial equation (2.3) contained four of them (including the wavenumber). The gas bubble mass, the drift force and the wavelength, are normalized in a way in this equation making it easier to analyze the effect of the two dissipation terms on the solution. The constants α and β depend on the parameters characterizing the gas bubble and the wave. The constant α depends on the intensity of the drift force field, and on the kind of drift.

Assuming that same numerical values which were used in calculating the quantity A_D, one can estimate the constants α and β, and, thus, evaluate the two terms representing friction in the equation of motion.

Figures 2 a, b, c show plots of the constants α and β of equation (2.12) as a functions of the gas bubble and frequency. The symbols R, L and A distinguish the considered types of drift.

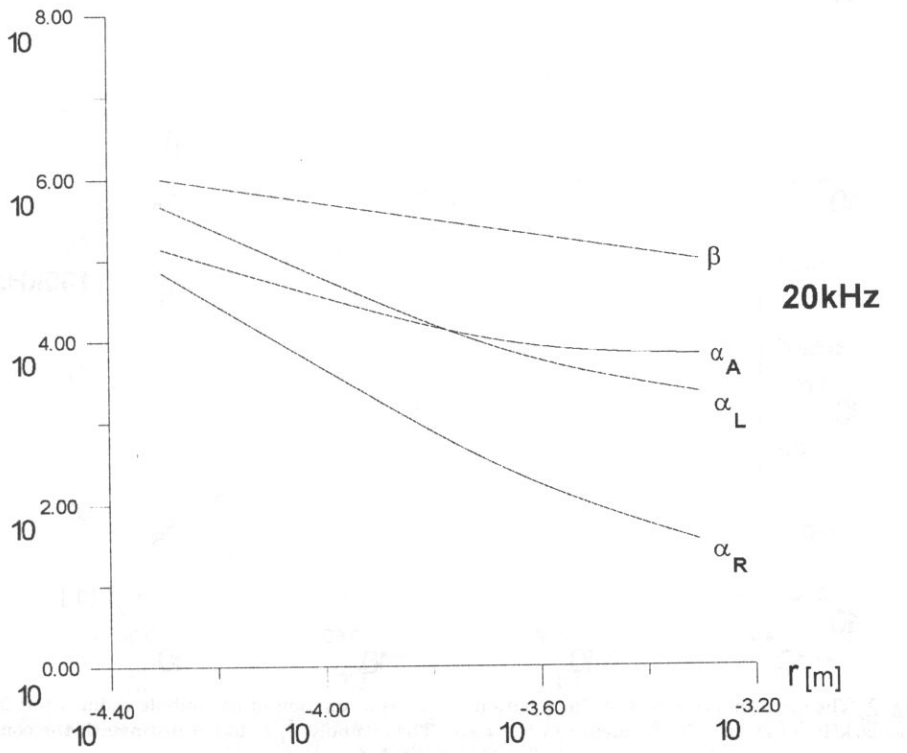

[FIG. 2 a]

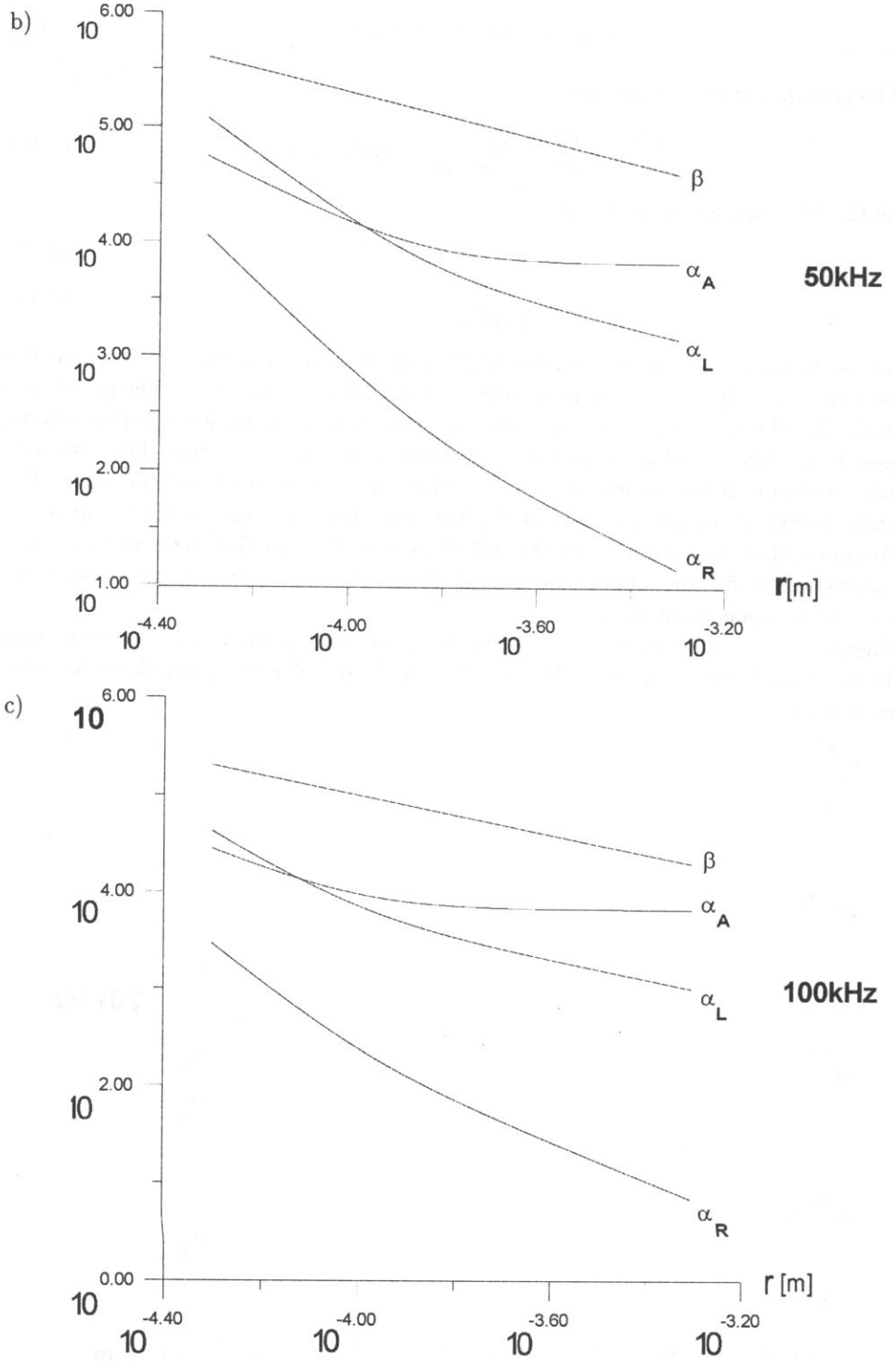

Fig. 2. The constants α and β of the equation (2.12) as a function of gas bubble radius a) at 20 kHz, b) at 50 kHz, c) at 100 kHz frequency of the wave. The symbols R, L and A distinguish the considered types of the drift.

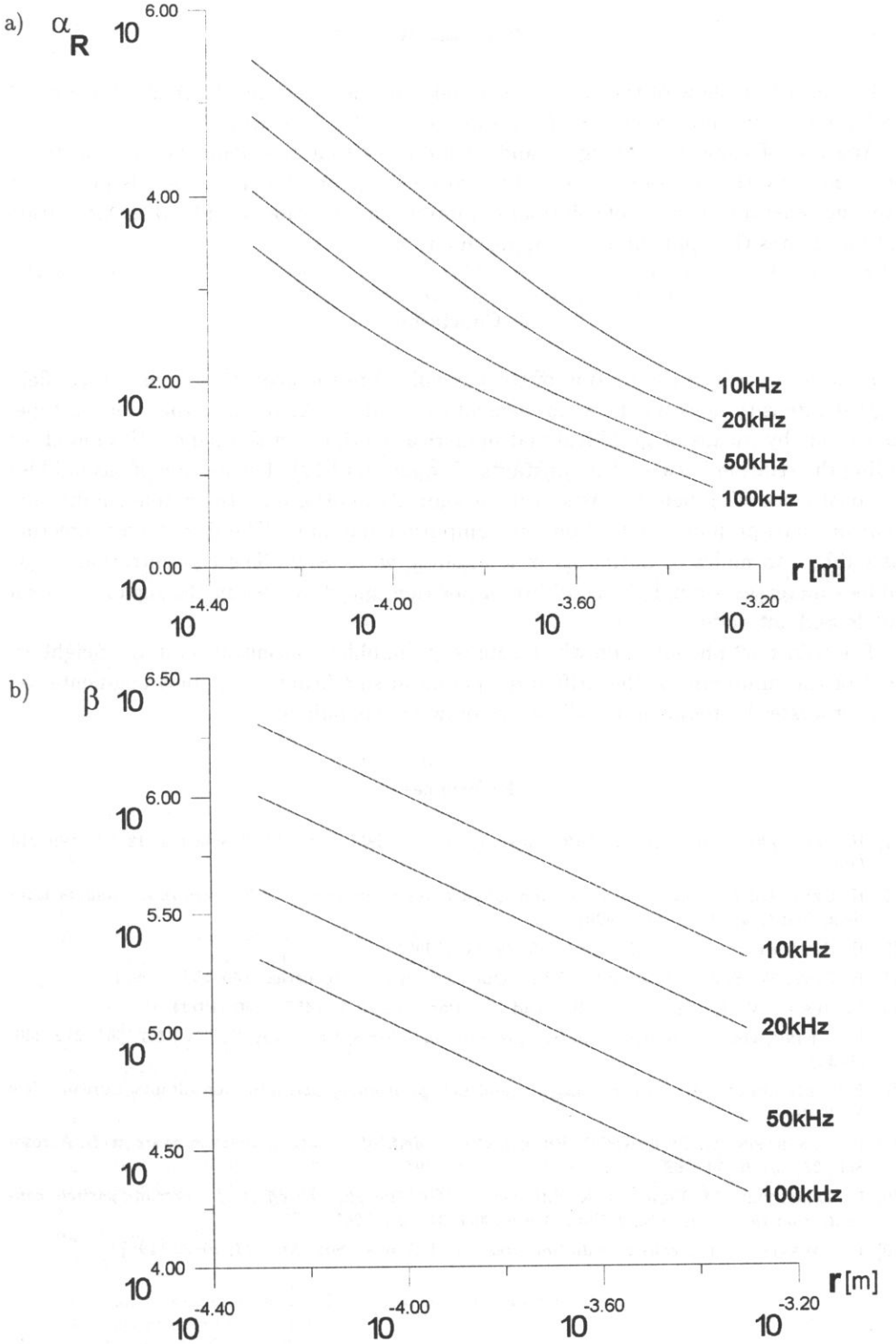

Fig. 3. The constants a) α, b) β of the equation of motion (2.12) as a function of the gas bubble radius at 10 kHz, 20 kHz, 50 kHz, 100 kHz, for R – type of drift.

Figures 3 a, b show of the constants α and β of the equation (2.12) as a function of gas bubble radius and frequency of the wave for the R – type drift.

Analysis of these plots (Figs. 2 and 3) indicates that the nonlinear friction term, represented by the constant β (the Ossen correction) can play a role in this motion. It gives the general properties of solutions of motion equations for considerable attenuation and formulates the applicability of approximation.

3. Conclusion

Equation (2.12) of the motion of the gas bubble in the acoustic standing wave field of great intensity does not have an elementary solution. Analysis of the solution type, carried out by means of graphical and numerical methods in the paper [1] allowed for finding the relation between the constants of equation (2.12). The motion of gas bubbles in acoustic standing field consists in monotonically approaching the stable equilibrium point or quasi-periodical vibration with amplitude damping. The drift forces directing gas bubbles to nodes or antinodes of a standing wave [8, 9]. The concentration of gas bubbles increases around the equilibrium position and decreases in the region between a node and antinode.

The transport phenomenon which causes gas bubbles concentration in the neighborhood of the minimum of the drift force potential significantly supports augmentation microprocesses by reducing the distances between gas bubbles.

References

[1] H. CZYŻ, *The aerosol particle drift in a standing wave field*, Archives of Acoustics, **12**, 3-4, 199–214 (1987).

[2] H. CZYŻ, *On the concentration of aerosol particles by means of drift forces in a standing wave field*, Acustica, **70**, 23–28, (1990).

[3] H. CZYŻ, Proc. of the XIIIth SHA' 96, 79–84, (1996).

[4] H. CZYŻ, W. ŚCIUK, Proc. of the XLIII Open Seminar on Acoustics, 149–154, (1996).

[5] M. JESSEL, V. TIMOSHENKO, C.R. Acad. Sci. Paris, vol. 272, 1457–1460 (1971).

[6] L.V. KING, *On the acoustic radiation pressure on spheres*, Proc. Roy. Soc. A., **147**, 861, 212–240, (1934).

[7] E.P. MEDNIKOV, *Acoustic coagulation and precipitation of aerosols*, Consultants Bureau, New York 1966.

[8] P. VAINSHTEIN, M. FICHMAN, D. PNUELI, *On the drift of aerosol particles in sonic fields*, Aerosol Sci., **23**, 631–637 (1992).

[9] P. VAINSHTEIN, M. FICHMAN, K. SHUSTER, C. GUTFINGER, *The effect of centerline particle concentration in a wave tube*, J. Fluid Mech., **306**, 31–42 (1996).

[10] P.J. WESTERVELT, *Acoustic radiation pressure*, J. Acoust. Soc. Am., **23**, 26–29 (1957).

ARCHIVES OF ACOUSTICS
22, 4, 455–462 (1997)

THE REAL ACOUSTIC POWER OF A PLANAR ANNULAR MEMBRANE RADIATION FOR AXIALLY-SYMMETRIC FREE VIBRATIONS

W.J. RDZANEK and W.P. RDZANEK, JR

Institute of Physics, Pedagogical University
(35–311 Rzeszów, Rejtana 16a, Poland)

The real part of the acoustic power radiated by a planar annular membrane is considered for axially-symmetric free vibrations. The membrane is located in a planar, rigid baffle and radiate acoustic wave into a lossless and homogeneous fluid medium. Sinusoidal in time processes are examined. The real power is obtained as elementary form for high-frequency radiated waves.

Notations

c propagation velocity of an acoustic wave in a fluid medium of density ϱ_0,
$J_m(x)$ Bessel function of the m-th order,
k $= r_2/r_1$,
k_n $= \omega_n\sqrt{\sigma/T}$,
k_0 $= 2\pi/\lambda$,
N acoustic power radiated by the membrane (3.1),
N' normalised power radiated by the membrane,
$N_m(x)$ Neumann function of the m-th order,
p acoustic pressure,
r radial variable,
r_1, r_2 radii of the annular membrane,
S $= \pi(r_2^2 - r_1^2)$,
T stretching force of the membrane, referred to unit length,
t time,
v normal component of vibration velocity of points of the membrane surface,
v_n vibration velocity of points on the surface of the membrane for mode $(0, n)$,
W characteristic function of planar annular source for $(0, n)$ vibration mode $(6')$,
x_n n-th root of the equation (2.2),
α_n $= J_0(x_n)/J_0(kx_n)$,
β $= k_0 r_1$,
δ_n $= x_n/\beta$,
η transverse displacement of points of the membrane surface,
λ wavelength in a fluid medium,
ϱ_0 density of a fluid medium,
σ surface density of the membrane,
ω_n angular frequency of free vibrations, corresponding to mode $(0, n)$.

1. Introduction

Planar vibrating sources are important for problems of generation and propagation of acoustic waves in a fluid medium. Most of research concentrates on analyse of rectangular and axially-symmetric sources. Extensive universal research of axially-symmetric sources are realised on acoustic wave radiation by: vibrating circular pistons (e.g. PRITCHARD [5], PORTER [4]), planar angular pistons (e.g. THOMPSON [8], MERRIWEATHER [3]) and membranes and circular plates (e.g. LEVINE and LEPPINGTON [2], RDZANEK [6] and [7]). Those papers, concerning membranes and circular plates, includes problems: the energetic aspect of radiating sources, acoustic interactions of particular elements of the source surface, constituent elements of sources array, vibration form influence on the resultant field radiated by vibrating array.

Up to now there were no elementary equations of acoustic power radiated by the planar annular vibrating membrane.

The classical mathematical method was used and the equation of the form of the Bouwkamp's integral [8] for the real part of acoustic power radiated by a planar annular membrane in case of axially-symmetric free vibrations. The considered processes were varying sinusoidally with time. Use of LEVIN and LEPINGTON'S mathematical method [2] based on Cauchy's theorem of residua allowed the derivation of the equation of real part of acoustic power of elementary form in special case for high-frequency waves' radiation. Frequency characteristics of described acoustic power are also presented graphically.

2. The annular membrane's free vibrations

The membrane is tight on two circles with radii r_1 and r_2, and $r_1 < r_2$. We consider axially-symmetric free vibrations sinusoidal in time. The transverse deflection of points of the membrane surface $\eta(r,t) = \eta(r)\exp(i\omega t)$ with boundary conditions $\eta(r_2,t) = \eta(r_1,t) = 0$ is represented by the n-th radial form of free vibrations

$$\eta_n(r)/A_n = J_0\left(x_n\frac{r}{r_1}\right) - \frac{J_0(x_n)}{N_0(x_n)}N_0\left(x_n\frac{r}{r_1}\right), \tag{2.1}$$

where J_0, N_0 are cylindrical functions of null order correspondingly Bessel's and Neumann's. The value $x_n = k_n r_1$ is the n-th frequency equation's root

$$\frac{J_0(kx_n)}{J_0(x_n)} = \frac{N_0(kx_n)}{N_0(x_n)}, \tag{2.2}$$

where $k = r_2/r_1 \geq 1$ and $k_n = \omega_n\sqrt{\sigma/T}$, ω_n is n-th free frequency, σ is surface density of the membrane, T is the stretching force of the membrane. The Table 1 includes some values of the frequency equation's roots (2.2) (compare [1]).

We calculate the constant A_n from the normalisation condition

$$\int_{r_1}^{r_2} \eta_n^2(r)r\,dr = \frac{1}{2}(r_2^2 - r_1^2). \tag{2.3}$$

Table 1. Roots x_n of equation $J_0(x_n)N_0(kx_n) - J_0(kx_n)N_0(x_n) = 0$.

	k					
n	1.1	1.2	1.5	2	3	5
1	31.412314	15.701344	6.270239	3.123029	1.548459	0.7631913
2	62.830045	31.412615	12.559773	6.273438	3.129084	1.5571072
3	94.246574	47.121681	18.845157	9.418203	4.703797	2.3464207
4	125.662802	62.830196	25.129431	12.561424	6.276664	3.1340324
5	157.078909	78.538490	31.413277	15.703999	7.848734	3.9208424
6	188.494956	94.246675	37.696903	18.846253	9.420391	4.7072157

We get than

$$A_n = \frac{\pi}{2} x_n (k^2 - 1)^{1/2} \left\{ \frac{1}{N_0^2(kx_n)} - \frac{1}{N_0^2(x_n)} \right\}^{-1/2}. \tag{2.3'}$$

3. An integral form of the acoustic power

Let the source of surface S of the normal component of the vibration velocity v radiate acoustic pressure p. Than $N = \frac{1}{2} \int_S pv^* \, dS$ is the acoustic power radiated by the source. v^* is here a value conjugate with a complex value v.

We calculate the acoustic power of the source of the axial symmetry on the basis of the integral equation (compare the Bouwkap's integral [8] and the paper [6])

$$N = \pi \varrho_0 c k_0^2 \int_0^{\pi/2 - i\infty} W^2(\vartheta) \sin\vartheta \, d\vartheta, \tag{3.1}$$

where c is the velocity of propagation of the wave in a fluid medium of density in rest stage ϱ_0, $k_0 = 2\pi/\lambda$ is a wave number, λ is wavelength and

$$W(\vartheta) = \int_{r_1}^{r_2} v(r) J_0(k_0 r \sin\vartheta) r \, dr \tag{3.2}$$

is the characteristic function of planar annular sound source, constraints radii of which are r_1 and r_2, $v_n(r) = -i\omega_n \eta_n(r)$ is the normal component of vibration velocity in the case of $(0, n)$ vibration mode. The integral (3.1) is calculated in the plane of the complex variable $\vartheta = \vartheta' + i\vartheta''$.

If $k_0 \to \infty$ then $p(r) = \varrho_0 c v(r)$, $N^{(\infty)} = \frac{1}{2} \varrho_0 c \int_S v^2 \, dS$ and than it is comfortable to use for calculations the normalised radiation power $N/N^{(\infty)}$.

Inserting the characteristic function

$$\frac{W_n(\vartheta)}{-i\omega_n A_n} = \frac{2}{\pi} \frac{r_1^2}{x_n^2 - \beta^2 \sin^2\vartheta} \frac{1}{N_0(x_n)} \{\alpha_n J_0(k\beta \sin\vartheta) - J_0(\beta \sin\vartheta)\}, \tag{3.3}$$

calculated on the basis of equations (3.2) and (2.1), into the equation (3.1), we get

$$\frac{N_n}{N_n^{(\infty)}} = \frac{2\delta_n^2}{\alpha_n^2 - 1} \int_0^{\pi/2 - i\infty} \left\{ \frac{\alpha_n J_0(k\beta \sin\vartheta) - J_0(\beta \sin\vartheta)}{\sin^2\vartheta - \delta_n^2} \right\}^2 \sin\vartheta \, d\vartheta, \tag{3.4}$$

where $\delta_n = x_n/\beta$, $\beta = k_0 r_1$, $\alpha_n = J_0(x_n)/J_0(kx_n)$.

If we confine integration in equation (3.4) to real values $0 \leq \mathrm{Re}(\vartheta) \leq \pi/2$ and substitute $\sin\vartheta' = x$, then we get integral equation

$$N_n' = \frac{2\delta_n^2}{\alpha_n^2 - 1} \int_0^1 \left\{ \frac{\alpha_n J_0(k\beta x) - J_0(\beta x)}{x^2 - \delta_n^2} \right\}^2 \frac{x \, dx}{\sqrt{1 - x^2}}, \tag{3.4'}$$

where $N_n' = \mathrm{Re}\{N_n/N_n^{(\infty)}\}$ is the real component of the normalised acoustic power radiated by the n-th axially-symmetric mode of the planar annular membrane.

4. The membrane's radiation for the high frequency range

If $\delta_n < 1$ ($\delta_n^2 \ll 1$) then analysing equation (3.4') is much more easy. We use the mathematical method of LEVIN and LEPPINGTON [2] and we introduce a function of a complex variable

$$F(z) = \left\{\alpha_n^2 J_0(k\beta z) - 2\alpha_n J_0(\beta z)\right\} H_0^{(1)}(k\beta z) + J_0(\beta z) H_0^{(1)}(\beta z) \tag{4.1}$$

such that

$$\mathrm{Re}\, F(z) = \{\alpha_n J_0(k\beta x) - J_0(\beta x)\}^2, \tag{4.1'}$$

where x is a real variable, $H_0^{(1)}$ is the Hankel's function of 1-st kind and null order.

The base of analysis is the equation which left side is the contour integral

$$\int_C \frac{zF(z)\, dz}{\sqrt{1 - z^2}(z^2 - \delta_n^2)^2} = 0 \tag{4.2}$$

calculated for contour C (Fig. 1) inside which the integrand is single-valued and regular (comp. [9]). There are no contributions during integration both over a big circle when its radius increases infinitely and over arcs of small circles around the points of branching ($z = 0$, $z = 1$), when their radii decreases tending to null. At the point $z = \delta_n$ the integrand (4.2) has a pole of 2-nd order.

On applying the Cauchy's theorem concerning residua, we get the integral (4.2) of the form

$$\mathcal{P} \int_0^1 \frac{xF(x)\, dx}{\sqrt{1 - x^2}(x^2 - \delta_n^2)^2} - \pi i \, \mathcal{F}'(\delta_n) + \int_1^\infty \frac{xF(x)\, dx}{-i\sqrt{x^2 - 1}(x^2 - \delta_n^2)^2} + \int_\infty^0 \frac{-yF(iy)\, dy}{\sqrt{y^2 + 1}(y^2 + \delta_n^2)^2} = 0, \tag{4.2'}$$

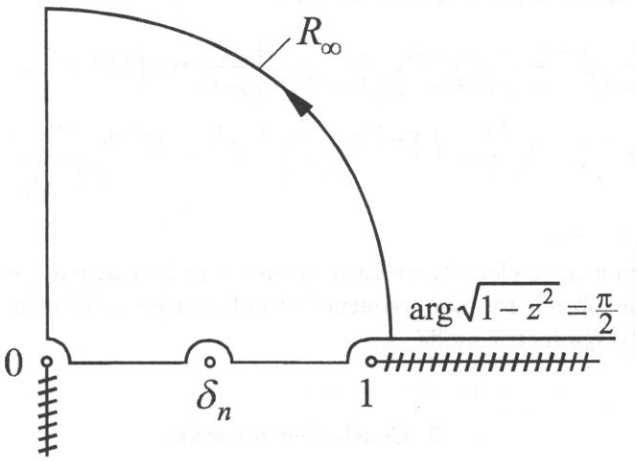

Fig. 1. The integration contour C for pattern (4.2) (comp. the paper [2]).

where the auxiliary function is introduced

$$\mathcal{F}(z) = \frac{zF(z)}{\sqrt{1-z^2}(z+\delta_n)^2} \tag{4.3}$$

and the integral $\mathcal{P}\int_0^1$ is interpreted as a principal value. We take into account that $\operatorname{Re} F(iy) = 0$, then

$$\operatorname{Re}\left\{\mathcal{P}\int_0^1 \frac{xF(x)\,dx}{\sqrt{1-x^2}(x^2-\delta_n^2)^2}\right\} = \int_0^1 \left\{\frac{\alpha_n J_0(k\beta x) - J_0(\beta x)}{x^2-\delta_n^2}\right\}^2 \frac{x\,dx}{\sqrt{1-x^2}}$$

$$= \int_0^1 \frac{\alpha_n N_0(k\beta x)\,[\alpha_n J_0(k\beta x) - 2J_0(\beta x)] + J_0(\beta x)N_0(\beta x)}{(x^2-\delta_n^2)^2} \frac{x\,dx}{\sqrt{x^2-1}}$$

$$+ \operatorname{Re}\{\pi i\,\mathcal{F}'(\delta_n)\}. \tag{4.4}$$

We also take into account that $F(\delta_n) = 0$, $\operatorname{Re} F'(\delta_n) = 0$, $\operatorname{Im} F'(\delta_n) = \frac{2}{\pi\delta_n}(1-\alpha_n^2)$ and finally

$$\operatorname{Re}\{\pi i\,\mathcal{F}'(\delta_n)\} = \frac{\alpha_n^2 - 1}{2\delta_n^2\sqrt{1-\delta_n^2}}. \tag{4.5}$$

Now we calculate the integral (4.4) inside of interval $[1,\infty)$, applying the asymptotic expressions

$$J_0(ax)N_0(bx) \sim \frac{1}{\pi x\sqrt{ab}}\{\sin(b-a)x - \cos(b+a)x\}, \tag{4.6}$$

$$\int_1^\infty \frac{e^{imx}\,dx}{\sqrt{x^2-1}(x^2-\delta_n^2)^2} = \sqrt{\frac{\pi}{2m}}\left\{(1-\delta_n^2)^{-2} + O\left(\frac{1}{m}\right)\right\} e^{i(m+\pi/4)}. \tag{4.7}$$

In this way, we obtain instead of equation (3.4′)

$$N'_n = \frac{1}{\sqrt{1-\delta_n^2}} + \frac{\delta_n^2}{\beta\sqrt{\pi\beta}(1-\alpha_n^2)(1-\delta_n^2)^2}\left\{\frac{\alpha_n^2}{k\sqrt{k}}\cos\left(2k\beta+\frac{\pi}{4}\right)\right.$$
$$\left. + \cos\left(2\beta+\frac{\pi}{4}\right) + 2\sqrt{\frac{2}{k}}\alpha_n\left(\frac{\sin\left((k-1)\beta+\frac{\pi}{4}\right)}{\sqrt{k-1}} - \frac{\cos\left((k+1)\beta+\frac{\pi}{4}\right)}{\sqrt{k+1}}\right)\right\} \tag{4.8}$$

with error $o(\delta_n^2\beta^{-3/2})$.

This equation is of an elementary form – convenient for calculations of the real power of the annular membrane for high frequency of radiated waves if the membrane vibrates with n-th axially-symmetric mode.

5. Concluding remarks

As result of theoretical analysis of the problem of radiation of a planar annular membrane the elementary expression was derived for normalised real acoustic power of axially-symmetric modes of free vibrations. This expression can be used for digital calculations only if the condition $x_n < \beta = k_0 r_1$ is satisfied.

There were given proper components which have essentially an "oscillating" character of changes of the real component of power of annular membrane (Fig. 2 and Fig. 3).

In case when the condition $x_n < k_0 r_1$ is not satisfied or when we need high accuracy of results, one should perform numerical calculations based on the integral equation (3.4′).

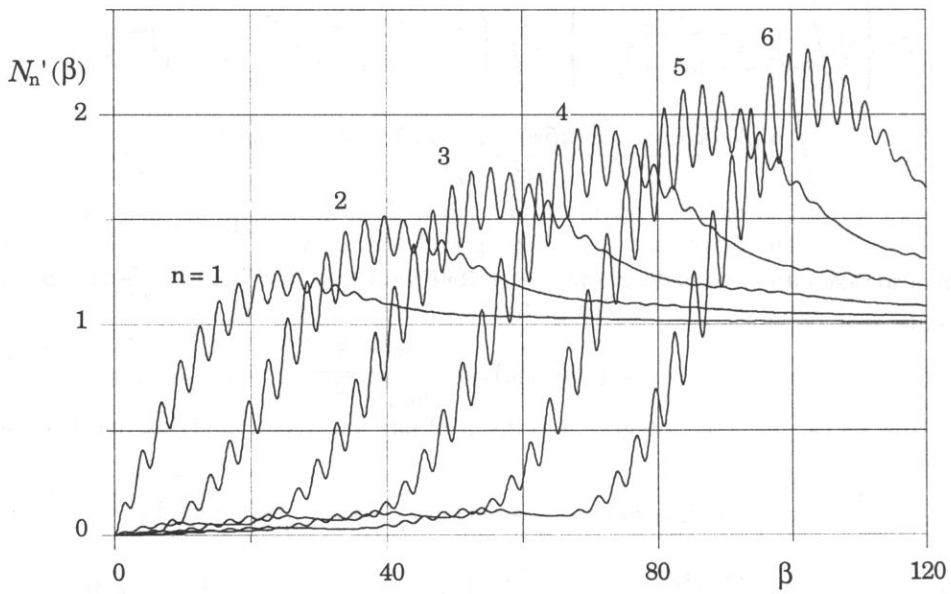

Fig. 2. Normalised real component of acoustic power radiated by the planar annular membrane versus β for modes $(0, n)$ and $k = 1.2$.

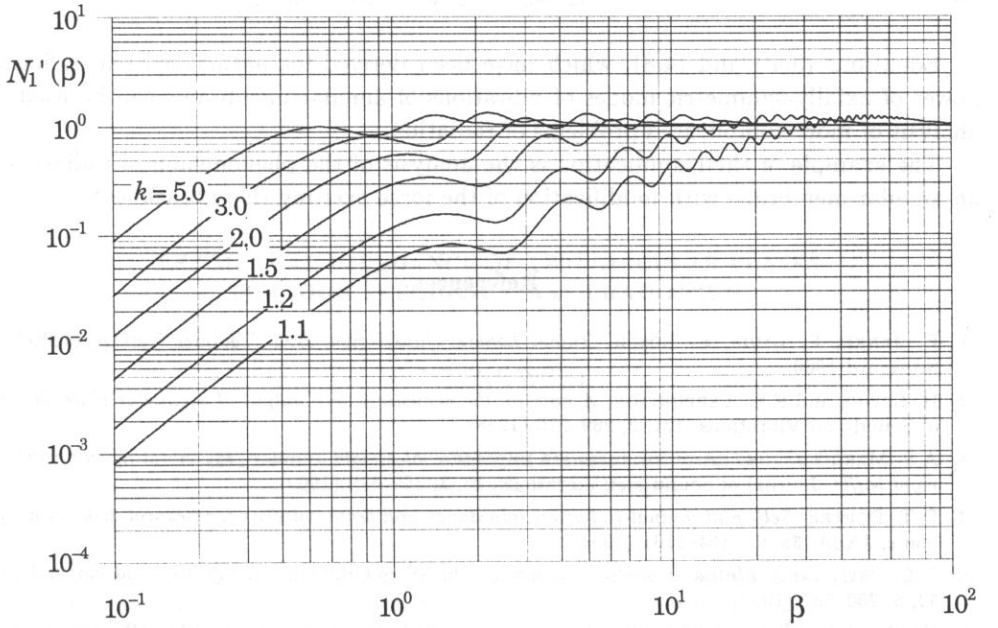

Fig. 3. Normalised real component of acoustic power radiated by the planar annular membrane versus β for different k and mode (0,1).

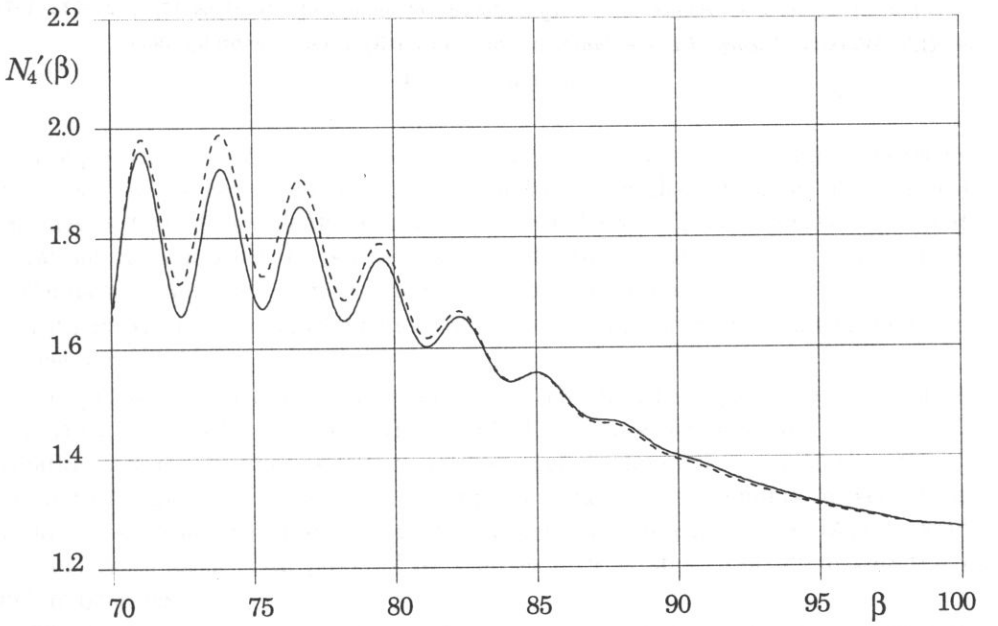

Fig. 4. Normalised real component of acoustic power radiated by the planar annular membrane versus β for the mode (0,4) and $k = 1.2$ – obtained from the formula (3.4′) (the solid line). The curve obtained from the formula (4.8) is dashed.

Equations (3.4′) and (4.8), which have been derived for normalised real radiation power of axially-symmetric modes of vibrations of annular membrane, can be used for analysis of more complicated problems of radiation.

The example of their application is the analysis of the phenomenon of radiation of an annular membrane with modification of the force exciting the vibrations.

References

[1] E. JANKE, F. EMDE, F. LÖSCH, *Tafeln höherer funktionen*, B.G. Teubner Verlagsgesellschaft, Stuttgard 1960.

[2] H. LEVINE and F.G. LEPPINGTON, *A note on the acoustic power output of a circular plate*, Journal of Sound and Vibrations, **121**, 2, 269–275 (1988).

[3] A.S. MERRIWEATHER, *Acoustic radiation impedance of a rigid annular ring vibrating in an infinite rigid baffle*, Journal of Sound and Vibrations, **10**, 3, 369–379 (1969).

[4] D.T. PORTER, *Self- and mutual-radiation impedance and beam patterns for flexural disks in a rigid plane*, JASA, **36**, 6, 1154–1161 (1964).

[5] R.L. PRITCHARD, *Mutual acoustic impedance between radiators in an infinite rigid plane*, JASA, **32**, 6, 730–737 (1960).

[6] W. RDZANEK, *Acoustical impedance of a circular membrane vibrating under the influence of a force with a uniform surface distribution*, Archives of Acoustics, **11**, 1, 39–52 (1986).

[7] W. RDZANEK, *Mutual impedance of circular plate for axially symmetric free vibrations at high frequency of radiating waves*, Archives of Acoustics, **17**, 3, 439–448 (1992).

[8] W. THOMPSON, jr, *The computation of self- and mutual-radiation impedances for annular and elliptical pistons using Bouwkamp's integral*, Journal of Sound and Vibrations, **17**, 2, 221–233 (1971).

[9] G.N. WATSON, *Theory of Bessel functions*, 2nd, University Press, Cambridge 1966.

ARCHIVES OF ACOUSTICS
22, 4, 463–471 (1997)

THE MUTUAL IMPEDANCE OF TWO CIRCULAR PLATES FOR HIGH FREQUENCY WAVE RADIATION

P. WITKOWSKI

Institute of Physics, Pedagogical University of Rzeszów
(34-310 Rzeszów, Rejtana 16a, Poland)

In this paper the mutual impedance of two thin circular plates with non-axisymmetric, time-harmonic free vibrations is analyzed. It is assumed that plates clamped at the circumference are placed in a rigid, planar baffle and radiate into a lossless and homogeneous fluid medium. Damping in plates is ignored.

Using the Cauchy theorem on residues and asymptotic formulae for the Bessel functions, an approximate expression is derived for a normalized mutual resistance and reactance for high frequencies.

1. Introduction

The practical application of a system of two plates as a sound transmitter or receiver of acoustic waves requires the knowledge of frequency characteristics of its acoustic parameters. One of them is the mutual impedance describing the influence of the plates vibrations on each other. In general case the vibrations of plates are non-axisymmetric so the mutual impedance concerns non-axisymmetric modes.

Hitherto the problem of interactions of non-axisymmetric modes was considered only for one plate [4, 8].

The problem of the mutual impedance of two elastic circular pistons was investigated in 1964 by PORTER [5] and CHAN [1] in 1967. They expressed an axially symmetric distribution of velocity in terms of the radial variable by a power series. In the paper [6], the mutual impedance of two circular co-planar sources with nonuniform velocity distributions: gaussian, parabolic and bessel has been considered. In paper [2], expressions were presented for acoustic power of two sources with parabolic velocity distribution for high frequencies.

The present paper deals with the mutual impedance of circular plates supporting non-axisymmetric free vibrations. By using the LEVINE and LEPPINGTON'S method [3], which is based on the Cauchy theorem, an elementary formula is derived for a normalized mutual impedance.

2. Mutual impedance of two circular plates

An acoustic radiator vibrating in an elastic medium encounters a counteraction of the medium. The measure of the source loading is the acoustic impedance defined as follows:

$$Z_a = \frac{1}{\sigma \langle v^2 \rangle} \int_\sigma p(r,\varphi)\, v^*(r,\varphi)\, d\sigma\,, \tag{2.1}$$

where

$$\langle v^2 \rangle = \frac{1}{\sigma} \int_\sigma v(r,\varphi)\, v^*(r,\varphi)\, d\sigma \tag{2.2}$$

is the mean value of the second power of the normal velocity of points on the source surface σ. Values $p(r,\varphi)$, $v(r,\varphi)$ stand for the surface distribution of pressure and normal velocity, respectively, r, φ denote the radial and angular coordinates of a point of the source with respect to the polar reference system. Now we find the analytical form of the definition (2.1) for two plates on which the distribution of velocity is defined as a superposition of free vibrations.

Let us consider two thin plates of the radii a_1, a_2, fixed on the rim in a rigid and flat acoustic baffle. The plates radiate into lossless and homogeneous fluid medium. The distance between the centres of the plates is denoted by l (Fig. 1).

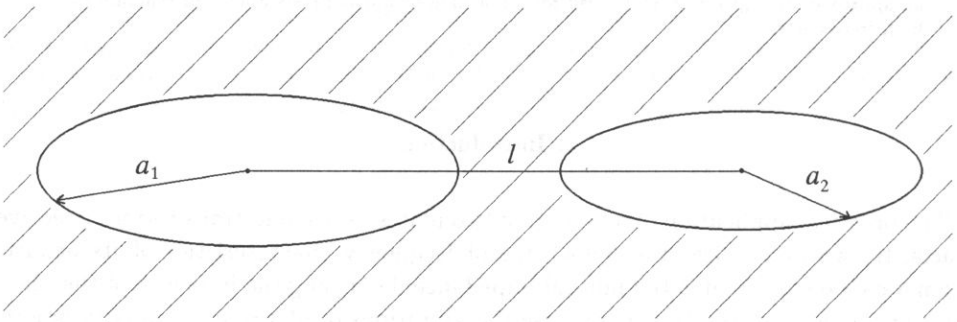

Fig. 1. The geometry of plates.

The normal velocity of the first plate is given in the form of a double, infinite sum:

$$v^{(1)}(r,\varphi) = \sum_{m=0}^{\infty} \sum_{n=1}^{\infty} c_{mn}^{(1)}\, v_{mn}^{(1)}(r,\varphi), \tag{2.3}$$

where $c_{mn}^{(1)}$ is an expansion coefficient of velocity in a series of eigenfunctions for the first plate and $v_{mn}^{(1)}(r,\varphi)$ are the normal velocity mode functions

$$v_{mn}^{(1)}(r,\varphi) = \mathcal{V}_{mn}^{(1)} \left\{ \begin{matrix} \sin(m\varphi) \\ \cos(m\varphi) \end{matrix} \right\} \left[J_m\left(\gamma_{mn} \frac{r}{a_1}\right) - \frac{J_m(\gamma_{mn})}{I_m(\gamma_{mn})} I_m\left(\gamma_{mn} \frac{r}{a_1}\right) \right], \tag{2.4}$$

where $J_m(\cdot)$ denotes the Bessel function of the m-th order, $I_m(\cdot)$ is the modified Bessel function of the m-th order, γ_{mn} stands for the roots of the characteristic equation $J_m(\gamma_{mn}) I'_m(\gamma_{mn}) - I_m(\gamma_{mn}) J'_m(\gamma_{mn}) = 0$.

In general case, the expansion coefficients of velocity in a series of eigenfunctions are complex, e.g. when we take into account the losses into material of the plates or the influence of radiated wave on the vibrations of the plates. The normalization factors

$$\mathcal{V}_{mn}^{(1)} = \frac{\sqrt{\varepsilon_m}}{\sqrt{2\pi} a_1 J_m(\gamma_{mn})}, \qquad \varepsilon_m = \begin{cases} 1, & m = 0, \\ 2, & m \geq 1, \end{cases} \tag{2.5}$$

are chosen such that the eigenfunctions are orthonormal.

Each of the normal velocity modes $v_{kl}^{(2)}$ of the second plate gives rise to an extra acoustic pressure on the surface of the first plate, p_{kl}^{21}. The total such a pressure is equal to an infinite sum of particular pressures p_{kl}^{21}

$$p^{21}(r, \varphi) = \sum_{k=0}^{\infty} \sum_{l=1}^{\infty} c_{kl}^{(2)} p_{kl}^{21}(r, \varphi), \tag{2.6}$$

where $c_{kl}^{(2)}$ is an expansion coefficient of the velocity on the second plate. Substituting the velocity (2.3) and the pressure (2.6) into the definition (2.1), we get:

$$Z_a^{21} = \sum_{m=0}^{\infty} \sum_{n=1}^{\infty} \sum_{k=0}^{\infty} \sum_{l=1}^{\infty} c_{mn}^{(1)*} c_{kl}^{(2)} \sqrt{\frac{\langle v_{kl}^{(2)2} \rangle}{\langle v_{mn}^{(1)2} \rangle}} Z_{\substack{kl \\ mn}}^{21}, \tag{2.7}$$

where

$$Z_{\substack{kl \\ mn}}^{21} = \frac{1}{\sigma \sqrt{\langle v_{mn}^{(1)2} \rangle \langle v_{kl}^{(2)2} \rangle}} \int_{\sigma_1} p_{kl}^{21}(r, \varphi)\, v_{mn}^{(1)*}(r, \varphi)\, d\sigma, \tag{2.8}$$

$\sigma = \pi a_1 a_2$, $\sigma_1 = \pi a_1^2$.

The quantity $Z_{\substack{kl \\ mn}}^{21}$ is the mutual impedance of two circular plates excited with radiating non-axisymmetric modes.

The pressure p_{kl}^{21} is calculated with using the Huygens-Rayleigh formula [6]. It has the following integral form:

$$p_{kl}^{21}(r, \varphi) = \frac{k_0 \varrho_0 \omega (i)^k}{2\pi} \int_0^{\frac{\pi}{2} - i\infty} \int_0^{2\pi} W_{kl}^{(2)}(\vartheta) e^{ik_0 r \sin\vartheta \cos(\varphi - \gamma)} \times \begin{Bmatrix} \sin(k\gamma) \\ \cos(k\gamma) \end{Bmatrix} e^{-ik_0 l \sin\vartheta \cos\gamma} \sin\vartheta \, d\vartheta \, d\gamma, \tag{2.9}$$

where

$$W_{kl}^{(2)}(\vartheta) = \mathcal{V}_{kl}^{(2)} \int_0^{a_2} J_k(k_0 r_2 \sin\vartheta) \left[J_k\left(\gamma_{kl} \frac{r_2}{a_2}\right) - \frac{J_k(\gamma_{kl})}{I_k(\gamma_{kl})} I_k\left(\gamma_{kl} \frac{r_2}{a_2}\right) \right] r_2 \, dr_2, \tag{2.10}$$

k_0 denotes the wave number in the gaseous medium, ϱ_0 is the equilibrium density of the gaseous medium, ω stands for the angular frequency of the vibrations.

Upon performing the integration in (2.8) with p_{kl}^{21} and $v_{mn}^{(1)}$ replaced by (2.9) and (2.4), respectively, and referring the impedance $Z_{\substack{kl \\ mn}}^{21}$ to the specific resistance of a fluid

medium $\varrho_0 c_0$, the normalized mutual impedance between (k,l) and (m,n) modes is obtained as follows

$$\zeta_{\substack{kl\\mn}}^{21} = \frac{\sqrt{\varepsilon_k \varepsilon_m}\, 2k_0^2 a_1 a_2}{\gamma_{mn}\gamma_{kl}}(-1)^k \int_0^{\frac{\pi}{2}-i\infty} \frac{\alpha_{mn} J_m(k_0 a_1 \sin\vartheta) - \dfrac{k_0 a_1 \sin\vartheta}{\gamma_{mn}} J_{m+1}(k_0 a_1 \sin\vartheta)}{1 - \left(\dfrac{k_0 a_1 \sin\vartheta}{\gamma_{mn}}\right)^4}$$

$$\times \frac{\alpha_{kl} J_k(k_0 a_2 \sin\vartheta) - \dfrac{k_0 a_2 \sin\vartheta}{\gamma_{kl}} J_{k+1}(k_0 a_2 \sin\vartheta)}{1 - \left(\dfrac{k_0 a_2 \sin\vartheta}{\gamma_{mn}}\right)^4}$$

$$\times [(-1)^m J_{k-m}(k_0 l \sin\vartheta) \pm J_{k+m}(k_0 l \sin\vartheta)] \sin\vartheta \, d\vartheta, \qquad (2.11)$$

where $\alpha_{mn} = J_{m+1}(\gamma_{mn})/J_m(\gamma_{mn})$. The signs plus and minus in the last term corrrespond to the choice of the cosine and sine functions, respectively, in the normal velocity distribution function (2.4).

This solution (2.11) is a generalization of the pattern obtained in [7] where $k = m = 0$, $a_1 = a_2$.

3. Acoustic resistance for high frequencies

The normalized mutual impedance (2.11) has no exact analytical solution. But there is a possibility to calculate its value using an approximate method.

As shown below, one can obtain an approximate representation for the mutual resistance by replacing the Bessel functions with their asymptotic expansions and then making use of the method of stationary phase.

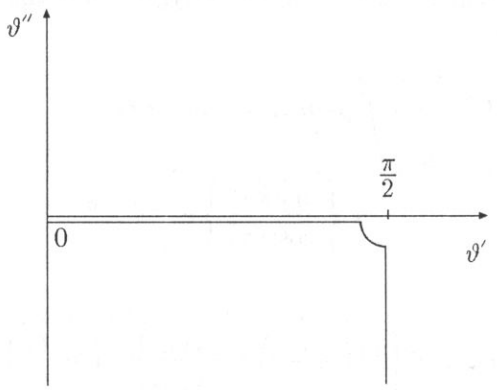

Fig. 2. The integration contour in the complex plate $\vartheta = \vartheta' + i\vartheta''$.

In order to separate the mutual resistance from impedance (2.11) let us substitute $\vartheta = \vartheta' + i\vartheta''$ and consider the integral along the segment $(0, \pi/2)$ of the real axis (Fig. 2). Let us substitute $x = \sin\vartheta'$ and use the abbreviations: $s = a_1/a_2$, $p = l/a_1$, $\beta = k_0 a_1$,

$\delta_{mn} = \gamma_{mn}/k_0 a_1$, $\delta_{kl} = \gamma_{kl}/k_0 a_1$. Then we get the expression:

$$\Theta^{21}_{\substack{kl \\ mn}} = 2\sqrt{\varepsilon_k \varepsilon_m}\, s^2 \delta_{kl}^2 \delta_{mn}^2 (-1)^k \int_0^1 \frac{\alpha_{mn}\delta_{mn} J_m(\beta x) - x J_{m+1}(\beta x)}{x^4 - \delta_{mn}^4}$$

$$\times \frac{s\alpha_{kl}\delta_{kl} J_k\left(\frac{\beta}{s}x\right) - x J_{k+1}\left(\frac{\beta}{s}x\right)}{x^4 - (s\delta_{kl})^4} \left[(-1)^m J_{k-m}(\beta p x) \pm J_{k+m}(\beta p x)\right] \frac{x\, dx}{\sqrt{1-x^2}}. \tag{3.1}$$

Let us introduce the function of a complex variable z [3]

$$F(z) = \left[\alpha_{mn}\delta_{mn} J_m(\beta z) - z J_{m+1}(\beta z)\right] \left[s\alpha_{kl}\delta_{kl} J_k\left(\frac{\beta}{s}z\right) - z J_{k+1}\left(\frac{\beta}{s}z\right)\right]$$

$$\times \left[(-1)^m H^{(1)}_{k-m}(\beta p z) \pm H^{(1)}_{k+m}(\beta p z)\right]. \tag{3.2}$$

Now, let us consider the complex integral:

$$\int_C \frac{F(z)\, z\, dz}{\sqrt{1-z^2}\,[z^4 - \delta_{mn}^4]\,[z^4 - (s\delta_{kl})^4]}. \tag{3.3}$$

The contour (Fig. 3) by-passes singular points of the integrand δ_{mn}, $s\delta_{kl}$, $i\delta_{mn}$, $is\delta_{kl}$ and branch point at $z = 0$ (of the Hankel function $H^{(1)}_{k\pm m}(\cdot) = J_{k\pm m}(\cdot) + iN_{k\pm m}(\cdot)$). Part of the contour follows the upper side of the branch cut between $z = 1$ and $z = \infty$ (of the function $\sqrt{1-z^2}$).

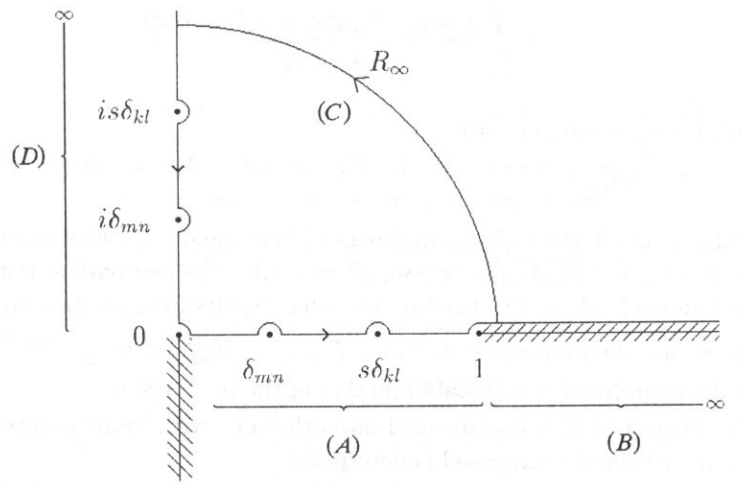

Fig. 3. The integration contour C.

The Cauchy theorem implies that the following is true for the integrals:

$$\wp \int_{\substack{0 \\ (A)}}^{1} + \int_{\substack{1 \\ (B)}}^{\infty} + \int_{\substack{R_\infty \\ (C)}} + \wp \int_{\substack{\infty \\ (D)}}^{0} = \pi i \sum_{j=1}^{4} \operatorname{res} f(z_j), \tag{3.4}$$

where $\wp\int$ denotes the principal value of an integral, $f(z)$ is equal to the integrand in (3.3), $z_j = \delta_{mn}, i\delta_{mn}, s\delta_{kl}, is\delta_{kl}$ are the first order poles.

The integral along a large circle vanish with increasing its radius. Also, integrals along small circles around the points $z = 0$ and $z = 1$ vanish when their radii tend to zero.

Then it remains:

$$\wp\int_0^1 \frac{F(x)x\,dx}{\sqrt{1-x^2}\,[x^4-\delta_{mn}^4]\,[x^4-(s\delta_{kl})^4]} + \int_1^\infty \frac{F(x)x\,dx}{-i\sqrt{x^2-1}\,[x^4-\delta_{mn}^4]\,[x^4-(s\delta_{kl})^4]}$$
$$+\wp\int_\infty^0 \frac{F(iy)iy\,d(iy)}{\sqrt{1+y^2}\,[y^4-\delta_{mn}^4]\,[y^4-(s\delta_{kl})^4]} = \pi i\sum_{j=1}^4 \operatorname{res} f(z_j). \tag{3.5}$$

Taking the real part of the left-hand side of (3.5), we arrive at the integral (3.1)

$$\int_0^1 \frac{\alpha_{mn}\delta_{mn}J_m(\beta x) - xJ_{m+1}(\beta x)}{x^4-\delta_{mn}^4}$$
$$\times \frac{s\alpha_{kl}\delta_{kl}J_k\left(\frac{\beta}{s}x\right) - xJ_{k+1}\left(\frac{\beta}{s}x\right)}{x^4-(s\delta_{kl})^4}\,[(-1)^m J_{k-m}(\beta px) \pm J_{k+m}(\beta px)]\,\frac{x\,dx}{\sqrt{1-x^2}}$$
$$= \int_1^\infty \frac{\alpha_{mn}\delta_{mn}J_m(\beta x) - xJ_{m+1}(\beta x)}{x^4-\delta_{mn}^4}$$
$$\times \frac{s\alpha_{kl}\delta_{kl}J_k\left(\frac{\beta}{s}x\right) - xJ_{k+1}\left(\frac{\beta}{s}x\right)}{x^4-(s\delta_{kl})^4}\,[(-1)^m N_{k-m}(\beta px) \pm N_{k+m}(\beta px)]\,\frac{x\,dx}{\sqrt{x^2-1}}. \tag{3.6}$$

The sum of residues in the right-hand side of (3.5) is equal zero, what is a consequence of $F(\delta_{mn}) = F(s\delta_{mn}) = F(i\delta_{mn}) = F(is\delta_{mn}) = 0$. Also the real part of the third integral in the left-hand side of Eq. (3.5) is equal 0, what results from relation $\Re eF(iy) = 0$. To prove this, we use the properties: $J_m(iy) = I_m(y)i^m$, $H_m^{(1)}(iy) = \frac{2}{\pi}i^{-(m+1)}K_m(y)$, where $K_m(y)$ is the cylindrical MacDonald function of the m-th order.

So, the integral (3.1) is transformed into other one with limits of integration from 1 to infinity, for which the integrand is determind.

All cylindrical functions in the integrand on the right-hand side of (3.6) we expand asymptotically [4] as x tends to infinity

$$J_m(x) \simeq \sqrt{\frac{2}{\pi x}}\cos\left(x - \frac{2m+1}{4}\pi\right),$$
$$N_m(x) \simeq \sqrt{\frac{2}{\pi x}}\sin\left(x - \frac{2m+1}{4}\pi\right). \tag{3.7}$$

After computing the integral on the right-hand side of (3.6) by using the method of stationary phase, we get finally:

$$\Theta_{\substack{kl\\mn}}^{21} = 2\sqrt{\varepsilon_k\varepsilon_m}\,\frac{s^3\delta_{kl}^2\delta_{mn}^2}{\pi\beta^2\sqrt{p}\,[1-\delta_{mn}^4]\,[1-(s\delta_{kl})^4]}$$
$$\times\left[\mathcal{A}\left(\frac{\sin\frac{\beta}{s}(ps-s+1)}{\sqrt{ps-s+1}}+(-1)^{k+m}\frac{\sin\frac{\beta}{s}(ps+s-1)}{\sqrt{ps+s-1}}\right)\right.$$
$$-\mathcal{B}\left(\frac{\cos\frac{\beta}{s}(ps-s+1)}{\sqrt{ps-s+1}}-(-1)^{k+m}\frac{\cos\frac{\beta}{s}(ps+s-1)}{\sqrt{ps+s-1}}\right)$$
$$-\mathcal{C}\left((-1)^m\frac{\cos\frac{\beta}{s}(ps+s+1)}{\sqrt{ps+s+1}}-(-1)^k\frac{\cos\frac{\beta}{s}(ps-s-1)}{\sqrt{ps-s-1}}\right)$$
$$\left.+\mathcal{D}\left((-1)^m\frac{\sin\frac{\beta}{s}(ps+s+1)}{\sqrt{ps+s+1}}+(-1)^k\frac{\sin\frac{\beta}{s}(ps-s-1)}{\sqrt{ps-s-1}}\right)\right], \tag{3.8}$$

where

$$\begin{aligned}\mathcal{A} &= (s\alpha_{kl}\alpha_{mn}\delta_{kl}\delta_{mn}+1),\\ \mathcal{B} &= (s\alpha_{kl}\delta_{kl}-\alpha_{mn}\delta_{mn}),\\ \mathcal{C} &= (s\alpha_{kl}\alpha_{mn}\delta_{kl}\delta_{mn}-1),\\ \mathcal{D} &= (s\alpha_{kl}\delta_{kl}+\alpha_{mn}\delta_{mn}).\end{aligned} \tag{3.9}$$

4. Acoustic reactance for high frequencies

Acoustic reactance, which is the imaginary part of impedance (2.11), has the form:

$$\chi_{\substack{kl\\mn}}^{21} = \frac{2\sqrt{\varepsilon_k\varepsilon_m}k_0^2a_1a_2}{\gamma_{mn}\gamma_{kl}}(-1)^k$$
$$\times\int_0^\infty\frac{\alpha_{mn}J_m(k_0a_1\cosh\vartheta'')-\dfrac{k_0a_1\cosh\vartheta''}{\gamma_{mn}}J_{m+1}(k_0a_1\cosh\vartheta'')}{1-\left(\dfrac{k_0a_1\cosh\vartheta''}{\gamma_{mn}}\right)^4}$$
$$\times\frac{\alpha_{kl}J_k(k_0a_2\cosh\vartheta'')-\dfrac{k_0a_2\cosh\vartheta''}{\gamma_{kl}}J_{k+1}(k_0a_2\cosh\vartheta'')}{1-\left(\dfrac{k_0a_2\cosh\vartheta''}{\gamma_{kl}}\right)^4}$$
$$\times[(-1)^mJ_{k-m}(k_0l\cosh\vartheta'')\pm J_{k+m}(k_0l\cosh\vartheta'')]\cosh\vartheta''\,d\vartheta''. \tag{4.1}$$

By substituting $x = \cosh\vartheta''$ and using the same notations as for resistance, we get the expression:

$$\chi_{\substack{kl\\mn}}^{21} = 2\sqrt{\varepsilon_k\varepsilon_m}\, s^2\delta_{kl}^2\delta_{mn}^2(-1)^k \times \int_0^\infty \frac{\alpha_{mn}\delta_{mn}J_m(\beta x) - xJ_{m+1}(\beta x)}{x^4 - \delta_{mn}^4} \frac{s\alpha_{kl}\delta_{kl}J_k\left(\frac{\beta}{s}x\right) - xJ_{k+1}\left(\frac{\beta}{s}x\right)}{x^4 - (s\delta_{kl})^4} \times [(-1)^m J_{k-m}(\beta p x) \pm J_{k+m}(\beta p x)] \frac{x\,dx}{\sqrt{1-x^2}}. \tag{4.2}$$

The calculation of this integral is much easier then that of the resistance because we do not have to change the limits of integrations. We can immediately change all cylindrical functions in (4.2) by inserting their asymptotic forms (3.7) and using the stationary phase method. In this way we arrive at the following equation:

$$\chi_{\substack{kl\\mn}}^{21} = 2\sqrt{\varepsilon_k\varepsilon_m}\frac{s^3\delta_{kl}^2\delta_{mn}^2}{\pi\beta^2\sqrt{p}\,[1-\delta_{mn}^4]\,[1-(s\delta_{kl})^4]} \times \left[\mathcal{A}\left(\frac{\cos\frac{\beta}{s}(ps-s+1)}{\sqrt{ps-s+1}} + (-1)^{k+m}\frac{\cos\frac{\beta}{s}(ps+s-1)}{\sqrt{ps+s-1}}\right) + \mathcal{B}\left(\frac{\sin\frac{\beta}{s}(ps-s+1)}{\sqrt{ps-s+1}} - (-1)^{k+m}\frac{\sin\frac{\beta}{s}(ps+s-1)}{\sqrt{ps+s-1}}\right) + \mathcal{C}\left((-1)^m\frac{\sin\frac{\beta}{s}(ps+s+1)}{\sqrt{ps+s+1}} - (-1)^k\frac{\sin\frac{\beta}{s}(ps-s-1)}{\sqrt{ps-s-1}}\right) + \mathcal{D}\left((-1)^m\frac{\cos\frac{\beta}{s}(ps+s+1)}{\sqrt{ps+s+1}} + (-1)^k\frac{\cos\frac{\beta}{s}(ps-s-1)}{\sqrt{ps-s-1}}\right)\right], \tag{4.3}$$

where

$$\begin{aligned} \mathcal{A} &= (s\alpha_{kl}\alpha_{mn}\delta_{kl}\delta_{mn} + 1),\\ \mathcal{B} &= (s\alpha_{kl}\delta_{kl} - \alpha_{mn}\delta_{mn}),\\ \mathcal{C} &= (s\alpha_{kl}\alpha_{mn}\delta_{kl}\delta_{mn} - 1),\\ \mathcal{D} &= (s\alpha_{kl}\delta_{kl} + \alpha_{mn}\delta_{mn}). \end{aligned} \tag{4.4}$$

5. Conclusions

The theoretical analysis makes it possible to obtain an integral formula for normalized mutual impedance with non-axisymmetric modes of free vibrations. It can be calculated

for short acoustic waves with approximate methods. The obtained formulae for acoustic resistance (3.8) and reactance (4.3) are similar to each other in the form and have "oscillatory" character of variations.

The expression obtained for normalized impedance (2.11) can be used in the analysis of more complicated vibrations, e.g. with taking into account losses in the plate material [3].

References

[1] K.C. CHAN, *Mutual acoustic impedance between flexible disks of different sizes in an infinite plane*, JASA, **42**, 5, 1060–1063 (1967).

[2] L. LENIOWSKA, W. RDZANEK, P. WITKOWSKI, *Mutual acoustic impedance of circular sources with parabolic vibration velocity distribution for high frequencies*, Archives of Acoustics, **17**, 3, 425–431 (1992).

[3] H. LEVINE, F.G. LEPPINGTON, *A note on the acoustic power output of a circular plate*, Journal of Sound and Vibration, **121**, 2, 269–275 (1988).

[4] P.M. MORSE, K.U. INGARD, *Theoretical acoustic*, McGraw-Hill Book Company, New York, London 1968.

[5] D.T. PORTER, *Self- and mutual- radiation impedance and bean patterns for flexural disks in a rigid plane*, JASA, **36**, 6, 1154–1161 (1964).

[6] W. RDZANEK, *Mutual and total impedance of the system of sources with nonuniform surface distribution of velocity* [in Polish], Pedagogical University of Zielona Góra 1979.

[7] W. RDZANEK, *Mutual acoustic impedance of circular membranes and plates with bessel axially-symmetric vibration velocity distributions*, Archives of Acoustics, **5**, 3, 237–250 (1980).

[8] P. WITKOWSKI, *The mutual impedance of a circular plate in the case of non-axisymmetric vibrations*, Proceedings of 40th Open Seminar on Acoustics OSA'93, 113–117.

ARCHIVES OF ACOUSTICS
22, 4, 473–480 (1997)

C H R O N I C L E

2-nd meeting on Advances in Acousto-Optics

St. Petersburg, Russia, June 24-25, 1997

After the successful 1-st meeting on AA-O'96 started as the 10-th Topical Meeting (1st one of the European Acousto-Optic Club) of the European Optical Society organized by Dr J. Sapriel (CNET – Bagneux) in Paris, the second meeting of that kind (AA-O'97) took place in St. Petersburg on 24–25-th June, 1997. It was organized by the European Optical Society, the St. Petersburg State Academy of Aerospace Instrumentation and the Institute of Radio Engineering and Electronics of Russian Academy of Science, Russia.

The Organizing Committee consisted of:

The **Conference Co-Chairs:** Prof. Yuri Gulayev (Institute of Radio Engineering and Electronics RAS, Russia and Prof. Jacques Sapriel (Centre National d'Etudes des Telecommunications, France).

The **Executive Committee:**

Prof. S.V. Kulakov

Dr V.V. Molotok

both from the St. Petersburg State Academy of Aerospace Instrumentation, Russia and the **Programme Committee:**

Valery V. Proklov (Institute of Radio Engineering and Electronics RAS, Russia)

Vladislav I.Pustovoit (Institute of Radio Engineering and Electronics RAS, Russia)

Oswald Leroy (Katholieke Universiteit Leuven, Belgium)

Antoni Śliwiński (University of Gdańsk, Poland)

Mario Armenise (Politecnico di Bari, Italy)

Jean P. Huignard (Thomson, LCR, France)

Daniel Dolfi (Thomson, LCR, France)

Erik Blomme (Vrije Hogeschool voor Technologie en Informatica, Belgium)

Rudy Briers (Katholieke Universiteit Leuven, Belgium)

Victor V. Molotok (St. Petersburg State Academy of Aerospace Instrumentation, Russia).

The AA-O'97 Conference was sponsored by the Russian Fund of Fundamental Research and Ministry for Base and Special Education of Russia.

More than 60 participants from 6 countries of Europe gathered in the Hotel for Tourisme nearby the building of the State Academy of Aerospace Instrumentation for very topical conference on interaction of light and ultrasonics (including theoretical developments treated for a wide range of applications.

There were 7 oral sessions and 1 poster session in which 37 papers were presented.

Several papers were related to different problems of ultrasonic light diffraction taking into account many aspects of the phenomenon including mechanisms of light and ultrasonics interaction, polarization effects, interferometric measurements.

Papers grouped around application of acousto-optical devices to signal processing covered theoretical basis for the problem as well as many practical solutions for acousto-optical processors like analysers, filters, modulators etc.

Another group of papers concern application perspectives of acousto-optical devices in optical communication systems.

Some papers were devoted to holographic 3D image display or to recording and reproducing of wideband RF signals.

Also, there were papers on properties of acousto-optical materials and on acousto-optical devices metrology.

Most of the presentations were very interesting and of high level what was reflected in professional discussion after presentations as well as during the final discussion predicted in the programme.

During the meeting there was also discussion about some formal rules for the EAOC (European Acousto-Optic Club). Dr Molotok presented a proposal prepared by Dr E. Blomme (Belgium) and a kind of a by – law of the EAAC reflecting the main objectives and purposes of the every year 2 days meeting of the A.O. community of Europe has been accepted. The role of the European Optical Society as the main sponsor and initiator of the meetings was evidently stressed. Also relations between AA-O's meetings and the every 3 years Spring Schools on Acoustooptics was discussed.

The participants decided that the next AA-O'98 and the 7th International Spring School on Acoustooptics will be organized as a joint meeting in Gdańsk – Jurata, May 18 – 22, 1998.

Antoni Śliwiński

WORLD CONGRESS ON ULTRASONICS'97

Jokohama, Japan, 24–27 August 1997

The WCU-97 was the second world meeting of ultrasonics community following the 1-st WCU-95 congress started in Berlin 2 years ago.

The **International Steering Committee** for the Congress representing different countries and acoustical societies has been following:

Chairman: **Noriyoshi Chubachi**, JAPAN

A. Alippi ITALY	**O. Leroy** BELGIUM
E. Benes AUSTRIA	**T.J. Mason** UK
L. Bjørnø DENMARK	**W.G. Mayer** USA
L. Crum USA	**W.G. Pace** UK
M. Deschamps FRANCE	**R. Reibold** GERMANY
J.A. Gallego-Juarez SPAIN	**A. Śliwiński** POLAND
J. Herbertz GERMANY	**S. Ueha** JAPAN
H. Jones CANADA	**A. Zarembowitch** FRANCE

The Chairman of the Organizing Committee was Prof. N. CHUBACHI from Tohoku Gakuin University, the V-ce Chairman: Prof. K. YAMANONCHI, Tohoku University and the Secretary: Prof. S. UEHA, Tokyo Institute of Technology, the President of the Acoustical Society of Japan. Prof. K. TAKAGI, University of Tokyo was the Chairman of the Program and the Editor of the Proceedings of WCU 97. The whole local Organizing Committee contained 109 members in 70% from universities and technological institutes and 30% from industrial companies.

The Congress was sponsored by Science and Technology Agency, Kanagawa Prefecture and City of Yokohama and financially supported by the City of Yokohama, by 4 science and technological foundations and 62 industrial corporations and companies.

More than 360 participants from 22 countries gathered at the Pacifico Yokohama congress centre situated at the Yokohama Bay for presentation of contributions and common discussion on advanced topics of ultrasonic science and technology. 260 original contribution papers, 4 invited papers and 1 plenary lecture were presented. Among the contribution papers 115 were oral presentations (20 minutes) in special fields sessions and 145 were short (about 2 minutes) – for oral presentations correlated with the poster sessions. In this way everyone of poster papers could be shortly introduced by their authors.

The papers covered the whole field of ultrasonics and were grouped in eleven following sessions: Basic Ultrasound (2 sessions), Ultrasonic Transduction and Materials (1 session), Photoacoustics and acousto-optics (2 sessions), Ultrasonic Measurement (2 sessions), Physical and Molecular Acoustics (2 sessions), Devices (3 sessions), Power Ultrasonic and Maters (4 sessions), Non-destructive Evaluation (1 session), Sonochemistry (2 sessions), Medical Ultrasonics (3 sessions) and Underwater Acoustics (2 sessions).

The only one plenary invited paper on "Safety of Medical Ultrasound" was presented by Professor J. HERBERTZ of Gerhard-Mercator Universität, Duisburg, Germany. The author presented his "perspective on safety issues of ultrasound in the field of therapy and surgery and in the fields of medical diagnosis and his vision of establishing a trustworthy safety classification for ultrasonic diagnostic equipment".

Three other invited papers were correlated with topical sessions.

Professor K. YAMANOUCHI of Tohoku University, Japan, spoke on "Future trend of acoustic wave devices". He described several hot topics of acoustic wave technology important to investigate facing the coming 21 century requirements.

The main items to develope are:

1) high performore and high quality acoustic devices,

2) development and research of new piezoelectric materials and new theoretical analysis,

3) analysis of linear and non-linear propagation characteristics and new devices using new fundamental operation mechanism,

4) evaluation of materials using ultrasonic microscope,

5) ultrasonic motors and actuators,

6) high performance SAW devices in mobile communication,

7) piezoelectric gyroscope and SAW sensors,

8) high precise and high performance and high frequency ultrasonic medical diagnosis,

9) high precise time standard using ultrasonics.

Most of these items were examplified by up to date achievements in ultrasonic, acousto-electronic and acousto-optic technologies and in acoustic measurements and applications.

Professor R. APFEL of Yale University, USA talked about "Super oscillations of drops and surfactant studies in microgravity". He presented results of a wide programme which combined experimental work performed both on the ground and in space and theoretical and numerical modeling of the drop behaviour oscilations and the influence of the surfactant on them. There has been possible to establish idealized conditions for surface behaviour studies by levitating a drop of liquid in air, away from interacting of container wall surfaces, and manipulating the drop with acoustic radiation forces. Different free oscillations of initially deformed drops were studied and the influence of surfactants on these oscilations reflected in dynamic surface tension and the surface viscosities (shear and dilatational) were observed and determined.

The next invited paper was presented by Professor J.A. GALLEGO-JUÁRES of Consejo Superior de Investigationes Cientificas, Spain, on "Power ultrasonic technologies for industrial applications". He described the structure and performance of the new sonic/ultrasonic power generator constituted by a transducer with a flexural–vibrating plate radiator and an electronic unit for driving the transducer. The prototypes of generators were developed for the frequency range 10 – 40 kHz and power capacities between 100 W and 1 kW. 3 kW new model of 1 meter radiating plate is being constructed, presently. Several examples of industrial applications like fine particle removal from industrial fumes, defoaning, food dehydration and cleaning of textiles were described.

It is impossible to talk over many very interesting contributed and poster papers among those presented in the congress. The majority of papers presented have a good level and illustrated topical achievements of ultrasonics in science technology medicine and industry.

In parallel to sessions the ultrasonic equipment exhibition of 12 exhibitors mainly from Japan was very succeded.

During the Congress there was a special competition on the best poster evaluation organized. Participants voted (using the ballot box) and 5 posters were selected and awarded by the Organizing Committee. Among them one Polish poster presented by E. Kotlicka from the Technical University of Warsaw was distinguished.

The participants as well as accompanied persons had many opportunities for sightseeing and experiencing the Japanese customs and culture. A special events were prepared nearby the lecture rooms: the flower arrangement (Ikebana), Kimono (Japanese traditional clothes), tea ceremony (Cha) and Koto music, calligraphy (Shodo) and colored paper folding (Origami) in which taking part one can enjoy very much.

The participants had opportunity to attend interesting post Congress technical tours. One of them was the tour to the Seidensha Electronics Co., Ltd. and the Tokyo Institute of Technology Lab. in which the undersigned below took part. There was a possibility to visit the factory producing ultrasonic and electromagnetic welding equipment of wide field of applications. In the Tokyo Institute of Technology, in the Precision and Intelligence Laboratory, the group was hosted by Professor Sadayuki Ueha, the head of the Applied Acoustic Devices Section. Many interesting experiments are curried on in this Laboratory. The current topics are: fundamentals of ultrasonics applied in various engineering fields, ultrasonic actuators and motors and ultrasonic measurements. Several kinds of hybrid transducer tipe ultrasonic motors, the noncontact transportation system using acoustic radiation pressure, ultrasonic diagnosis of osteoporosis system and others, were demonstrated to the visitors. At the end of the visit a very warm reception (barbecue party) took place.

The undersigned below having the opportunity to write this report wants to express his cordial thanks to Professor S. Ueha for his kind invitation to Japan and the essential support enabling him to participate the Congress.

The 2-nd World Congress on Ultrasonics in Jokohama, similarly as the 1st one in Berlin has occured very succesfull and fruitful. The Steering Committee of WCU's during its meeting in Jokohama declined with thanks to the Organizers for their great efforts and the excellent organization. Also, the Steering Committee discussed and accepted the By-Law for World Congress on Ultrasonics. It has been decided that the next WCU-99 meeting joint with Ultrasonic International 99 Conference will take place in Copenhagen, Denmark and will be organized by Prof. L. Bjørnø.

Antoni Śliwiński

103rd AES Convention, New York

26 – 29 September 1997

This Convention was a Jubilee of fifty years unbroken tradition of AES Conventions. "AES goes gold" – this sentence was visible from numerous green posters, which marked organizers' stands in the huge indoor volume of the New York Javits Center, where the 103rd Convention was located. The Javits Center, stretches along the Hudson River on Manhattans west-side, near to the entrance to the famous Lincoln Tunnel, linking Manhattan with New Jersey. The Center is very large, one can say, too large in comparison with other convention sites. It is enough to say that the building contains over 167000 square meter (1.8 million square feet) of floor space, thus walking among various stands, lecture halls, meeting rooms and hundreds of exhibition booths was somewhat tiring.

The opening ceremony was devoted to celebrate and emphasize the AES Gold Jubilee. Traditional AES awards were presented during the special ceremony, to acknowledge the contributions of those individuals who have furthered the advancement of the audio domain and the development of the Society. This year the awards were more numerous than previously due to the Jubilee occasion. An informal reception with a buffet completed the opening ceremony creating for the recipients of awards together with all invited guests, a relaxed atmosphere and an opportunity for individual meetings and exchange of ideas.

The scientific part of the Convention consisted, first of all, of the 16 paper sessions, each of them devoted to a specific domain of audio engineering. 142 papers were presented by 270 authors and co-authors from 18 countries (USA – 96, UK – 50, Japan – 27, Germany – 19, Finland – 11, Italy – 11, The Netherlands – 11, France – 10, Canada – 7, Denmark – 6, Austria – 5, Korea – 4, Russia – 3, Urugway – 3, Israel – 2, Poland – 2, Spain – 2, Switzerland – 1). Besides of the paper sessions mentioned, the 16 workshop sessions, devoted to most actual topics, were organized and held parallel to paper sessions.

As usual, most of the papers were edited as Preprints prior to the debates, which helped presentations and efficient discussions after presentations. Moreover, this year, for the first time, all Preprints have been edited as a set in the form of a CD-ROM-disc, sold to attendees.

It is difficult to compare the scientific achievements presented during this Convention with those of previous ones. It is easier to assess its commercial impact. The approximate number of 18000 visitors to the exhibition area means an undoubted advertising success of all the 348 companies of the audio industry all over the world, participating in this gigantic fair.

Besides the scientific and industrial importance, the Convention played a significant organizational role. The Board of Governors meeting, held traditionally the day after the closing of the Convention, was, as usual, an important event of the entire AES

annual activity. The meeting preceeded the date of 6 October, being the terminal point of passing organizational functions from those ending their term to those elected for the next term. The actual President, Elizabeth Cohen, presided the meeting for the last time, thus future meetings will be presided by the President-elect Subir Pramanik. Other AES officers will also be changed according to bylaws. Among other things I delivered the final report of my activities as Vice-President for the Central Europe Region.

In my report I quoted as main achievements the six new AES Sections which I successfully coorganized within the Region: Lithuanian, Russian-St.Petersburg, Russian-Baltic State Technical University–Student, Gdansk Technical University–Student, Ukrainian, Byelorussian. Thus the total number of Sections within the CE Region increased to seventeen, while above three hundred new members entered into AES community. This creates a new organizational situation in Central and Eastern Europe facilitating professional contacts among sound engineers working in the neighbouring countries. Regional AES meetings become desirable and just such initiative was undertaken, proposed to the Board of Governors and preliminarily accepted. The initiative was undertaken by the St. Petersburg Section which will organize a regional conference in 1999.

Other decisions were also undertaken by the BoG meeting, namely, those concerning future AES Conventions. The nearest one, the 104th, will take place in Amsterdam, from May 16 – 19,1998, and the next one, the 105th, in San Francisco, from September 26 – 29, 1998.

From my experience during functioning as AES officer, I would like to formulate a final concise conclusion and advice. The national AES Sections, especially in the countries undergoing transformation from centrally controlled to the democratic system of social life, are of great value as a substantial relief and help for introducing acousticians, sound engineers and other related professional local communities into a world wide area, of scientific, professional and commercial contacts. Those possibilities, offered to local Sections by the AES must not be overlooked. Now, the future activities of the AES Central Region will be coordinated by the new Vice-President for the CE Region, Dr Karl-Otto Baeder from Switzerland. I wish him the most successful term leading to the further fruitful development of our Region.

I think, moreover, that the above mentioned Sections of Central and Eastern Europe should be grateful to those long-sighted AES officers, who seven years ago decided to extend the Europe AES Region to the East and offer substantial help in organizing new Sections. The Audio Engineering Society may be proud of the fulfilment of one of its major aims.

Marianna Sankiewicz

DISSERTATION

"Investigations of inclusion complexes of organic ions with α- and β-cyclodextrin by means of ultrasonic spectroscopy methods" Andrzej Balcerzak, Institute of Fundamental Technological Research, Polish Academy of Sciences, Warsaw. Ph.D. Thesis in material science, supervised by Associate Professor Adam Juszkiewicz.

The aim of the Thesis was to obtain thermodynamic and kinetic characteristics of complexation process, information about its mechanism, and to determine the influence of different parameters (sterical, chemical) on this process.

Measurements of the absorption of ultrasonic waves in the frequency range 1 – 150 MHz were carried out for aqueous solutions of α- and β-cyclodextrin with surfactants which were the source of organic ions. The additional measurements of velocity of the acoustical wave and density were also made. All these measurements were made for the equimolar solutions of cyclodextrin + surfactant at 15, 25, 35 and 45° C. The concentrations were equal to 0.01 – 0.04 M and 0.01 M for solutions with α-cyclodextrin and β-cyclodextrin (due to its low solubility), respectively.

The measurements were made by means of the resonator (1 – 10 MHz) and pulse (10 – 150 MHz) methods.

The most important results:

— there are ultrasonic relaxation processes in the aqueous solutions of α- and β-cyclodextrin with surfactants; these processes can be described by one or two relaxation times,

— each of these processes fulfils the scheme of first-order or pseudo-first-order reaction,

— the calculated kinetic and thermodynamic parameters enable to attribute molecular phenomena to the observed relaxation processes,

— the low-frequency process is connected with the exchange of water molecules in hydratation shell of cyclodextrin,

— the high-frequency process, which occurs for organic ions with long alkyl chains, is connected with penetration of the chain of the organic ion to the cavity of cyclodextrin,

— a kind of the hydrophilic group of the surfactant has diminutive influence on this penetration,

— the experimental results are explained by the proposed three-step kinetic model of complexation.